

Polarization transfer in relativistic magnetized plasmas

Jean Heyvaerts^{1,2}, Christophe Pichon^{1,3}, Simon Prunet¹, Jérôme Thiébaud¹

¹ *Institut d’Astrophysique de Paris, UMR 7095, CNRS, UPMC Univ. Paris VI, 98 bis boulevard Arago, 75014 Paris, France*

² *Observatoire Astronomique de Strasbourg, 11 Rue de l’Université, 67000 Strasbourg (France)*

³ *CEA Saclay, DSM/IPhT, Bâtiment 774, 91191 Gif-sur-Yvette, France*

16 March 2019

ABSTRACT

The polarization transfer coefficients of a relativistic magnetized plasma are derived. These results apply to any momentum distribution function of the particles, isotropic or anisotropic. Particles interact with the radiation either in a non-resonant mode when the frequency of the radiation exceeds their characteristic synchrotron emission frequency, or quasi-resonantly otherwise. These two classes of particles contribute differently to the polarization transfer coefficients. For a given frequency, this dichotomy corresponds to a regime change in the dependence of the transfer coefficients on the parameters of the particle’s population, since these parameters control the relative weight of the contribution of each class of particles. Our results apply to either regimes as well as the intermediate one. The derivation of the transfer coefficients involves an exact expression of the conductivity tensor of the relativistic magnetized plasma that has not been used hitherto in this context. Suitable expansions valid at frequencies much larger than the cyclotron frequency allow us to analytically perform the summation over all resonances at high harmonics of the relativistic gyrofrequency.

The transfer coefficients are represented in the form of two-variable integrals that can be conveniently computed for any set of parameters by using Olver’s expansion of high-order Bessel functions. We particularize our results to a number of distribution functions, isotropic, thermal or power-law, with different multipolar anisotropies of low order, or strongly beamed. Specifically, earlier exact results for thermal distributions are recovered. For isotropic distributions, the Faraday coefficients are expressed in the form of a one-variable quadrature over energy, for which we provide the kernels in the high-frequency limit and in the asymptotic low-frequency limit. An interpolation formula extending over the full energy range is proposed for these kernels. A similar reduction to a one-variable quadrature over energy is derived at high-frequency for a large class of anisotropic distribution functions that may form a basis on which any smoothly anisotropic distribution could be expanded.

Key words: polarization, plasmas, radiative transfer, galaxies: magnetic fields

1 INTRODUCTION AND MOTIVATION

The transfer of the intensity and polarization of radiation propagating in a relativistic magnetized plasma has been a long standing problem which still remains incompletely solved. Its potential diagnostic applications have long been known (Cioffi & Jones 1980; Jones & O’Dell 1977) and it has recently attracted renewed interest (Brentjens & de Bruyn 2005; Thiébaud et al. 2010) in connection with the study of the magnetic field structure of synchrotron-emitting objects where the high-energy emitting particles may constitute the bulk of the plasma. Polarization data constrain the structure of geometrically complex sources and of magnetospheres. Astrophysical environments such as the vicinity of the central black hole in the Milky Way (Agol 2000; Beckert 2003; Shcherbakov 2011), jet-sources, galactic (Stirling et al. 2004) or extragalactic (Homan & Wardle 2004), pulsars (Kanbach et al. 2003; Dyks et al. 2004; Petri & Kirk 2005; Mc Donald et al. 2010; Yuen et al. 2012) or disks around black holes (Dovciak et al. 2008) have been studied by these methods. The perspectives of using polarization data to constrain magnetic fields have improved strongly by the deployment of LOFAR (Beck 2009),

and will blossom with the advent of SKA (Dewdney et al. 2009; Carilli 2004), ranging from the largest scales (Gaensler et al. 2004; Feretti & Johnston-Hollitt 2004) to the smallest ones (Bicknell 2004).

Understanding polarization data rests on the availability of good polarization transfer codes and on the knowledge of the transfer coefficients that would modify the intensity and the polarization of light as it propagates in the medium. Synchrotron radiation plays an important role in the emission of magnetized high energy sources. The polarization properties of its emission and absorption caused by the high-energy population are well known. The non-dissipative transfer coefficients of Faraday rotation and Faraday conversion from circular to linear polarization have been more difficult to derive. Substantial progress has nevertheless been achieved in time (Trubnikov 1958; Zhelezniakov 1967; Sazonov 1969b; Melrose 1997a; Shcherbakov 2008; Huang & Shcherbakov 2011). In this paper we buildup on this research by deriving explicit expressions for the polarization transfer coefficients in a relativistic homogeneous magnetized plasma for any isotropic distribution function and for a large class of non-isotropic ones. These results are obtained by a new exact method of derivation of the high frequency conductivity tensor of a magnetized relativistic plasma which involves, at some late stage of the derivation, well-justified approximations. Our results are shown to exactly coincide with known exact results in the case of thermal distributions.

Section 2 is devoted to introducing the polarization transfer equations of uniformly magnetized medium and deriving ab initio the corresponding conductivity. Section 3 presents in anticipation the end-results of our derivation of the polarization transfer coefficients as a double regular quadrature and illustrates it for isotropic and anisotropic distributions, where it can sometimes be reduced to a single quadrature. This unconventional presentation has been chosen because the derivation of these results from those in Section 2, which is carried in Section 4 and Section 5, is technical in some respects. These two sections can be skipped accordingly on a first read. Section 6 focuses on analytical results applicable to isotropic distribution functions in the low-frequency limit. Section 7 wraps up.

2 FORMULATION

2.1 Description of polarization transfer

The polarization properties of radiation are represented by a column vector of four Stokes parameters, $\mathbf{I} = {}^T(I, Q, U, V)$, ${}^T M$ denoting the transpose of the matrix M . The Stokes vector \mathbf{I} depends on the frequency and direction of propagation of the radiation, as well as on the point in space and on the time at which it is observed. In the limit where the frequency is higher than any gyrofrequency, the Stokes vector satisfies a radiative transfer equation in which the generalized emission coefficient is a four-component column vector $\mathbf{W} = {}^T(W_I, W_Q, W_U, W_V)$ and the generalized absorption coefficient is a 4×4 transfer matrix. This transfer equation can be written, for radiation of frequency ω and group velocity (based on an isotropic mean conductivity) \mathbf{v}_g as:

$$(\partial_t + \mathbf{v}_g \cdot \nabla) \begin{pmatrix} I \\ Q \\ U \\ V \end{pmatrix} = \begin{pmatrix} W_I \\ W_Q \\ W_U \\ W_V \end{pmatrix} - \begin{pmatrix} K_{II} & K_{IQ} & K_{IU} & K_{IV} \\ K_{IQ} & K_{II} & K_{QU} & K_{QV} \\ K_{IU} & -K_{QU} & K_{II} & K_{UV} \\ K_{IV} & -K_{QV} & -K_{UV} & K_{II} \end{pmatrix} \begin{pmatrix} I \\ Q \\ U \\ V \end{pmatrix}. \quad (1)$$

The four matrix elements K_{II} , K_{IQ} , K_{IU} , K_{IV} and the emission column vector \mathbf{W} result from dissipative effects. The emission column vector \mathbf{W} represents the emission rate and polarization of the spontaneously emitted radiation. The elements K_{QU} , K_{QV} , K_{UV} of the transfer matrix result from non-dissipative effects caused by the slowly varying phase difference between different components of the electric vector of the radiation. The elements of the matrix in equation (1) can be expressed in terms of the components of the high-frequency conductivity tensor $\boldsymbol{\sigma}(\mathbf{k}, \omega)$. Equation (1) has been established by a number of authors and by different methods (Sazonov & Tsytovitch 1968; Heyvaerts 1969; Zheleznyakov et al. 1974). A direct derivation of the absorption-like term is presented below. The derivation of the emission term is less straightforward (Sazonov & Tsytovitch 1968).

Since the wavelengths of the plasma eigenmodes of a given frequency ω do not differ by much from each other at high frequency, their phase difference evolves slowly in space and time. As a result, the correlations between these phases, which determine the state of polarization, are maintained over a length much longer than the wavelength, justifying a radiative transfer approach. When the plasma frequency ω_p exceeds by much the gyrofrequencies Ω_A of all particle species A , the wavelengths of the eigenmodes still differ by a little amount when $\omega \gg \Omega_A$ although the dispersion relation may depart from the vacuum one when ω is of order ω_p . In any other case, the difference of the phases of the transverse eigenmodes evolves on a wavelength scale and the radiative transfer approach is inappropriate. Assuming there are only two transverse eigenmodes, if their phases would be correlated at some point and time, the rapid growth of their difference would reduce this correlation to nothing in only a few wavelengths. Thus, the polarization state of radiation supported by modes of largely different wavelengths for a given frequency reduces to that of the sum of two mutually incoherent eigenmodes. Equation (1) is then only relevant in the high frequency limit, $\omega \gg \Omega_A$.

We now show how the elements of the absorption matrix relate to those of the conductivity tensor. We start from the propagation equation of the electric field $\mathbf{E}(\mathbf{r}, t)$, deduced from Maxwell's equations:

$$\frac{1}{c^2} \frac{\partial^2 \mathbf{E}}{\partial t^2} - \Delta \mathbf{E} + \mu_0 \frac{\partial \mathbf{J}}{\partial t} = 0. \quad (2)$$

Our equations are written in the MKSA system of units, where ε_0 is the dielectric permittivity of vacuum and μ_0 its magnetic permeability. The velocity of light in vacuo is $c = (\varepsilon_0 \mu_0)^{-1/2}$. In equation (2), \mathbf{E} is the electric field and \mathbf{J} the current density. The electric field is assumed to be transverse, so that $\text{div } \mathbf{E} = 0$, which is a good approximation at high frequencies. The microscopic electric field is then Fourier expanded, its complex vectorial amplitude $\hat{\mathbf{E}}_{\mathbf{k}, \omega}$ being regarded as slowly depending on space and time, which is equivalent to coarse-graining in Fourier space. The electric current density $\mathbf{J}(\mathbf{r}, t)$ is similarly expanded. The phase, and possibly the amplitude, of the microscopic electric field is a random variable. Omitting the indices \mathbf{k}, ω for simplicity, each term of the Fourier expansion can be written as

$$\mathbf{E}(\mathbf{r}, t) = \hat{\mathbf{E}}(\mathbf{r}, t) e^{i(\mathbf{k} \cdot \mathbf{r} - \omega t)}. \quad (3)$$

The current in equation (2) is the sum of an induced current \mathbf{J}' , which results from the electric field $\mathbf{E}(\mathbf{r}, t)$ and a spontaneous current \mathbf{J}'' , the microcurrent created by the individual plasma particles, which gives rise to spontaneous emission, while the induced current gives rise to the absorption-like term in equation (1). This latter part of the current is given in terms of the electric field by a linear non-local and causal conductivity tensor operator:

$$\mathbf{J}'(\mathbf{r}, t) = \int_0^\infty d\tau \iiint d^3R \Sigma(\mathbf{R}, \tau) \cdot \mathbf{E}(\mathbf{r} - \mathbf{R}, t - \tau). \quad (4)$$

The conductivity operator can be split into a scalar isotropic part, Σ_s , and a tensorial anisotropic part Σ_1 . The isotropic part may, for example, represent the dispersive properties of a cold population of relatively large density, neglecting the magnetization of these particles. An isotropic conductivity has no effect on the polarization but affects the propagation properties of electromagnetic waves. No component of the conductivity need to be separated out when the propagation is represented well enough by the vacuum dispersion relation. The tensorial anisotropic part consists of the anisotropic residual of the conductivity, not included in Σ_s , and of the conductivity of populations which negligibly contribute to the dispersive properties of the plasma waves. The frequency ω supposedly being much larger than all gyrofrequencies, the component Σ_1 must be small. Its contribution to the dispersion properties may be neglected but it nevertheless contributes to the polarization transfer matrix.

The form of the electric field in equation (3) is inserted in equations (2) and (4). When acting on the imaginary exponential phase factor the operators ∂_t and ∇ are of order ω and k respectively, but when acting on the slowly varying amplitude $\hat{\mathbf{E}}(\mathbf{r}, t)$ they are of order $1/T$ and $1/L$, T and L being the time and length scales on which $\hat{\mathbf{E}}$ varies, which are much longer than the wave period and wavelength. Only the terms of first order in $1/(\omega T)$ and $1/(kL)$ are retained. For consistency, this requires that $\hat{\mathbf{E}}(\mathbf{r} - \mathbf{R}, t - \tau)$ in equation (4) be expanded as:

$$\hat{\mathbf{E}}(\mathbf{r} - \mathbf{R}, t - \tau) = \hat{\mathbf{E}}(\mathbf{r}, t) - \tau \partial_t \hat{\mathbf{E}} - (\mathbf{R} \cdot \nabla) \hat{\mathbf{E}}. \quad (5)$$

The time and space integrations in equation (4) then involve the Fourier transforms of Σ_s and Σ_1 , $\sigma_s(\mathbf{k}, \omega)$ and $\sigma(\mathbf{k}, \omega)$ (no index 1), the latter being a tensor, and the derivatives of σ_s with respect to ω and \mathbf{k} . This results in:

$$\left(\omega^2 - c^2 k^2 + \frac{i\omega}{\varepsilon_0} \sigma_s \right) \hat{\mathbf{E}} + \left(2i\omega - \frac{1}{\varepsilon_0} \frac{\partial(\omega \sigma_s)}{\partial \omega} \right) \partial_t \hat{\mathbf{E}} + \left(\left(2ic^2 \mathbf{k} + \frac{\omega}{\varepsilon_0} \nabla_{\mathbf{k}} \sigma_s \right) \cdot \nabla \right) \hat{\mathbf{E}} = -\frac{i\omega}{\varepsilon_0} \sigma(\mathbf{k}, \omega) \cdot \hat{\mathbf{E}}. \quad (6)$$

The term of dominant order in equation (6) is the first one. The two other terms on the left are of first order in $1/(\omega T)$ and $1/(kL)$ and the term on the right is also regarded as small. Equation (6) is satisfied at the dominant order when the factor of $\hat{\mathbf{E}}$ vanishes, which means that the electric field consists of fluctuations, the frequency of which is ω_k , the solution of the isotropic dispersion relation:

$$\omega^2 - c^2 k^2 + \frac{i\omega}{\varepsilon_0} \sigma_s(k, \omega) = 0. \quad (7)$$

The corresponding group velocity, \mathbf{v}_g , is obtained by differentiating equation (7) with respect to ω and k . When σ_s represents the dispersion due to a cold unmagnetized plasma, which we assume for simplicity, $\omega \sigma_s$ does not depend on ω nor on k . With these simplifications, the three sub-dominant terms in equation (6) reduce to:

$$(\partial_t + (\mathbf{v}_g \cdot \nabla)) \hat{\mathbf{E}} = -\frac{\sigma(\mathbf{k}, \omega_k) \cdot \hat{\mathbf{E}}}{2\varepsilon_0}, \quad (8)$$

where the amplitude $\hat{\mathbf{E}}$, which slowly varies with position and time, is only non-vanishing when the wave vector \mathbf{k} and the frequency ω_k are linked by the dispersion relation in equation (7). An equation for the correlation tensor of the electric field of this radiation, $\langle \hat{\mathbf{E}} \otimes \hat{\mathbf{E}}^* \rangle$ can be derived from equation (8) by tensorial multiplication by $\hat{\mathbf{E}}^*$, the superscript * denoting complex conjugation, and averaging over the statistical distribution of the phases (and possibly of the amplitudes) of the

components of $\hat{\mathbf{E}}$. This operation is represented by brackets. The electric field supposedly being transverse, it pertains the plane perpendicular to the propagation direction \mathbf{n} and may be represented by its components on two arbitrarily chosen unit basis vectors \mathbf{e}_1 and \mathbf{e}_2 in this plane. An intensity tensor with components I_{ij} relative to this basis that is proportional to the two-dimensional electric field correlation tensor must be defined such that it has the dimension of a specific intensity. The Stokes parameters of the radiation are related to this intensity tensor by

$$I_{ij} \equiv v_g \frac{k^2 dk}{d\omega_k} \begin{pmatrix} \varepsilon_0 \langle \hat{E}_1 \hat{E}_1^* \rangle & \varepsilon_0 \langle \hat{E}_1 \hat{E}_2^* \rangle \\ \varepsilon_0 \langle \hat{E}_2 \hat{E}_1^* \rangle & \varepsilon_0 \langle \hat{E}_2 \hat{E}_2^* \rangle \end{pmatrix} = \begin{pmatrix} I + Q & U + iV \\ U - iV & I - Q \end{pmatrix}. \quad (9)$$

The definition of the Stokes parameter V is a matter of convention which fixes its sign, since $\langle \hat{E}_1 \hat{E}_2^* \rangle$ could have been taken to be proportional to $U - iV$ instead. Shcherbakov & Huang (2011) use a convention opposite to ours. The transfer equation for the components I_{ij} can be deduced from equation (8) which writes, using the dummy index rule

$$(\partial_t + (\mathbf{v}_g \cdot \nabla)) I_{ij} = -\frac{1}{2\varepsilon_0} (\sigma_{ip} \delta_{jq} + \delta_{ip} \sigma_{jq}^*) I_{pq}. \quad (10)$$

By equation (9), the term on the right of equation (10) can be converted into the transfer matrix term in equation (1), some elements of which turn out to involve the hermitian (dissipative) part of the conductivity while others involve its anthermitian (non-dissipative) part. These parts are respectively defined by:

$$\sigma_{ij}^H = \frac{1}{2} (\sigma_{ij} + \sigma_{ji}^*), \quad \sigma_{ij}^A = \frac{1}{2} (\sigma_{ij} - \sigma_{ji}^*). \quad (11)$$

The elements of the transfer matrix in equation (1) are given in terms of these parts of the conductivity by:

$$\begin{aligned} K_{II} &= \frac{\mathcal{R}e(\sigma_{11}^H + \sigma_{22}^H)}{2\varepsilon_0}, & K_{IQ} &= \frac{\mathcal{R}e(\sigma_{11}^H - \sigma_{22}^H)}{2\varepsilon_0}, & K_{IU} &= \frac{\mathcal{R}e(\sigma_{12}^H)}{\varepsilon_0}, & K_{IV} &= \frac{\mathcal{I}m(\sigma_{12}^H)}{\varepsilon_0}, \\ K_{QU} &= \frac{\mathcal{R}e(\sigma_{12}^A)}{\varepsilon_0}, & K_{UV} &= \frac{\mathcal{I}m(\sigma_{22}^A - \sigma_{11}^A)}{2\varepsilon_0}, & K_{QV} &= \frac{\mathcal{I}m(\sigma_{12}^A)}{\varepsilon_0}. \end{aligned} \quad (12)$$

These matrix elements refer to the components of the local conductivity for the wave vector \mathbf{k} and frequency $\omega_{\mathbf{k}}$ related to it by the dispersion relation in equation (7). The relations in equation (12) between the transfer coefficients and the elements of the conductivity matrix agree with those in Shcherbakov & Huang (2011) given the relation between conductivity and dielectric tensors for perturbations varying as in equation (3) and accounting for the fact, mentioned above, that their definition of the Stokes parameter V differs from ours by a sign.

The polarization properties of the synchrotron emission are well known, both in vacuo (Westfold 1959) and in a cold plasma (Tsyvovitch 1950; Razin 1960; Ramaty 1968). The dissipative absorption coefficients K_{II} , K_{IQ} , K_{IU} , K_{IV} given in equation (12) in terms of the components of the hermitian part of the conductivity have also been presented in the literature (Ginzburg & Sirovatskii 1969; Sazonov 1969a). These components can be calculated using the same well-known approximations which also provide the emission coefficient. The dissipative absorption can be derived from the emission by Einstein's coefficients method, ignoring dispersion (Wild et al. 1963), or not (Zhelezniakov 1967).

The non-dissipative coefficients K_{QU} , K_{UV} , K_{QV} have proved more difficult to calculate. This paper concentrates on their calculation in the case of ultrarelativistic plasma particles immersed in a static uniform magnetic field \mathbf{B}_0 . The motion of the particles is described in the Vlasov approximation. We neglect the dispersive properties of a cold population that might be present, so that the dispersion relation (7) supposedly reduces to $\omega = ck$.

2.2 Formal solution for the high frequency conductivity tensor

The conductivity tensor is found by calculating the high frequency current \mathbf{J} resulting from a high frequency electric field \mathbf{E} by solving the linearized Vlasov equation for the perturbation $f(\mathbf{r}, \mathbf{p})$ of the distribution function,

$$\partial_t f + \mathbf{v} \cdot \nabla f + (q\mathbf{v} \times \mathbf{B}_0) \cdot \nabla_{\mathbf{p}} f = -q(\mathbf{E} + \mathbf{v} \times \mathbf{B}) \cdot \nabla_{\mathbf{p}} f_0, \quad (13)$$

where q is the charge (with its sign) of the particle species considered. In equation (13) $f_0(\mathbf{p})$ is the unperturbed homogeneous distribution function of the species considered, that only depends on the component p_{\parallel} of the particle's momentum along the magnetic field and on the modulus p_{\perp} of its component perpendicular to it, normalized to the density of particles, so that

$$\int_0^{\infty} \int_{-\infty}^{+\infty} 2\pi p_{\perp} dp_{\perp} dp_{\parallel} f_0(p_{\perp}, p_{\parallel}) = n, \quad (14)$$

where n is the volume density of this species of particles. The gradient with respect to position is denoted as ∇ and the gradient with respect to some other vectorial variable \mathbf{u} , such as the momentum \mathbf{p} , is denoted by $\nabla_{\mathbf{u}}$. The first three terms of equation (13) represent the time-derivative of f following the unperturbed particle's motion, described by the position and momentum $\mathbf{r}(t')$ and $\mathbf{p}(t')$ of this particle at time t' , following the unperturbed motion. At time t , the particle is at \mathbf{r} with

momentum \mathbf{p} . We then obtain the perturbation f by integrating in time the right hand side term of equation (13) following the unperturbed particle's motion, which gives

$$f(\mathbf{r}, \mathbf{p}, t) = -q \int_{-\infty}^t dt' (\mathbf{E}(\mathbf{r}(t'), t') + \mathbf{v}(t') \times \mathbf{B}(\mathbf{r}(t'), t') \cdot \nabla_{\mathbf{p}} f_0(\mathbf{p}(t'))). \quad (15)$$

The integration is over all times t' earlier than t . The unperturbed motion is easily expressed in a frame where \mathbf{B}_0 is along the Z axis so that $\mathbf{B}_0 = B_0 \mathbf{e}_Z$ and the two unit vectors \mathbf{e}_X and \mathbf{e}_Y are perpendicular to it, but otherwise unspecified. The velocity of a particle can be written as

$$\mathbf{v} = v_{\perp} \cos \phi \mathbf{e}_X + v_{\perp} \sin \phi \mathbf{e}_Y + v_{\parallel} \mathbf{e}_Z, \quad (16)$$

where v_{\perp} and v_{\parallel} are conserved by the unperturbed motion, as are also the modulus p of the momentum, the associated Lorentz factor γ and the particle's pitch angle ϑ . The angle ϕ , the gyration angle of the particle, rotates in time at the synchrotron frequency Ω_* , which for non-relativistic particles reduces to the cyclotron frequency Ω . These frequencies, which have the sign opposite to that of the charge, s_q , depend on the rest mass m of the particles and are given by

$$\Omega_* = -\frac{q B_0}{\gamma m}, \quad \Omega = -\frac{q B_0}{m}, \quad \text{and} \quad s_q = \text{sign}(q). \quad (17)$$

At a time $t' = t - \tau$ earlier than t , the components of the velocity of a freely-moving particle having at time t a gyration angle ϕ and a position X, Y, Z were

$$v_X(t - \tau) = v_{\perp}(t) \cos(\phi - \Omega_* \tau), \quad v_Y(t - \tau) = v_{\perp}(t) \sin(\phi - \Omega_* \tau), \quad v_Z(t - \tau) = v_{\parallel}(t). \quad (18)$$

The position of that particle at time $t - \tau$ was

$$X(t - \tau) = X - \frac{v_{\perp}}{\Omega_*} (\sin \phi - \sin(\phi - \Omega_* \tau)), \quad Y(t - \tau) = Y + \frac{v_{\perp}}{\Omega_*} (\cos \phi - \cos(\phi - \Omega_* \tau)), \quad Z(t - \tau) = Z - v_{\parallel} \tau. \quad (19)$$

The magnetic perturbation is related to the electric one by the Faraday equation, $\text{curl } \mathbf{E} = -\partial_t \mathbf{B}$. The perturbation in the distribution function which develops as a result of an electric field perturbation such as that in equation (3) can be written as $f(\mathbf{r}, \mathbf{p}, t) = \hat{f}(\mathbf{p}) \exp(i(\mathbf{k} \cdot \mathbf{r} - \omega t))$. It depends linearly on the perturbation field by equation (15) and can be expressed in terms of operators acting on the unperturbed distribution function, such as the anisotropy operator D , defined by:

$$D(f_0) = \left(v_{\perp} \frac{\partial f_0}{\partial p_{\parallel}} - v_{\parallel} \frac{\partial f_0}{\partial p_{\perp}} \right). \quad (20)$$

$D(f_0)$ vanishes for an isotropic distribution function. The wave vector \mathbf{k} is taken to be in the $X - Z$ plane and has components $k_X = k \sin \alpha$ and $k_Z = k \cos \alpha$, the propagation angle α being comprised between 0 and π . When fully expanded, the solution for \hat{f} can be written from equation (15) as

$$\begin{aligned} \hat{f}(\mathbf{p}) = & -\frac{q}{\omega} \int_0^{\infty} d\tau \exp \left(i \left((\omega - k_{\parallel} v_{\parallel}) \tau - \frac{k_{\perp} v_{\perp}}{\Omega_*} (\sin \phi - \sin(\phi - \Omega_* \tau)) \right) \right) \times \\ & \left[\left(\hat{E}_X \cos(\phi - \Omega_* \tau) + \hat{E}_Y \sin(\phi - \Omega_* \tau) \right) \left(\omega \frac{\partial f_0}{\partial p_{\perp}} + k_{\parallel} D(f_0) \right) + \hat{E}_Z \left(\omega \frac{\partial f_0}{\partial p_{\parallel}} - \cos(\phi - \Omega_* \tau) k_{\perp} D(f_0) \right) \right]. \end{aligned} \quad (21)$$

The associated Fourier coefficient of the current density is the average value of $q\mathbf{v}$ weighted by $\hat{f}(\mathbf{p})$. Using the solution for \hat{f} in equation (21), each component of the current appears to be a linear function of the electric field components \hat{E}_X , \hat{E}_Y and \hat{E}_Z from which the components of the conductivity tensor may be identified. Each one involves a fourfold integral on the variables p_{\parallel} , p_{\perp} , ϕ of the particle momentum and on the delay time τ . As can be seen in equation (21), integration over the delay time involves imaginary exponentials with an argument linear and trigonometric in τ . We refer to these integrals as phase integrals. Expanding the trigonometric functions of $(\phi - \Omega_* \tau)$ on the second line of equation (21) in imaginary exponentials, three phase integrals appear, that can be written as

$$P_{\varepsilon}(\omega, k_{\perp}, k_{\parallel}, \mathbf{v}) = \int_0^{\infty} d\tau \exp \left(i \left((\omega - k_{\parallel} v_{\parallel}) \tau - \frac{k_{\perp} v_{\perp}}{\Omega_*} (\sin \phi - \sin(\phi - \Omega_* \tau)) + \varepsilon(\phi - \Omega_* \tau) \right) \right). \quad (22)$$

The index ε may take the three values $(-1, 0, +1)$, or $(-, 0, +)$. At this point, it is necessary to take care of the sign of the charge, and to introduce dimensionless variables, simpler than those in equation (22), by:

$$x = \frac{k_{\perp} v_{\perp}}{|\Omega_*|}, \quad \sigma = \frac{\omega - k_{\parallel} v_{\parallel}}{|\Omega_*|}, \quad u = \frac{\omega}{|\Omega|}, \quad \sigma_0 = u \sin \alpha, \quad \varpi = \frac{ck_{\parallel} - v_{\parallel} k}{|\Omega_*|}. \quad (23)$$

The variables x (not a coordinate), σ and u are all positive and usually large since $\omega = ck \gg |\Omega|$. The variable ϖ , which plays the role of an angular variable, may be positive or negative. The modulus of ϖ assumes values of the same order as σ . The properties of the variables ϖ and σ , which may replace p_{\parallel} and p_{\perp} as dynamical variables of freely moving particles, are

detailed in Appendix A. From equation (21), the current density can be written in terms of the three phase integrals as:

$$\hat{\mathbf{J}} = -\frac{2\pi q^2}{\omega} \int_{-\infty}^{+\infty} dp_{\parallel} \int_0^{\infty} p_{\perp} dp_{\perp} \int_0^{2\pi} \frac{d\phi}{2\pi} \left[v_{\perp} \cos \phi \mathbf{e}_X + v_{\perp} \sin \phi \mathbf{e}_Y + v_{\parallel} \mathbf{e}_Z \right] \times \left[\frac{P_+ + P_-}{2} \left(\omega \frac{\partial f_0}{\partial p_{\perp}} + k_{\parallel} D(f_0) \right) \hat{E}_X + \frac{P_+ - P_-}{2i} \left(\omega \frac{\partial f_0}{\partial p_{\perp}} + k_{\parallel} D(f_0) \right) \hat{E}_Y + \left(P_0 \omega \frac{\partial f_0}{\partial p_{\parallel}} - \frac{P_+ + P_-}{2} k_{\perp} D(f_0) \right) \hat{E}_Z \right]. \quad (24)$$

3 RESULTS

We derive in section 4 the components of the conductivity tensor for a relativistic plasma at frequencies much higher than the gyrofrequency and carry out two out of the four integrals involved in equations (22) and (24). In particular cases, the corresponding quadrature may be pursued one step farther.

In this section we anticipate the polarization transfer coefficients and illustrate them for isotropic and anisotropic distributions.

3.1 Dissipation-less polarization transfer coefficients

3.1.1 Quasi exact expressions

We obtain in section 4.4 a general expression for the Faraday rotation and conversion coefficients f and h , defined $f = K_{QU}/c$ and $h = K_{UV}/c$, where K_{QU} and K_{UV} are given by equation (12). These coefficients can be explicitly written as in equations (86)–(87), which we reproduce here neglecting the principal value terms that are shown in section 4.4 to be safely negligible. These equations are therefore almost exact. They can be written as

$$f = -\frac{2\pi^2 s_q}{c} \frac{\omega_{\text{pr}}^2 \Omega^2}{\omega^3} \iint \frac{m^3 c^3}{\sin^2 \alpha} d\varpi d\sigma \varpi x \frac{\partial F_0}{\partial \sigma} \left[J'_{\sigma}(x) N_{\sigma}(x) + \frac{1}{\pi x} \right], \quad (25)$$

$$h = \frac{\pi^2 \omega_{\text{pr}}^2 \Omega^2}{c \omega^3} \iint \frac{m^3 c^3}{\sin^2 \alpha} d\varpi d\sigma \left[\frac{\partial F_0}{\partial \sigma} (x^2 J'_{\sigma}(x) N'_{\sigma}(x) - \varpi^2 J_{\sigma}(x) N_{\sigma}(x)) + \frac{1}{\pi} \left(\varpi \frac{\partial F_0}{\partial \varpi} - \sigma \frac{\partial F_0}{\partial \sigma} \right) \right]. \quad (26)$$

The particle's dynamical variables ϖ and σ , defined in equation (23), incorporate properties of the radiation of interest. Much of the dependence of f and h on the propagation angle α and on the frequency is in fact hidden in these variables. The distribution function F_0 is normalized to unity (in the sense of equation (75) below), the particle density n being implicit in the square of the specie's plasma frequency $\omega_{\text{pr}}^2 = nq^2/m\epsilon_0$. The integrals in equations (25) and (26) involve two-variable kernels in which one of the variables, σ , appears as a continuous Bessel function index. This index is larger than their argument x , as can be seen from equation (23), but possibly not much larger, which complicates the search for suitable approximations.

There are essentially two very different regimes, defined in section 5, for the wave-particle interaction which we refer to as non-resonant (NR) and quasi-resonant (QR). Different particles make very different contributions to the transfer coefficients depending on whether they interact in the NR or in the QR regime. Equations (25) and (26) however encompass all regimes, being written in a form that does not require any regioning of the ϖ - σ domain for their evaluation. The domain of validity of specific approximations, non-resonant or quasi-resonant, to the functions in equations (25) and (26) are different and complementary (figure 6).

3.1.2 High-frequency limit (HF)

It is shown in section 5.1 that when the inequality

$$\frac{3\gamma^2 \sin \alpha |\Omega|}{\omega} < 1 \quad (27)$$

holds true, only the non-resonant domain, defined in that section, contributes to the transfer coefficients. For a given value of the Lorentz factor γ , the inequality (27) is satisfied when the radiation's frequency ω exceeds the characteristic synchrotron frequency $\omega_c(\gamma, \alpha)$ for particles of this energy travelling in the direction of the radiation (equation (101)). We therefore refer to this situation as the high-frequency limit. When all particles in the distribution interact with the wave in this regime, the integration on the non-resonant domain actually extends over the full ϖ - σ domain. In this case, the Faraday coefficients f and h result from equations (115) and (119), expanded to the first non-vanishing order in Ω/ω :

$$f_{\text{HF}} = 2\pi s_q \frac{\omega_{\text{pr}}^2 \Omega^2}{c \omega^3} \iint \frac{m^3 c^3}{\sin^2 \alpha} d\varpi d\sigma \left(\frac{\varpi x^2}{2(\sigma^2 - x^2)^{3/2}} \right) \frac{\partial F_0}{\partial \sigma}. \quad (28)$$

$$h_{\text{HF}} = -\pi \frac{\omega_{\text{pr}}^2 \Omega^2}{c \omega^3} \iint \frac{m^3 c^3}{\sin^2 \alpha} d\varpi d\sigma \left(\frac{2x^4(\sigma^2 - x^2) + \sigma_0^2 x^2(4\sigma^2 + x^2)}{8(\sigma^2 - x^2)^{7/2}} \right) \frac{\partial F_0}{\partial \sigma}. \quad (29)$$

Equations (28) and (29) do not assume isotropy of the distribution function F_0 but are only valid when the quasi-resonant contribution can be neglected, which makes them less general than equations (25)–(26).

3.1.3 Medium-frequency (MF): cutting through the quasi-resonant domain

The integration over the non-resonant domain cannot be extended to the full domain when the inequality in equation (27) is not satisfied for a non-negligible number of particles in the distribution. This arises in particular when the parameter on the left of equation (27) is of order unity, which we refer to as a medium-frequency situation. A slightly more sophisticated approach is then needed, which we now describe. The double quadratures in equations (28)–(29) should in this case be extended over the non-resonant (NR) domain only and the contribution of the quasi-resonant (QR) domain should be added to it. When it is not dominant, the integral over the QR domain may be approximately evaluated. Our proposed approximation rests on separating the non-resonant from the quasi-resonant domain, and expressing the integral over the quasi-resonant one by using a very simple approximation. The boundary \mathcal{B}_{QR} between the NR and QR regions is where the variable g defined in equation (94) below is near unity. Since $x \approx \sigma$ in the vicinity of this limit, \mathcal{B}_{QR} is represented in the ϖ – σ plane by the equation

$$B_{\text{QR}}(\varpi, \sigma) \equiv \varpi^2 - 3^{2/3} \sigma^{4/3} + \sigma_0^2 = 0. \quad (30)$$

The sign of $B_{\text{QR}}(\varpi, \sigma)$ tells whether the point ϖ – σ is in the non-resonant domain ($B_{\text{QR}} > 0$) or in the quasi-resonant one ($B_{\text{QR}} < 0$). The QR domain is then cut out of the ϖ – σ domain, the remainder constituting the properly-defined NR domain. The kernels of the integrands in equations (28)–(29) are kept at their non-resonant values when in the NR domain. For perfect accuracy, the kernels in the QR region should be taken to be those in equations (99)–(100). When however the QR region does not contribute predominantly, these complicated kernels can be replaced by simple approximations. Their effect essentially being to limit the growth of the modulus of the non-resonant kernels when the QR region is reached, we replace them by linear interpolations in ϖ , at fixed σ , between the values of the non-resonant kernels evaluated on the border \mathcal{B}_{QR} for that value of σ . Let $\Theta_{\text{H}}(y)$ denote the Heaviside function, equal to unity for positive argument y and zero otherwise. The above-described approximations to f and h can be written as:

$$f_{\text{MF}} = 2\pi s_q \frac{\omega_{\text{pr}}^2 \Omega^2}{c \omega^3} \iint \frac{m^3 c^3}{\sin^2 \alpha} d\varpi d\sigma \varpi \left[\Theta_{\text{H}}^+ \frac{x^2}{2(\sigma^2 - x^2)^{3/2}} + \Theta_{\text{H}}^- \frac{x_{\text{QR}}^2}{2(\sigma^2 - x_{\text{QR}}^2)^{3/2}} \right] \frac{\partial F_0}{\partial \sigma}, \quad (31)$$

$$h_{\text{MF}} = -\pi \frac{\omega_{\text{pr}}^2 \Omega^2}{c \omega^3} \iint \frac{m^3 c^3}{\sin^2 \alpha} d\varpi d\sigma \left[\Theta_{\text{H}}^+ \frac{2x^4(\sigma^2 - x^2) + \sigma_0^2 x^2(4\sigma^2 + x^2)}{8(\sigma^2 - x^2)^{7/2}} + \Theta_{\text{H}}^- \frac{2x_{\text{QR}}^4(\sigma^2 - x_{\text{QR}}^2) + \sigma_0^2 x_{\text{QR}}^2(4\sigma^2 + x_{\text{QR}}^2)}{8(\sigma^2 - x_{\text{QR}}^2)^{7/2}} \right] \frac{\partial F_0}{\partial \sigma}. \quad (32)$$

where $\Theta_{\text{H}}^{\pm} = \Theta_{\text{H}}(\pm B_{\text{QR}}(\varpi, \sigma))$ and $\varpi_{\text{QR}}(\sigma)$ and $x_{\text{QR}}(\sigma)$ are the values of $|\varpi|$ and x on the boundary \mathcal{B}_{QR} for the given value of σ (equation (30)). Equations (31) and (32) provide approximate values of the transfer coefficients f and h valid for isotropic as well as for non-isotropic distribution functions. The approximations in equations (31) and (32) will be illustrated on the example of a thermal distribution function in section 3.2.4.

3.1.4 Low-frequency limit(LF)

When the reverse inequality to equation (27) applies in a strong sense, both the non-resonant and quasi-resonant domains contribute to the transfer coefficients. For a given frequency and a given propagation angle, α , this essentially happens when the dynamical variable σ of the particle is above the limit defined by equation (30) for $\varpi = 0$ or when its Lorentz factor γ largely exceeds the threshold defined by the reverse of inequality (27), which happens when the frequency ω is much less than the critical synchrotron frequency, for a particle of Lorentz factor γ travelling in the direction of the considered radiation (equation (101)). We refer to this situation as the low-frequency limit. The low-frequency contribution to the Faraday coefficients comprises both NR and QR parts, which we calculate for isotropic distributions in sections 6.3 and 6.4.

3.2 Kernels of polarization transfer coefficients for isotropic distribution functions

Let us illustrate how to use equations (25) and (26) on isotropic models of the distribution function. When the distribution function is isotropic, it depends only on the Lorentz factor γ of the particles, but nevertheless depends on both variables ϖ and σ . When dealing with isotropic distribution functions, it is therefore wise to change from the variables ϖ, σ to the variables ϖ, γ . Integrating over ϖ , which then does not involve the distribution function, equations (25) and (26) can be written in the general form

$$f = \frac{\omega_{\text{pr}}^2 \Omega^2}{c \omega^3} m^3 c^3 \int_1^\infty d\gamma \frac{dF_0}{d\gamma} F^{\text{iso}}(\gamma), \quad h = \frac{\omega_{\text{pr}}^2 \Omega^2}{c \omega^3} m^3 c^3 \int_1^\infty d\gamma \frac{dF_0}{d\gamma} H^{\text{iso}}(\gamma), \quad (33)$$

where $F^{\text{iso}}(\gamma)$ and $H^{\text{iso}}(\gamma)$ are one-variable kernels for isotropic distribution functions.

3.2.1 Isotropic distributions in the high-frequency limit

In the high-frequency limit, the integration over ϖ in equations (28)–(29), which defines these kernels, extends, for a given value of γ , over the full domain. The kernels F^{iso} and H^{iso} can then be written in this case as

$$F_{\text{HF}}^{\text{iso}}(\gamma) = \frac{2\pi s_q}{\sin^2 \alpha} \int_{\varpi_-}^{\varpi_+} d\varpi \left(\frac{\varpi x^2}{2(\sigma^2 - x^2)^{3/2}} \right). \quad (34)$$

$$H_{\text{HF}}^{\text{iso}}(\gamma) = -\frac{\pi}{\sin^2 \alpha} \int_{\varpi_-}^{\varpi_+} d\varpi \left(\frac{2x^4(\sigma^2 - x^2) + \sigma_0^2 x^2(4\sigma^2 + x^2)}{8(\sigma^2 - x^2)^{7/2}} \right). \quad (35)$$

The variables σ , x and $(\sigma^2 - x^2)$ can be expressed from equation (A2) in terms of γ , ϖ and parameters in equation (23) as

$$\sigma = \gamma u \sin^2 \alpha + \varpi \cos \alpha, \quad x^2 = (u^2(\gamma^2 \sin^2 \alpha - 1) + 2\gamma u \varpi \cos \alpha - \varpi^2) \sin^2 \alpha, \quad \sigma^2 - x^2 = \varpi^2 + u^2 \sin^2 \alpha. \quad (36)$$

The boundaries $\varpi_-(\gamma)$ and $\varpi_+(\gamma)$ of the integration over ϖ at a given γ are the abscissas of the intersection of the line of constant γ with the boundary of the physical domain in the ϖ - σ plane (figure A1). Since this boundary is where $x = 0$, equation (36) implies that

$$\varpi_{\pm}(\gamma) = u \left(\gamma \cos \alpha \pm \sqrt{\gamma^2 - 1} \right), \quad (37)$$

The integration over ϖ in equations (34) and (35) plays the role of an angular integration. It can be performed analytically, the results, valid at high frequency, eventually being

$$F_{\text{HF}}^{\text{iso}}(\gamma) = 4\pi s_q \frac{\omega \cos \alpha}{|\Omega|} \left(\gamma \mathcal{L}(\gamma) - \sqrt{\gamma^2 - 1} \right), \quad \text{where} \quad \mathcal{L}(\gamma) = \cosh^{-1}(\gamma) = \ln \left(\sqrt{\gamma^2 - 1} + \gamma \right), \quad (38)$$

$$H_{\text{HF}}^{\text{iso}}(\gamma) = -\pi \frac{\sin^2 \alpha}{2} \left(\gamma \sqrt{\gamma^2 - 1} (2\gamma^2 - 3) + \mathcal{L}(\gamma) \right). \quad (39)$$

3.2.2 Isotropic distributions in the low-frequency limit

It comes out of the discussion in section 5.4 that the coefficient of Faraday rotation f does not depart much from its non-resonant approximation, although corrections are necessary for a quantitative agreement in low-frequency situations. We find in section 6 that the isotropic kernel for f can be written in the low-frequency limit as

$$F_{\text{LF}}^{\text{iso}}(\gamma) = \pi s_q \frac{\omega \cos \alpha}{|\Omega|} \gamma \left(\frac{4}{3} \ln \left(\frac{\gamma u}{\sin \alpha} \right) - 1.26072439 \right). \quad (40)$$

By contrast, the Faraday conversion coefficient h drastically differs from its high-frequency expression when there is a quasi-resonant contribution. The kernel of this coefficient is derived in section 6.3 in the low-frequency limit and for an isotropic distribution function. It can then be written as:

$$H_{\text{LF}}^{\text{iso}}(\gamma) = \frac{\pi}{8} \left(\frac{\omega^2 \sin \alpha}{\Omega^2} \right)^{2/3} \left(4 - \frac{1}{3^{4/3}} \right) \gamma^{4/3}. \quad (41)$$

3.2.3 Exact isotropic kernels and composite approximations to them

The results in sections 3.2.1 and 3.2.2 apply in different regions of the energy space. For distributions with only very few particles in the low-frequency regime, the high-frequency approximation is sufficient. When the distribution is more extended in energy than the threshold γ_{qr} defined in equation (98), the kernels should account for the QR contribution in the LF regime. They may then be calculated by integrating over ϖ at fixed γ the right hand sides of equations (25)–(26). This however requires a double numerical integration. Section 6.5 proposes an approximate formula interpolating between the HF expression of these kernels, valid when $\gamma < \gamma_{\text{qr}}$, and their asymptotic LF expressions, valid for $\gamma \gg \gamma_{\text{qr}}$. Huang & Shcherbakov (2011) adopt a similar approach by providing fits to their numerically computed kernels and claim similar accuracy.

For extended energy distributions, the region at $\gamma \sim \gamma_{\text{qr}}$ should not dominantly contribute to integrals such as those in equation (33). These interpolation formulae then provide about 10% accuracy on h for power law distributions and slightly better accuracy on f . When on the contrary the energy range close to γ_{qr} is determinant, the medium frequency approximations in equations (31)–(32) could be used instead or, if accurate results are needed, the transfer coefficients would be numerically calculated from equations (25) and (26) by double-integrating over the variables ϖ and σ .

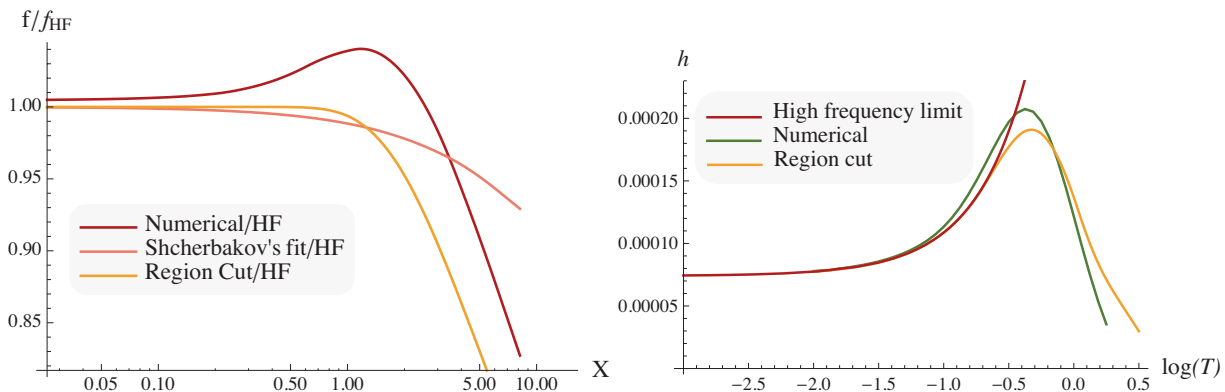


Figure 1. *Left:* ratio to the high frequency expression $f_{\text{HF}}^{\text{th}}$ in equation (43) of resp. the numerically-computed value of the thermal Faraday rotation coefficient f^{th} for the isothermal model of equation (42), based on equation (25), the fit formula provided for it by Shcherbakov (2008) and the region-cut approximation in equation (31), as labeled. These ratios are displayed as a function of the scaling parameter X introduced by Shcherbakov (2008), defined in equation (47). *Right:* the high frequency limit of the Faraday conversion coefficient h^{th} from equation (43), the region-cut formula from equation (32) and the almost exact value numerically computed from equation (25), as a function of the temperature, T (as labeled). In both cases, the region-cut procedure around the resonant particles seems to improve significantly the domain of validity of the match to the exact transfer coefficients.

3.2.4 Illustrations and comparison to known results

Previous approaches to polarization transfer coefficients

The polarization transfer coefficients for a thermal distribution have been previously derived exactly, by a method entirely different from ours, in a form that eventually requires only one numerical quadrature (Trubnikov 1958). It is therefore of interest to test different approximate results against this exact result, or against results proposed for the thermal case by different authors. Trubnikov (1958) considers a Jüttner distribution, as in equation (42) below. The conductivity is derived by integrating the changes of the perturbed distribution function over the delay time along unperturbed trajectories, just as we did in section 2, then taking suitable moments of the components of momentum. The exponential dependence of the Jüttner distribution on energy can be associated to the complex exponential that arises from the evolution over time of the phase functions, as in equation (57). The integration over the particle's energy can then be carried out, yielding a result that involves a modified Bessel function of the second kind of a complex argument depending on the delay time (Melrose 1997a; Shcherbakov & Huang 2011). The integration over the delay time then remains to be carried out. This can be done by different numerical strategies (Shcherbakov & Huang 2011; Huang & Shcherbakov 2011), yielding exact results. Else, it can be carried out analytically in an approximate way in different limits (Melrose 1997c; Shcherbakov 2008) or by using the method of stationary phase (Melrose 1997d). Huang & Shcherbakov (2011) have extended this approach to other distribution functions, the integration with respect to delay time being performed first for a given value of the Lorentz factor. These authors numerically calculate transfer coefficients for Dirac distributions in energy and provide fitting formulae for the kernels of Faraday rotation and conversion. The coefficients for arbitrary isotropic distributions may be obtained by a further integration over energy. Examples are provided for power law distributions covering a finite energy interval and for thermal distributions. In the next sections we compare our results for a thermal distribution to results obtained by these approaches.

Polarization transfer coefficients for a thermal distribution in the high-frequency limit

Following Shcherbakov (2008) we express the thermal Jüttner distribution as

$$F_0(\gamma) = \frac{\exp(-\gamma/T)}{4\pi m^3 c^3 T K_2(T^{-1})}, \quad \text{normalized so that} \quad \int 4\pi \gamma \sqrt{\gamma^2 - 1} m^3 c^3 F_0(\gamma) d\gamma = 1. \quad (42)$$

where T is the ratio of the thermal energy to the rest mass energy of the particles. By Trubnikov's method, Shcherbakov (2008) finds the following polarization transfer coefficients in the high-frequency limit

$$f_{\text{HF}}^{\text{th}} = \frac{\Omega \cos \alpha \omega_{\text{pr}}^2 K_0(T^{-1})}{c \omega^2 K_2(T^{-1})}, \quad \text{and} \quad h_{\text{HF}}^{\text{th}} = \frac{\Omega^2 \sin^2 \alpha \omega_{\text{pr}}^2 (K_1(T^{-1}) + 6TK_2(T^{-1}))}{2c\omega^3 K_2(T^{-1})}, \quad (43)$$

where K_1 and K_2 are modified Bessel functions of the second kind. In this high-frequency limit his results are identical to ours. To compare them, we evaluate f and h from equations (38)–(39), also valid in this limit, considering the case of an electronic population, so that $s_q = -1$. The f coefficient, derived from equations (33) and (38), becomes in this case

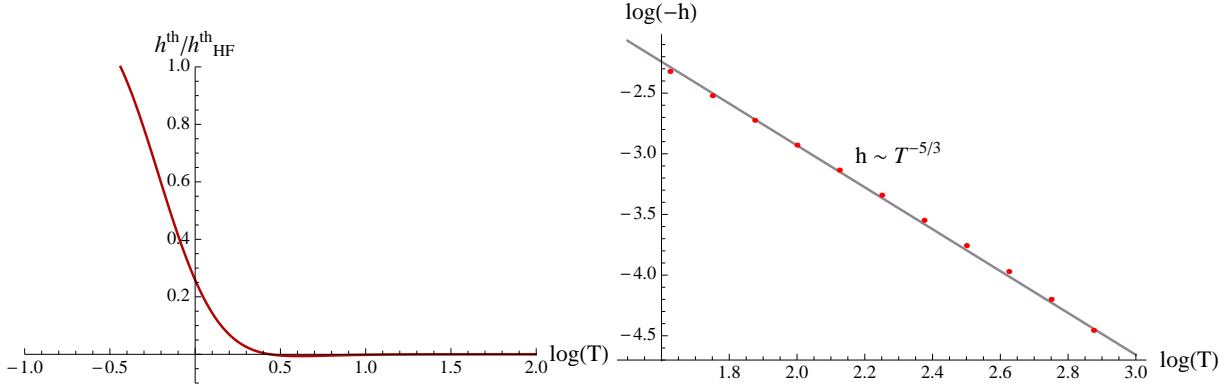


Figure 2. *Left:* The evolution with temperature T of the ratio of h^{th} to its high-frequency approximation $h_{\text{HF}}^{\text{th}}$. *Right:* The evolution of $\log|h|$ versus $\log T$. The $T^{-5/3}$ asymptote at large T is a direct consequence of the $\gamma^{4/3}$ asymptotic behaviour of the isotropic kernel of the Faraday coefficient h at large γ .

$$f_{\text{HF}}^{\text{th}} = \frac{\Omega \cos \alpha \omega_{\text{pr}}^2}{c \omega^2} \frac{1}{T^2 K_2(T^{-1})} \int_1^\infty d\gamma e^{-\gamma/T} \left(\gamma \mathcal{L}(\gamma) - \sqrt{\gamma^2 - 1} \right). \quad (44)$$

Keeping the integrand part in $\sqrt{\gamma^2 - 1}$ untouched, the term $\gamma \mathcal{L}(\gamma) \exp(-\gamma/T)$ is integrated by parts, giving successively

$$\int_1^\infty d\gamma \gamma \mathcal{L}(\gamma) e^{-\gamma/T} = T^2 \int_1^\infty d\gamma \frac{e^{-\gamma/T}}{\sqrt{\gamma^2 - 1}} + T \int_1^\infty d\gamma \frac{\gamma}{\sqrt{\gamma^2 - 1}} e^{-\gamma/T} = T^2 K_0(T^{-1}) + \int_1^\infty d\gamma \sqrt{\gamma^2 - 1} e^{-\gamma/T}, \quad (45)$$

where the last equality has been obtained again by integrating by parts the second integral of the middle part. Substituting this into equation (44), we recover f^{th} in equation (43). Starting from equations (33) and (39) for $h_{\text{HF}}^{\text{iso}}$ we similarly recover $h_{\text{HF}}^{\text{th}}$ in equation (43) by noting that $\int d\gamma \mathcal{L}(\gamma) \exp(-\gamma/T) = T K_0(T^{-1})$ and that

$$\int_1^\infty d\gamma \gamma (2\gamma^2 - 3) \sqrt{\gamma^2 - 1} e^{-\gamma/T} = T (-K_2(T^{-1}) + 6T K_3(T^{-1})) = -T K_0(T^{-1}) + 4T^2 (K_1(T^{-1}) + 6T K_2(T^{-1})). \quad (46)$$

Polarization transfer coefficients for a thermal distribution in the medium-frequency regime

Stepping out of the domain of validity of the high-frequency approximation, Figure 1 comparatively illustrates the behaviour of different approximations to the polarization coefficients by representing their high frequency approximations (43) and contrasting them to the numerical estimation of their exact counterparts (equations (25) and (26)) and to the fits provided by Shcherbakov (2008) to describe this regime. The difference between the approximations to f^{th} being small, the left panel of Figure 1 represents their ratio to their HF approximation. These ratios are displayed as a function of the parameter

$$X = T \left(10^3 \sqrt{2} \sin \alpha / u \right)^{1/2}, \quad (47)$$

defined in Shcherbakov (2008), which is proportional to the square root of the left hand side of the inequality in equation (27). The right panel of Figure 1 shows the corresponding approximations to h^{th} as a function of temperature, the quantity represented in this case being the coefficient itself. This figure uses the following fiducial parameters $m = c = 1$, $\alpha = \pi/4$, $u = 15$. It is found that the region-cut approximation to the intermediate regime discussed in Section 3.1 and represented by the expressions in equations (31) and (32) provides a good extension of these coefficients to higher temperatures where the high-frequency limit becomes insufficient.

Polarization transfer coefficients for a thermal distribution in the low-frequency limit

As an illustration of equation (41) let us consider again the Isothermal distribution, equation (42). It follows that when most particles interact with the radiation in the low-frequency regime we expect

$$h_{\text{LF}}^{\text{th}} \propto -\frac{1}{8\pi} \left(\frac{1}{T} \right)^{5/3} \Gamma \left(\frac{7}{3} \right), \quad (48)$$

which corresponds indeed to the asymptotic behaviour that can be computed numerically (using the Olver uniform expansion, see section 6.2 and Appendix G), as shown on figure 2.

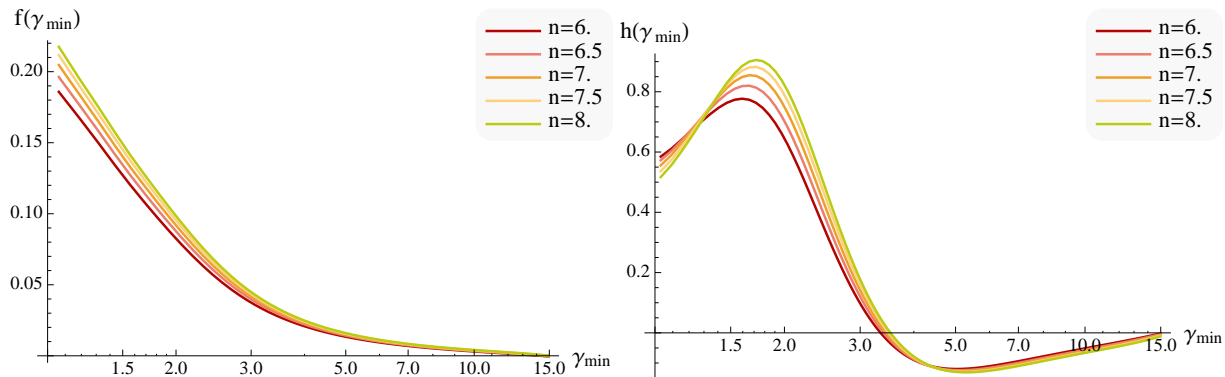


Figure 3. Polarization transfer coefficients (left: $f_{\text{iso}}^{\text{pl}}$ and right: $h_{\text{iso}}^{\text{pl}}$) for an isotropic power law distribution function as a function of the low energy cutoff γ_{min} for different values of the power law index n , as labeled. The coefficient f is normalized to $-\pi s_d \cos \alpha (\omega_{\text{pr}}^2 |\Omega| / c\omega^2)$ and h to $\omega_{\text{pr}}^2 \Omega^2 / c\omega^3$. This figure has been produced by numerically integrating equations (25)–(26) over ϖ and σ for the distribution (49).

Polarization transfer coefficients for an isotropic power law distribution function

Let us also consider a power law distribution scaling like γ^n with a low-energy cutoff γ_m , such as:

$$F_0(\gamma) = \frac{\Theta_{\text{H}}(\gamma - \gamma_m)}{N(\gamma_m, n) \gamma^n}. \quad (49)$$

For an isotropic distribution, assuming $n > 3$ for convergence, the normalization factor $N(\gamma_m, n)$ results from equation (42)

$$\frac{4\pi m^3 c^3}{N(\gamma_m, n)} \int_{\gamma_m}^{\infty} \frac{\sqrt{\gamma^2 - 1} \gamma d\gamma}{\gamma^n} = 1. \quad (50)$$

The Faraday coefficients can be expressed for such distribution functions in terms of a γ -dependent kernel as in equations (33). The low-energy cutoff introduces a Dirac-type singularity in the derivative $dF_0/d\gamma$ at γ_m , that should be taken care of when equations (33) are used. Alternatively, these relations may be integrated by parts, the integrated term vanishing because F_0 vanishes at infinity and the kernels do at $\gamma = 1$.

The figure 3 shows the polarization transfer coefficients for power-law distributions of various exponents as a function of the low-energy cutoff γ_{min} . These coefficients have been numerically calculated from equations (25)–(26) by integrating over ϖ and σ for the distribution (49), using equation (A1) to express γ in terms of σ and ϖ .

Approximations to the one-variable kernels could have been used instead. We derive in section 6.5 approximations to $F^{\text{iso}}(\gamma)$ and $H^{\text{iso}}(\gamma)$ obtained by interpolating between their high-frequency expressions and their asymptotic low-frequency limits. They provide results of reasonable, though limited, accuracy, but conveniently reduce the calculation to a simple one-variable quadrature. The figure L1 in appendix L compares the results in figure 3 with those obtained from these approximations. Equations (33), (50) and (40) indicate that f^{pl} scales for large γ_m as $\ln(\gamma_m)/\gamma_m^2$.

In a distribution that is extended in energy, particles of Lorentz factor γ less than the upper limit γ_{qr} defined by equation (27) contribute in the high-frequency regime, as in equations (38) and (39), while particles of a larger Lorentz factor bring a quasi-resonant contribution that should be added to their non-resonant one. For $\gamma \gg \gamma_{\text{qr}}$, these two contributions add to form the asymptotic low-frequency contribution to the coefficients in equations (40) and (41). The QR contribution to the coefficient f is small but does not vanish, being the integral of an almost odd function over an interval almost symmetrical with respect to zero (appendix J). The isotropic low-frequency kernel that results for f has been derived in section 6 and is shown in equation (130).

3.3 Polarization transfer coefficients for anisotropic distribution functions

The high-frequency results in equations (28) and (29) make no assumption about the isotropy, or otherwise, of the distribution function F_0 . But for the work of Melrose (1997b) on anisotropic thermal plasmas, there does not seem to be any other result published so far in the literature on general anisotropic distributions. Huang & Shcherbakov (2011) give results and fits for a number of isotropic distribution functions, including monoenergetic ones. The form in which our results are obtained allows to calculate transfer coefficients in the high-frequency approximation not only for isotropic distribution functions but also for a large class of anisotropic ones, providing the first terms of an expansion of the anisotropy in multipoles. Strong anisotropies still demand a two-variable quadrature, as exemplified by the beam model below. Stepping out of the high-frequency limit in

this case would provide one-variable quadratures that are no simpler than the two-variable ones from which they originate. We therefore restrict in this section to high-frequency results for different anisotropic distribution functions.

3.3.1 Quadrupolar and higher multipolar anisotropies at high frequency

Let us parametrize quadrupolar-type anisotropic distribution functions as the product of a function of the Lorentz factor γ of the particles by a second order Legendre function of the cosine of the particle's pitch angle ϑ , defined such that $p_{\parallel} = p \cos \vartheta$:

$$F(\gamma, \vartheta) = F_2(\gamma)P_2(\cos \vartheta). \quad (51)$$

For such distributions it is best to switch to the spherical coordinates γ and ϑ . The σ - and ϖ -derivatives of the distribution function in equations (25)–(26) or in equations (28)–(29) always separate into the sum of two terms, one of which is proportional to $dF_2/d\gamma$ and the other is proportional to F_2 . Generically, owing to the factorization property of the distribution function as in equation (51), the transfer coefficient could be written, for example in the case of the Faraday rotation coefficient f , as

$$f_{\text{HF}}^{\text{aniso}} = A_f \int_1^{\infty} \gamma d\gamma \left(\frac{dF_2}{d\gamma} D'_f(\gamma, \mu) + F_2(\gamma)D_f(\gamma, \mu) \right), \quad (52)$$

where A_f is a constant factor, still dependent on ω and α , and the functions respectively multiplying $F_2'(\gamma)$ and $F_2(\gamma)$, $D'_f(\gamma, \mu)$ and $D_f(\gamma, \mu)$, depend on γ and on the parameter $\mu = \cos \alpha$, α being the propagation angle of the radiation (figure 5). Similar quantities referring to the coefficient h can be defined. From equations (28), (29), using equations (36) and (A1), it follows after integration over ϑ that, for the quadrupolar model in equation (51)

$$\begin{aligned} f_{\text{HF}}^{\text{aniso}} = & \pi s_q \frac{\omega_{\text{pr}}^2 |\Omega|}{c\omega^2} m^3 c^3 \int \gamma d\gamma \frac{dF_2}{d\gamma} \left(\frac{4\mathcal{L}(\gamma)(3(2\gamma^2+3)P_3(\mu) - (\gamma^2-1)\mu)}{5(\gamma^2-1)} + \frac{4((\gamma^2-1)\mu - (11\gamma^2+4)P_3(\mu))}{5\gamma\sqrt{\gamma^2-1}} \right) \\ & + \pi s_q \frac{\omega_{\text{pr}}^2 |\Omega|}{c\omega^2} m^3 c^3 \int \gamma d\gamma F_2(\gamma) \left(\frac{6\mathcal{L}(\gamma)(2(\gamma^4-1)\mu - (2\gamma^4+15\gamma^2+3)P_3(\mu))}{5\gamma(\gamma^2-1)^2} + \frac{(34\gamma^2+86)P_3(\mu) - 24(\gamma^2-1)\mu}{5(\gamma^2-1)^{3/2}} \right), \end{aligned} \quad (53)$$

and

$$\begin{aligned} h_{\text{HF}}^{\text{aniso}} = & \pi \frac{\omega_{\text{pr}}^2 \Omega^2}{c\omega^3} m^3 c^3 \int \gamma d\gamma F_2(\gamma) \left(\frac{\mathcal{L}(\gamma)((24\gamma^2+5)P_2(\mu) - 12(2\gamma^2+1)P_4(\mu) + 7)}{7(\gamma^2-1)^2} - \frac{7(-6\gamma^4+17\gamma^2+4) + 5(18\gamma^4+65\gamma^2+4)P_2(\mu) - 12(4\gamma^4+37\gamma^2+4)P_4(\mu)}{105\gamma(\gamma^2-1)^{3/2}} \right) \\ & + \pi \frac{\omega_{\text{pr}}^2 \Omega^2}{c\omega^3} m^3 c^3 \int \gamma d\gamma \frac{dF_2}{d\gamma} \left(\frac{\mathcal{L}(\gamma)(14\gamma^2 - 108\gamma^2 P_4(\mu) + (94\gamma^2 - 7)P_2(\mu) + 7)}{42\gamma(\gamma^2-1)} + \frac{7(4\gamma^4 - 8\gamma^2 + 19) + 5(-20\gamma^4 + 76\gamma^2 + 31)P_2(\mu) + 36(2\gamma^4 - 9\gamma^2 - 8)P_4(\mu)}{210\sqrt{\gamma^2-1}} \right). \end{aligned} \quad (54)$$

Equations (53) and (54) are analytical expressions, valid in the high-frequency limit, for the Faraday coefficients f and h for an anisotropic distribution function of the form (51). Appendix I gives the corresponding coefficients D'_f and D_f for higher multipoles of the form $F_n(\gamma)P_n(\mu)$ for $n = 0, 1 \dots 6$. Any axisymmetric distribution $F(\gamma, \vartheta)$ can be represented as a linear combination of such functions, as $F(\gamma, \vartheta) = \sum_n F_n(\gamma)P_n(\cos \vartheta)$. Since the conductivity depends linearly on the unperturbed distribution function, the conductivity of a sum of functions is the sum of the corresponding conductivities. In each individual term, neither the multipole “distribution function” $F_n(\gamma)$ nor the angular factor $P_n(\cos \vartheta)$ need to be positive. The only constraint is that the sum over n be positive for any γ and ϑ .

As expected, the coefficients f and h depend on the direction of propagation α in a different manner than those associated to an isotropic distribution function given in equations (38)–(39). For a quadrupolar distribution, f varies with α as a combination of $P_1(\cos \alpha)$ and $P_3(\cos \alpha)$ while h varies as a combination of $P_2(\cos \alpha)$ and $P_4(\cos \alpha)$.

3.3.2 Beam model at high frequency

Let us consider now an anisotropic distribution representing a beam. Since theory is constructed for particles, the unperturbed motion of which is ruled only by the static magnetic field in the chosen frame of reference, the beam must be assumed to propagate parallel to the magnetic field. Otherwise, for example for winds propagating at an angle to the magnetic field, a static convection electric field would also be present in the observer's frame and the calculation in section 2.2 would then have to be revisited or the Stokes parameters transformed from the beam proper frame to the observer's frame. We form the beam distribution F_{\star} by boosting an isothermal distribution, so that

$$F_{\star}(\gamma, \theta) \propto \exp(-\gamma_{\star}(p, \theta)/T), \quad \text{where } \gamma_{\star}(p, \theta) \text{ obeys } c^2 m^2 \gamma_{\star}^2(p, \theta) = c^2 m^2 + (p_{\star} + p \cos(\theta))^2 + p^2 \sin^2(\theta). \quad (55)$$

For such a distribution, the derivative of F_{\star} w.r.t. σ entering equations (28)–(29) is given by

$$\frac{\partial F_{\star}}{\partial \sigma} = -F_{\star} \frac{|\Omega|}{T \omega \gamma_{\star} \sin^2 \alpha} \left(\sqrt{c^2 m^2 + p^2} + \cos(\alpha) p_{\star} \right). \quad (56)$$

For the purpose of numerical integration, equations (28)–(29) and (56) are expressed as a function of p_{\perp} and p_{\parallel} . The result of this integration, valid in the high-frequency limit, is shown on Figure 4 for our beam model and for different values of p_{\star}

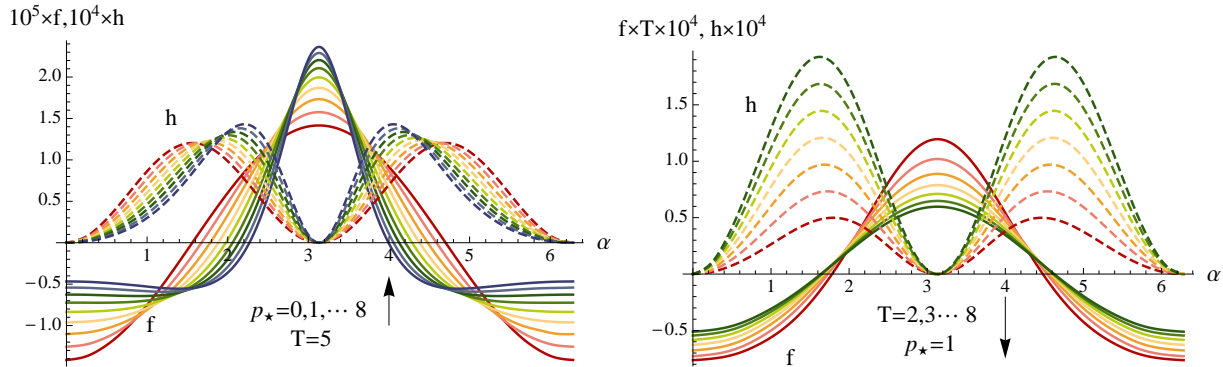


Figure 4. Polarization transfer coefficients (f, h) versus the angle of propagation α , represented here on the interval $[0, 2\pi]$ for the “beam” model of Section 3.3.2 as a function of the beam momentum parameter p_* (left panel) and the temperature T (right panel), as labeled. The vertical arrows indicate in which sense the parameter varies at $\alpha = \pi$. The Faraday response becomes more collimated along the magnetic field direction as the distribution becomes more anisotropic or colder.

and T as labeled, with the same fiducial parameters as above. As expected, for $p_* = 0$ we recover the thermal solution of Section 3.2.4, but as the beam becomes more anisotropic (i.e. p_* increases at fixed T , or T decreases at fixed $p_* \neq 0$), the Faraday coefficients are more focussed near the axis of symmetry. This may be understood from the fact that the values of the kernels depending on ϖ and σ in equations (28)–(29) are the largest where the difference $\sigma^2 - x^2$ is the smallest, that is where the pitch angle ϑ of the particle is closest to the direction of propagation α of the radiation, causing a larger response when the angle α is in the particle’s beam.

The next two sections formally carry out two of the four integrals involved in equation (24) in order to write equations (25) and (26), and investigate the corresponding resonant and non resonant regimes. A detailed analysis of the various frequency regimes allows us to write simple one dimensional quadrature. These two sections can be skipped as a first read.

4 DERIVATION OF THE POLARIZATION TRANSFER COEFFICIENTS

We now describe our derivation of the polarization transfer coefficients, which amounts to calculating the elements of the hermitian and antihermitian parts of the conductivity deduced from equation (24), that is, of the phase integrals in equation (22). The usual approach to the phase integrals is to integrate over the time delay τ by expanding $\exp(ix \sin \phi)$, or any similar expression, in discrete Fourier series such as for example $\exp(ix \sin \phi) = \sum_n J_n(x) \exp(in \phi)$ where $J_n(x)$ is a Bessel function of relative integer order. An integration over times t' earlier than t (that is over positive delay times $\tau = t - t'$) is then performed that yields resonant denominators $\omega - k_{\parallel} v_{\parallel} - n\Omega_*$. The integrand being proportional to $\exp(+i\omega\tau)$, and it being understood that ω really is a complex Laplace variable, the resonant denominators should be regarded as having an infinitesimal positive imaginary part, ensuring the convergence of integrals over τ at $\tau = +\infty$. These denominators are then to be understood as complex numbers with an infinitesimal positive imaginary part, the real part of which is the Cauchy principal value, the imaginary part being $-i\pi\delta_{\text{D}}(\omega - k_{\parallel} v_{\parallel} - n\Omega_*)$. This gives an exact expression of the conductivity (Bekefi 1966) in the form of series, each term of which involves one such resonant denominator.

However, since any approximation to the sum of these series has, in the present context, to be carried out up to very large values of n , of order $\omega / |\Omega_*|$ at least, this representation of the conductivity is not suitable for our purpose. As when deriving the synchrotron emission spectrum, it would be preferable to somehow substitute to the discrete series a representation in which the discrete summation is replaced by an integration over a continuous variable. Sazonov (1969b) attempted this by changing the discrete sums into integrals, considering the index n of the Bessel functions as being a continuous variable which can be identified with the variable σ defined in equation (23). This approach is known to be successful when evaluating the dissipative part of the conductivity, in which the many resonant Dirac functions form a sum similar to a Riemann one that can be approached by the integral of the so-defined interpolating function, $F(\sigma)$ say. But this is an unfortunate approach for calculating the non-dissipative part, in which principal values are involved. A continuous approximation to the derivative of $F(\sigma)$ would have been preferable in this case, although any a-priori choice of such an interpolation would be tainted with arbitrariness.

4.1 An exact continuous-spectrum type representation of the conductivity

We improve here over Sazonov’s approach by deriving exact expressions for the phase integrals in equation (22) as functions of the continuous variable σ defined in equation (23). This variable will eventually appear as a continuous index of some

Bessel functions. This will achieve, without any arbitrariness, the desired continuous-spectrum-type representation. Qin et al. (2007) have derived this transformation by using the invariance associated to the periodicity of the unperturbed motion while Heyvaerts (1970) and Thiébaud (2010) derived it by exactly turning the familiar discrete series representation into a continuous one by means of an integral representation of the principle values involved in the series. To show here how this is achieved, we follow a method similar to that of Qin et al. (2007). The phase integrals in equation (22) are first expressed in terms of the variables in equation (23) and the delay time τ is replaced by a delay angle ψ , so that

$$P_\varepsilon(\sigma, x, \phi) = \exp(-i s_q(\sigma\phi - x \sin \phi)) \int_{s_q\phi}^{+\infty} \frac{d\psi}{|\Omega_*|} \exp(i((\sigma + s_q\varepsilon)\psi - x \sin \psi)), \quad \text{with} \quad \psi = s_q\phi + |\Omega_*| \tau. \quad (57)$$

To account for the periodicity of the unperturbed motion, the integration range over the angle ψ is separated into segments of length 2π , and the integration on the n^{th} segment is carried out by changing from ψ to $w = \psi - (s_q\phi + 2n\pi)$. Then,

$$P_\varepsilon(\sigma, x, \phi) = \frac{\exp(i(\varepsilon\phi + s_q x \sin \phi))}{|\Omega_*|} \left(\sum_{n=0}^{\infty} e^{2i\pi n(\sigma + s_q\varepsilon)} \right) \int_0^{2\pi} dw \exp(i((\sigma + s_q\varepsilon)w - x \sin(w + s_q\phi))). \quad (58)$$

The fact that the periodicity of the motion is fully taken into account in this exact transformation could be considered superfluous because, on the one hand, the period is very long in the ultrarelativistic limit and because, on the other hand, the integral over ψ in equation (57) could conceivably be evaluated by the method of stationary phase applied to a unique interval of quasi-stationarity. It will however become clear below that the antihermitian part of the conductivity is in fact not determined only by the properties of the motion near the quasi-stationary phase, a situation that may be compared to that of a classical plasma, in which the cyclotron resonances determine the rates of emission and absorption but where non-resonant particles make the most of the contribution to the medium's dispersive properties. From equation (58) we calculate the combinations of the phase integrals that appear in equation (24), namely

$$\begin{pmatrix} P_0 \\ (P_+ - P_-)/2i \\ (P_+ + P_-)/2 \end{pmatrix} = \frac{e^{is_q x \sin \phi}}{|\Omega_*|} \left(\sum_{n=0}^{\infty} e^{2i\pi n\sigma} \right) \int_0^{2\pi} dw e^{i(\sigma w - x \sin(w + s_q\phi))} \begin{pmatrix} 1 \\ \sin(\phi + s_q w) \\ \cos(\phi + s_q w) \end{pmatrix}. \quad (59)$$

The sum over n of the imaginary exponentials is not absolutely convergent. It should be regarded as a distribution rather than as a proper function because it enters an integration over the variable σ that will have to be performed at a later stage. We define three functions T_1, T_2, T_3 by

$$T_1 = 1, \quad T_2 = \sin, \quad T_3 = \cos. \quad (60)$$

The expressions in equation (59) are then inserted in equation (24) which gives the components of the current. Then gathering the terms which depend on the gyration angle ϕ and integrating over it, the components of the conductivity tensor can be written as

$$\sigma_{ij} = -\frac{2\pi q^2}{\omega} \int_{-\infty}^{+\infty} dp_{\parallel} \int_0^{\infty} p_{\perp} dp_{\perp} M_{ij}(p_{\perp}, p_{\parallel}, k_{\perp}, k_{\parallel}), \quad (61)$$

where the matrix M_{ij} is, with i a line index and j a column one:

$$\begin{pmatrix} v_{\perp}(\omega \frac{\partial f_0}{\partial p_{\perp}} + k_{\parallel} D(f_0)) Q_{33}(\sigma, x) & v_{\perp}(\omega \frac{\partial f_0}{\partial p_{\perp}} + k_{\parallel} D(f_0)) Q_{32}(\sigma, x) & (v_{\perp} \omega \frac{\partial f_0}{\partial p_{\parallel}} Q_{31}(\sigma, x) - k_{\perp} v_{\perp} D(f_0) Q_{33}(\sigma, x)) \\ v_{\perp}(\omega \frac{\partial f_0}{\partial p_{\perp}} + k_{\parallel} D(f_0)) Q_{23}(\sigma, x) & v_{\perp}(\omega \frac{\partial f_0}{\partial p_{\perp}} + k_{\parallel} D(f_0)) Q_{22}(\sigma, x) & (v_{\perp} \omega \frac{\partial f_0}{\partial p_{\parallel}} Q_{21}(\sigma, x) - k_{\perp} v_{\perp} D(f_0) Q_{23}(\sigma, x)) \\ v_{\parallel}(\omega \frac{\partial f_0}{\partial p_{\perp}} + k_{\parallel} D(f_0)) Q_{13}(\sigma, x) & v_{\parallel}(\omega \frac{\partial f_0}{\partial p_{\perp}} + k_{\parallel} D(f_0)) Q_{12}(\sigma, x) & (v_{\parallel} \omega \frac{\partial f_0}{\partial p_{\parallel}} Q_{11}(\sigma, x) - k_{\perp} v_{\parallel} D(f_0) Q_{13}(\sigma, x)) \end{pmatrix}. \quad (62)$$

The coefficients Q_{ab} that appear in equation (62), a and b varying between 1 and 3, encompass the results of the integrations over the delay angle and over the gyration angle. They depend on the sign s_q of the electric charge of the particle species and may eventually be written as

$$Q_{ab}(\sigma, x) = (-s_q)^{a+b} \left(2\pi \sum_{n=0}^{\infty} e^{2i\pi n\sigma} \right) G_{ab}(\sigma, x), \quad \text{with} \quad G_{ab} = \int_0^{2\pi} \frac{d\phi}{2\pi} \int_0^{2\pi} \frac{dw}{2\pi} T_a(\phi) T_b(\phi - w) e^{i(\sigma w + x(\sin(\phi - w) - \sin \phi))}. \quad (63)$$

The parenthesis in the first part of equation (63) can be more explicitly written as

$$2\pi \sum_{n=0}^{\infty} e^{2i\pi n\sigma} = i\pi \frac{e^{-i\pi\sigma}}{\sin \sigma\pi} \left(\lim_{N \rightarrow \infty} \left(1 - e^{2i\pi N\sigma} \right) \right). \quad (64)$$

The calculation of the elements G_{ab} involves integrations over the angles ϕ and w . Qin et al. (2007) perform these integrations along the lines described in Appendix B. The elements G_{ab} may finally be expressed in terms of Bessel functions of the first kind, with indices σ or $-\sigma$ and argument x , as listed below:

$$\begin{aligned}
 G_{11}(\sigma, x) &= e^{i\sigma\pi} J_\sigma(x) J_{-\sigma}(x) & G_{12}(\sigma, x) &= -\frac{i}{2} e^{i\sigma\pi} \frac{\partial}{\partial x} (J_\sigma(x) J_{-\sigma}(x)) , \\
 G_{13}(\sigma, x) &= e^{i\sigma\pi} \left(-\frac{\sin\sigma\pi}{\pi x} + \frac{\sigma}{x} J_\sigma(x) J_{-\sigma}(x) \right) & G_{22}(\sigma, x) &= \frac{\sin\sigma\pi}{\pi} e^{i\sigma\pi} \left(\frac{\pi}{\sin\sigma\pi} J'_\sigma(x) J'_{-\sigma}(x) + \frac{\sigma}{x^2} \right) , \\
 G_{23}(\sigma, x) &= \frac{is}{2x} e^{i\sigma\pi} \frac{\partial}{\partial x} (J_\sigma(x) J_{-\sigma}(x)) , & G_{33}(\sigma, x) &= -\frac{\sigma}{\pi x^2} \sin\sigma\pi e^{i\sigma\pi} \left(1 - \frac{\pi\sigma}{\sin\sigma\pi} J_\sigma(x) J_{-\sigma}(x) \right) , \\
 G_{21} &= -G_{12} , & G_{31} &= +G_{13} , & G_{32} &= -G_{23} .
 \end{aligned} \tag{65}$$

The elements Q_{ab} , and then the matrix elements M_{ij} , are given in terms of these coefficients in equation (63). The variable σ being positive, it is useful to eliminate the Bessel functions of negative indices for other Bessel functions with positive indices. This is possible since the Bessel function of the first kind and negative index $J_{-\sigma}(x)$ can be expressed in terms of Bessel functions of the first and second kind with positive indices, $J_\sigma(x)$ and $N_\sigma(x)$ by the left identity in equation (66) below (Abramowitz & Stegun 1964). When derivatives are involved, the second relation in equation (66), that gives the wronskian of the functions of the first and second kind (Abramowitz & Stegun 1964), may be used to eliminate N'_σ if needed. We then base the transformation to positive σ values on the relations:

$$J_{-\sigma}(x) = \cos\sigma\pi J_\sigma(x) - \sin\sigma\pi N_\sigma(x) , \quad J_\sigma(x) N'_\sigma(x) - J'_\sigma(x) N_\sigma(x) = \frac{2}{\pi x} . \tag{66}$$

Using equations (66), the elements Q_{ab} in equation (63) can all be expressed in terms of $J_\sigma(x)$, $N_\sigma(x)$ and their derivatives w.r.t. x . Some components of these expressions turn out to be regular at integer values of σ , while some other keep a singular denominator $\sin\sigma\pi$ which generates expressions that must, again, be understood in the sense of distributions. The matrix elements M_{ij} in equations (61)–(62) can then be explicitly written as

$$\begin{aligned}
 M_{XX} &= (+i) \lim_{N \rightarrow \infty} \left(1 - e^{2i\pi N\sigma} \right) \frac{v_\perp}{|\Omega_*|} \left(\omega \frac{\partial f_0}{\partial p_\perp} + k_\parallel D(f_0) \right) & \pi \frac{\sigma^2}{x^2} \left(\frac{\cos\sigma\pi}{\sin\sigma\pi} J_\sigma^2(x) - J_\sigma(x) N_\sigma(x) - \frac{1}{\sigma\pi} \right) , \\
 M_{XY} &= (-s_q) \lim_{N \rightarrow \infty} \left(1 - e^{2i\pi N\sigma} \right) \frac{v_\perp}{|\Omega_*|} \left(\omega \frac{\partial f_0}{\partial p_\perp} + k_\parallel D(f_0) \right) & \pi \frac{\sigma}{x} \left(\frac{\cos\sigma\pi}{\sin\sigma\pi} J_\sigma(x) J'_\sigma(x) - J'_\sigma(x) N_\sigma(x) - \frac{1}{\pi x} \right) , \\
 M_{XZ} &= (+i) \lim_{N \rightarrow \infty} \left(1 - e^{2i\pi N\sigma} \right) \frac{v_\perp}{|\Omega_*|} \left(\omega \frac{\partial f_0}{\partial p_\parallel} - k_\perp D(f_0) \frac{\sigma}{x} \right) & \pi \frac{\sigma}{x} \left(\frac{\cos\sigma\pi}{\sin\sigma\pi} J_\sigma^2(x) - J_\sigma(x) N_\sigma(x) - \frac{1}{\sigma\pi} \right) , \\
 M_{YX} &= (+s_q) \lim_{N \rightarrow \infty} \left(1 - e^{2i\pi N\sigma} \right) \frac{v_\perp}{|\Omega_*|} \left(\omega \frac{\partial f_0}{\partial p_\perp} + k_\parallel D(f_0) \right) & \pi \frac{\sigma}{x} \left(\frac{\cos\sigma\pi}{\sin\sigma\pi} J_\sigma(x) J'_\sigma(x) - J'_\sigma(x) N_\sigma(x) - \frac{1}{\pi x} \right) , \\
 M_{YY} &= (+i) \lim_{N \rightarrow \infty} \left(1 - e^{2i\pi N\sigma} \right) \frac{v_\perp}{|\Omega_*|} \left(\omega \frac{\partial f_0}{\partial p_\perp} + k_\parallel D(f_0) \right) & \pi \left(\frac{\cos\sigma\pi}{\sin\sigma\pi} J_\sigma^2(x) - J'_\sigma(x) N'_\sigma(x) + \frac{\sigma}{\pi x^2} \right) , \\
 M_{YZ} &= (+s_q) \lim_{N \rightarrow \infty} \left(1 - e^{2i\pi N\sigma} \right) \frac{v_\perp}{|\Omega_*|} \left(\omega \frac{\partial f_0}{\partial p_\parallel} - k_\perp D(f_0) \frac{\sigma}{x} \right) & \pi \left(\frac{\cos\sigma\pi}{\sin\sigma\pi} J_\sigma(x) J'_\sigma(x) - J'_\sigma(x) N_\sigma(x) - \frac{1}{\pi x} \right) , \\
 M_{ZX} &= (+i) \lim_{N \rightarrow \infty} \left(1 - e^{2i\pi N\sigma} \right) \frac{v_\parallel}{|\Omega_*|} \left(\omega \frac{\partial f_0}{\partial p_\perp} + k_\parallel D(f_0) \right) & \pi \frac{\sigma}{x} \left(\frac{\cos\sigma\pi}{\sin\sigma\pi} J_\sigma^2(x) - J_\sigma(x) N_\sigma(x) - \frac{1}{\pi\sigma} \right) , \\
 M_{ZY} &= (-s_q) \lim_{N \rightarrow \infty} \left(1 - e^{2i\pi N\sigma} \right) \frac{v_\parallel}{|\Omega_*|} \left(\omega \frac{\partial f_0}{\partial p_\perp} + k_\parallel D(f_0) \right) & \pi \left(\frac{\cos\sigma\pi}{\sin\sigma\pi} J_\sigma(x) J'_\sigma(x) - J'_\sigma(x) N_\sigma(x) - \frac{1}{\pi x} \right) , \\
 M_{ZZ} &= (+i) \lim_{N \rightarrow \infty} \left(1 - e^{2i\pi N\sigma} \right) \frac{v_\parallel}{|\Omega_*|} \left(\omega \frac{\partial f_0}{\partial p_\parallel} - k_\perp D(f_0) \frac{\sigma}{x} \right) & \pi \left(\frac{\cos\sigma\pi}{\sin\sigma\pi} J_\sigma^2(x) - J_\sigma(x) N_\sigma(x) \right) + \frac{1}{x} k_\perp D(f_0) .
 \end{aligned} \tag{67}$$

Let us now specify the meaning of $\lim_{N \rightarrow \infty} (1 - e^{2i\pi N\sigma})$, which enters with other factors in integrations over σ implied by the integration over momenta in equation (61). When this factor multiplies a regular function of σ , its limit is unity since, when N diverges, $\exp(2i\pi N\sigma)$ oscillates infinitely rapidly leaving in the limit a vanishing integral when multiplied by any regular function. The case when a factor $(\cos\sigma/\sin\sigma\pi)$ multiplies $(1 - \exp(2i\pi N\sigma))$ deserves closer scrutiny, since both $\sin\sigma\pi$ and $(1 - \exp(2i\pi N\sigma))$ vanish at integer values. It is shown in Appendix C that the limit of their product is the distribution

$$\lim_{N \rightarrow \infty} \left(1 - e^{2i\pi N\sigma} \right) \frac{\cos\sigma\pi}{\sin\sigma\pi} \equiv \mathcal{D} \left(\frac{\cos\sigma\pi}{\sin\sigma\pi} \right) = \left(\mathcal{P} \left(\frac{\cos\sigma\pi}{\sin\sigma\pi} \right) - i \sum_{n \in \mathbb{N}} \delta_D(\sigma - n) \right) . \tag{69}$$

where \mathbb{N} is the set of positive integers, δ_D a Dirac distribution and the notation \mathcal{P} means that the function which follows in the parenthesis should be taken as a Cauchy principal value near each of its singularities, which in this case are the integer values of σ . The effect of the multiple resonances at all integer values of σ that are involved in the matrix elements of the conductivity are concentrated on those terms in equations (68) in which factors $(\cos\sigma\pi/\sin\sigma\pi)$ subsist, although it could have been expected that resonances should be present in all terms since equation (64) exhibits such a singular factor. In changing according to equation (66) for Bessel functions with positive indices only, some of these singular factors have been disposed of, having been regularized owing to the favourably phased term proportional to $\sin\sigma\pi N_\sigma(x)$ in equation (66). This means that the transformation to Bessel functions with only positive indices has effected the summation over resonances for these favourably phased terms. Resonances only remain explicitly present in the unfavourably phased ones, that originate in the term $\cos\sigma\pi J_\sigma(x)$ in equation (66). It is shown in section 4.4 that these residual resonant terms eventually turn out to be negligible when $\omega/|\Omega| \gg 1$.

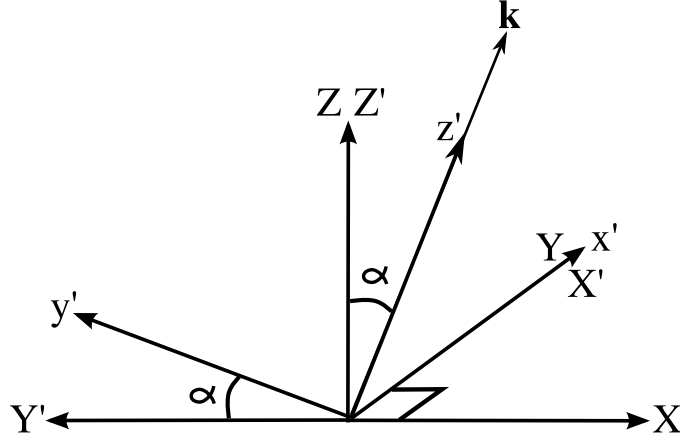


Figure 5. The Z axis is along the unperturbed magnetic field. The z' axis is along the wavevector $\mathbf{k} = k \cos \alpha \mathbf{e}_Z + k \sin \alpha \mathbf{e}_X$, where $0 \leq \alpha \leq \pi$. The axes Y and x' are identical

4.2 Polarization transfer coefficients from the conductivity

The elements of the transfer matrix are given in equation (12) in terms of the components of the conductivity tensor in the plane perpendicular to the direction of propagation of the radiation. Since the components of this tensor are known in a frame in which the static magnetic field is along the Z axis, the components in equations (68) must be transformed to the new reference frame x', y', z' represented in Fig. 5 in which the wave vector \mathbf{k} is along the z' axis. For our purpose, it suffices to calculate the transverse components $x'x', x'y', y'x', y'y'$ which are given by Thiébaud (2010)

$$M_{x'x'} = M_{YY}, \quad M_{x'y'} = \sin \alpha M_{YZ} - \cos \alpha M_{YX}, \quad M_{y'x'} = \sin \alpha M_{ZY} - \cos \alpha M_{XY}, \quad (70)$$

$$M_{y'y'} = \cos^2 \alpha M_{XX} + \sin^2 \alpha, \quad M_{ZZ} - \sin \alpha \cos \alpha (M_{ZX} + M_{XZ}). \quad (71)$$

These calculations are straightforward, but it nevertheless takes some algebra to reduce them to the simple form in equations (72)–(74). Some details are given in Appendix D. The transverse components of the M matrix can eventually be written as:

$$M_{x'x'} = \frac{i\pi}{\gamma m} x^2 \frac{\partial f_0}{\partial \sigma} \left(\mathcal{D} \left(\frac{\cos \sigma \pi}{\sin \sigma \pi} \right) J_\sigma'^2(x) - J_\sigma'(x) N_\sigma'(x) + \frac{\sigma}{\pi x^2} \right). \quad (72)$$

$$M_{x'y'} = -\frac{s_q \pi}{\gamma m} \varpi x \frac{\partial f_0}{\partial \sigma} \left(\mathcal{D} \left(\frac{\cos \sigma \pi}{\sin \sigma \pi} \right) J_\sigma(x) J_\sigma'(x) - J_\sigma'(x) N_\sigma(x) - \frac{1}{\pi x} \right), \quad M_{y'x'} = -M_{x'y'}. \quad (73)$$

$$M_{y'y'} = \frac{i\pi}{\gamma m} \varpi^2 \frac{\partial f_0}{\partial \sigma} \left(\mathcal{D} \left(\frac{\cos \sigma \pi}{\sin \sigma \pi} \right) J_\sigma^2(x) - J_\sigma(x) N_\sigma(x) \right) - \frac{i}{\gamma m} \left((\sigma \cos \alpha - \varpi) \frac{\partial f_0}{\partial \varpi} + \varpi \cos \alpha \frac{\partial f_0}{\partial \sigma} \right). \quad (74)$$

From equations (72)–(74), we may calculate the corresponding components of the conductivity. The density n of the particles is factored out of the distribution function by writing it as $f_0 = n F_0$, defining a reduced distribution function normalized to unity and a plasma frequency ω_{pr} for the relativistic species of particles considered:

$$f_0 = n F_0, \quad \int_0^\infty 2\pi p_\perp dp_\perp \int_{-\infty}^{+\infty} dp_\parallel F_0 = 1, \quad \omega_{\text{pr}}^2 = \frac{nq^2}{\varepsilon_0 m}. \quad (75)$$

The components of the antihermitian and hermitian parts of the conductivity can then be written as

$$\frac{\sigma_{x'x'}^A}{\varepsilon_0} = -2\pi^2 i \frac{\omega_{\text{pr}}^2 \Omega^2}{\omega^3} \iint \frac{m^3 c^3}{\sin^2 \alpha} d\varpi d\sigma x^2 \frac{\partial F_0}{\partial \sigma} \left(\mathcal{P} \left(\frac{\cos \sigma \pi}{\sin \sigma \pi} \right) J_\sigma'^2(x) - J_\sigma'(x) N_\sigma'(x) + \frac{\sigma}{\pi x^2} \right). \quad (76)$$

$$\frac{\sigma_{x'y'}^A}{\varepsilon_0} = +2\pi^2 s_q \frac{\omega_{\text{pr}}^2 \Omega^2}{\omega^3} \iint \frac{m^3 c^3}{\sin^2 \alpha} d\varpi d\sigma \varpi x \frac{\partial F_0}{\partial \sigma} \left(\mathcal{P} \left(\frac{\cos \sigma \pi}{\sin \sigma \pi} \right) J_\sigma(x) J_\sigma'(x) - J_\sigma'(x) N_\sigma(x) - \frac{1}{\pi x} \right), \quad \sigma_{y'x'}^A = -\sigma_{x'y'}^A. \quad (77)$$

$$\frac{\sigma_{y'y'}^A}{\varepsilon_0} = -2\pi^2 i \frac{\omega_{\text{pr}}^2 \Omega^2}{\omega^3} \iint \frac{m^3 c^3}{\sin^2 \alpha} d\varpi d\sigma \left[\varpi^2 \frac{\partial F_0}{\partial \sigma} \left(\mathcal{P} \left(\frac{\cos \sigma \pi}{\sin \sigma \pi} \right) J_\sigma^2(x) - J_\sigma(x) N_\sigma(x) \right) - \frac{1}{\pi} \left((\sigma \cos \alpha - \varpi) \frac{\partial F_0}{\partial \varpi} + \varpi \cos \alpha \frac{\partial F_0}{\partial \sigma} \right) \right]. \quad (78)$$

$$\frac{\sigma_{x'x'}^H}{\varepsilon_0} = -2\pi^2 \frac{\omega_{\text{pr}}^2 \Omega^2}{\omega^3} \sum_{n \in \mathbb{N}} \iint \frac{m^3 c^3}{\sin^2 \alpha} d\varpi d\sigma x^2 \frac{\partial F_0}{\partial \sigma} J_\sigma'^2(x) \delta_{\text{D}}(\sigma - n). \quad (79)$$

$$\frac{\sigma_{x'y'}^H}{\varepsilon_0} = -2\pi^2 i s_q \frac{\omega_{\text{pr}}^2 \Omega^2}{\omega^3} \sum_{n \in \mathbb{N}} \iint \frac{m^3 c^3}{\sin^2 \alpha} d\varpi d\sigma \varpi x \frac{\partial F_0}{\partial \sigma} J_\sigma(x) J_\sigma'(x) \delta_{\text{D}}(\sigma - n), \quad \sigma_{y'x'}^H = -\sigma_{x'y'}^H. \quad (80)$$

$$\frac{\sigma_{y'y'}^H}{\varepsilon_0} = -2\pi^2 \frac{\omega_{\text{pr}}^2 \Omega^2}{\omega^3} \sum_{n \in \mathbb{N}} \iint \frac{m^3 c^3}{\sin^2 \alpha} d\varpi d\sigma \varpi^2 \frac{\partial F_0}{\partial \sigma} J_\sigma^2(x) \delta_{\text{D}}(\sigma - n). \quad (81)$$

The elements of the transfer matrix in equation (1) can be found from these results by using equation (12). Our choice of reference axes in the plane perpendicular to \mathbf{k} results in the vanishing of the coefficients K_{QV} and K_{IU} , since $\sigma_{x'y'}^A$ is real and $\sigma_{x'y'}^H$ is imaginary. In equation (78) the integration over ϖ and σ of the terms $\cos \alpha (\sigma \partial_\varpi F_0 + \varpi \partial_\sigma F_0)$ can be reduced to an integral on the boundary of the physical domain which vanishes.

4.3 Formal expression of the polarization transfer coefficients

The components of the hermitian part of the conductivity in equations (79)–(81) are associated with dissipative radiative effects. Equations (12) relate them to the absorption coefficients per unit time which appear in equation (1). The transfer coefficients per unit length in a medium of negligible dispersion are obtained from them by dividing by the velocity of light. The discrete sum over the large positive integers n in equations (79)–(81) can be approximated by an integral, so that

$$\frac{K_{II}}{c} = -\pi^2 \frac{\omega_{\text{pr}}^2 \Omega^2}{c \omega^3} \iint \frac{m^3 c^3}{\sin^2 \alpha} d\varpi d\sigma \frac{\partial F_0}{\partial \sigma} \left[x^2 J_\sigma'^2(x) + \varpi^2 J_\sigma^2(x) \right]. \quad (82)$$

$$\frac{K_{IQ}}{c} = -\pi^2 \frac{\omega_{\text{pr}}^2 \Omega^2}{c \omega^3} \iint \frac{m^3 c^3}{\sin^2 \alpha} d\varpi d\sigma \frac{\partial F_0}{\partial \sigma} \left[x^2 J_\sigma'^2(x) - \varpi^2 J_\sigma^2(x) \right]. \quad (83)$$

$$\frac{K_{IV}}{c} = -2\pi^2 s_q \frac{\omega_{\text{pr}}^2 \Omega^2}{c \omega^3} \iint \frac{m^3 c^3}{\sin^2 \alpha} d\varpi d\sigma \frac{\partial F_0}{\partial \sigma} \varpi x J_\sigma(x) J_\sigma'(x). \quad (84)$$

We return to the dissipative coefficients in section 5.2. There are two non-dissipative coefficients, which in a stationary medium are usually defined per unit length. Assuming again no dispersion, they are $f = K_{QU}/c$ and $h = K_{UV}/c$. When acting alone on radiation propagating in the direction of the unit vector \mathbf{n} , they cause the Stokes parameters Q, U, V to vary according to the equation:

$$\mathbf{n} \cdot \nabla \begin{pmatrix} I \\ Q \\ U \\ V \end{pmatrix} = - \begin{pmatrix} 0 & 0 & 0 & 0 \\ 0 & 0 & f & 0 \\ 0 & -f & 0 & h \\ 0 & 0 & -h & 0 \end{pmatrix} \begin{pmatrix} I \\ Q \\ U \\ V \end{pmatrix}. \quad (85)$$

This simplified transfer equation leaves the intensity I invariant as well as the degree of polarisation $\sqrt{Q^2 + U^2 + V^2}/I$. The argument of all Bessel functions implicitly being x , the coefficients f and h can be written as

$$f = 2\pi^2 s_q \frac{\omega_{\text{pr}}^2 \Omega^2}{c \omega^3} \iint \frac{m^3 c^3}{\sin^2 \alpha} d\varpi d\sigma \varpi x \frac{\partial F_0}{\partial \sigma} \left[\mathcal{P} \left(\frac{\cos \sigma \pi}{\sin \sigma \pi} \right) J_\sigma J_\sigma' - J_\sigma' N_\sigma - \frac{1}{\pi x} \right], \quad (86)$$

$$h = \pi^2 \frac{\omega_{\text{pr}}^2 \Omega^2}{c \omega^3} \iint \frac{m^3 c^3}{\sin^2 \alpha} d\varpi d\sigma \left[\frac{\partial F_0}{\partial \sigma} \left(\mathcal{P} \left(\frac{\cos \sigma \pi}{\sin \sigma \pi} \right) (\varpi^2 J_\sigma^2 - x^2 J_\sigma'^2) + (x^2 J_\sigma' N_\sigma' - \varpi^2 J_\sigma N_\sigma) \right) + \frac{1}{\pi} \left(\varpi \frac{\partial F_0}{\partial \varpi} - \sigma \frac{\partial F_0}{\partial \sigma} \right) \right]. \quad (87)$$

4.4 The residual contribution of resonances to non-dissipative coefficients is negligible

The principal value terms in equations (86)–(87) are negligible in the limit $\omega \gg |\Omega|$ in which σ and x are large. To prove this, we use the fact that the interval between successive zeroes of $\sin \sigma \pi$ is unity, whereas the Bessel functions vary on a much longer scale because both their index and argument are large, the argument remaining smaller than their index, though. This can be seen from the definition of σ and x in equation (23). The contribution to the integral over σ of each unit interval $[n - \frac{1}{2}, n + \frac{1}{2}]$ can then be calculated at any accuracy by Taylor expanding about n the function which factors $\cot \sigma \pi$ in equations (86) and (87). This provides the result of the integration on $[n - \frac{1}{2}, n + \frac{1}{2}]$ in the form of a series. The summation of these functions of n over all unit intervals centered on integer values can then be approximately replaced, provided σ is large, by an integral over σ since they slowly vary with n . This integral turns out to be extremely small, owing to particular properties of the functions $J_\sigma(x)$ and $J_\sigma'(x)$ for large σ and small x . Details are to be found in Appendix E. With this further simplification, the polarization transfer coefficients in equations (86) and (87) lose their principal value terms. Terms in which no Bessel functions are involved can be reduced to a line integral on the boundary \mathcal{B} of the physical domain in the ϖ – σ plane (Appendix A), which is particularly useful to transform equation (87) in which the term devoid of Bessel functions is the divergence of the vector with components $V_\varpi = \varpi F_0$ and $V_\sigma = -\sigma F_0$. All calculations done, we get

$$f = -\frac{2\pi^2 s_q \omega_{\text{pr}}^2 \Omega^2}{c \omega^3} \iint \frac{m^3 c^3}{\sin^2 \alpha} d\varpi d\sigma \varpi x \left(J_\sigma'(x) N_\sigma(x) + \frac{1}{\pi x} \right) \frac{\partial F_0}{\partial \sigma}, \quad (88)$$

$$h = \frac{\pi^2 \omega_{\text{pr}}^2 \Omega^2}{c \omega^3} \iint \frac{m^3 c^3}{\sin^2 \alpha} d\varpi d\sigma (x^2 J_\sigma'(x) N_\sigma'(x) - \varpi^2 J_\sigma(x) N_\sigma(x)) \frac{\partial F_0}{\partial \sigma} + \frac{\pi \omega_{\text{pr}}^2 \Omega^2}{c \omega^3} \int_{-\infty}^{+\infty} \frac{m^3 c^3}{\sin^2 \alpha} d\varpi \frac{2\varpi^2 + \sigma_0^2}{\sqrt{\varpi^2 + \sigma_0^2}} F_0(\varpi, \sigma_b(\varpi)), \quad (89)$$

The notation $\sigma_b(\varpi) = \sqrt{\sigma_0^2 + \varpi^2}$ denotes the value of σ at a point of abscissa ϖ on the boundary \mathcal{B} of the physical domain in the ϖ - σ plane. It will soon be shown that, when expanding the Bessel functions in $|\Omega|/\omega$, the non-Bessel terms in equations (88) and (89) almost exactly cancel the zeroth-order terms of the development. Equations (88) and (89) are applicable to any distribution function. The integrals over σ and/or ϖ extend to the full range of physically relevant values and no other approximation has been made than neglecting the series of residual principal value terms, which is well justified. Equations (88) and (89) are then close to being exact. They however feature complicated kernels, which makes it desirable to find simpler and suitable approximations to them.

5 NON-RESONANT AND QUASI-RESONANT PARTS OF THE TRANSFER COEFFICIENTS

5.1 Quasi resonant contribution to transfer coefficients from Nicholson's approximation

The phase integrals in equation (22) involve the integration of trigonometric functions which may vary more or less rapidly with the delay time τ , depending on the values of the particle's parameters and the gyration angle ϕ . Let us denote by ϑ the pitch angle of a particle, that is, the angle of the particle's velocity with the magnetic field. According to equation (22), the characteristic variation frequency of the phase most often is of the order of ω . When however the modulus of the particle's velocity is close to the speed of light, the characteristic frequency of phase variations may occasionally be much less, when the angle between the particle's velocity and the wave vector becomes small enough. For example, equation (22) indicates that this frequency would be of order $|\Omega|$ or less when

$$\omega - k_{\parallel} v_{\parallel} - k_{\perp} v_{\perp} \cos \phi \leq |\Omega|, \quad \text{that is} \quad \left(1 - \frac{v}{c}\right) + \frac{v}{c} (1 - \cos(\vartheta - \alpha)) + \frac{v}{c} \sin \alpha \sin \vartheta (1 - \cos \phi) \leq \frac{|\Omega|}{ck}. \quad (90)$$

Since $u = ck/|\Omega|$ is very large, this requires that each term on the left of the second inequality in equation (90) be less than the term on the right, i.e. that

$$|\alpha - \vartheta| \leq \left(\frac{|\Omega|}{\omega}\right)^{1/2}, \quad |\phi| \leq \left(\frac{|\Omega|}{\omega}\right)^{1/2}, \quad (1/\gamma) \leq \left(\frac{|\Omega|}{\omega}\right)^{1/2}. \quad (91)$$

For quasi-resonance, the third inequality in equation (91) requires that ω should be less than $\gamma^2 |\Omega|$ which is of order of the characteristic frequency of the synchrotron emission spectrum by a particle of Lorentz factor γ (equation (101)). The other inequalities in equation (91) require that the angle between the wave vector and the particle's velocity be, for a frequency at the peak of synchrotron emission, less than $1/\gamma$. These inequalities are only satisfied by a restricted class of particles, which we refer to as quasi-resonant particles. For quasi-resonant particles, the characteristic frequency of the variations of the phase (the integrand in equation (22)) is, during a small fraction of the synchrotron gyration period, much less than ω and, because of this slow variation with τ , the phase integral is exceptionally large.

This induced some authors (Sazonov 1969b; Heyvaerts 1970; Melrose 1997c,d) to consider that quasi-resonant particles entirely determine the non-dissipative transfer coefficients, just as they determine the dissipative ones and the emission coefficients (Westfold 1959). This shows up when phase integrals are evaluated by the method of the (quasi-) stationary phase, resulting in the presence in the results of Airy-type functions. The dominance of the contribution of quasi-resonant particles to non-dissipative transfer coefficients is however not granted. The functions which determine the dissipative coefficients in equations (79)–(81) happen to be vanishingly small for non-resonant particles, but those determining the non-dissipative ones have a much wider support and are associated with a large number of non-resonant particles. At this point, we do not know whether the quasi-resonant contribution to the non-dissipative coefficients is negligible compared to the non-resonant one, or comparable to it. This will be discussed in section 5.4.

The first inequality in equation (90), which defines quasi-resonant particles, can be written for $\phi = 0$ in terms of the variables σ and x in equation (23) as $(\sigma - x) < \gamma$. The pitch angle ϑ of the particle and the propagation angle α of the wave being almost equal at quasi-resonance, $\sigma \approx \gamma u \sin^2 \alpha$. Considering the general case when α is not very small, this yields $\sigma \sim \gamma u$, a very large value. Imposing the condition $(\sigma - x) < \gamma$ to a wave with frequency in the peak of the the synchrotron emission, such that $\omega \sim \gamma^2 |\Omega|$, we get $\sigma \approx \gamma^3$, which then implies that for quasi-resonance

$$\frac{\sigma - x}{\sigma} < \frac{1}{\sigma^{2/3}}. \quad (92)$$

Thus, for quasi-resonant particles, σ and x are very close to each other, x being however slightly smaller, since, from equation (23), $(\sigma - x)$ must be positive. The inequality in equation (92) places the argument x in the intermediate region where the so-called Nicholson's approximation to Bessel functions of large index and argument is appropriate (Watson (1922) chap. 8, Olver (1952)). The Nicholson's approximation to $J_{\sigma}(x)$ is well known but the corresponding approximation to $N_{\sigma}(x)$ is not. Its derivation is outlined in Appendix F. The functions J_{σ} , N_{σ} and their derivatives may be represented in this range by modified Bessel functions of the second kind $K_{\nu}(g)$, with index $\nu = 1/3$ or $2/3$, and by a similar combination $L_{\nu}(g)$ of modified Bessel functions of the first kind, $I_{\pm\nu}(g)$. K_{ν} and L_{ν} are defined by

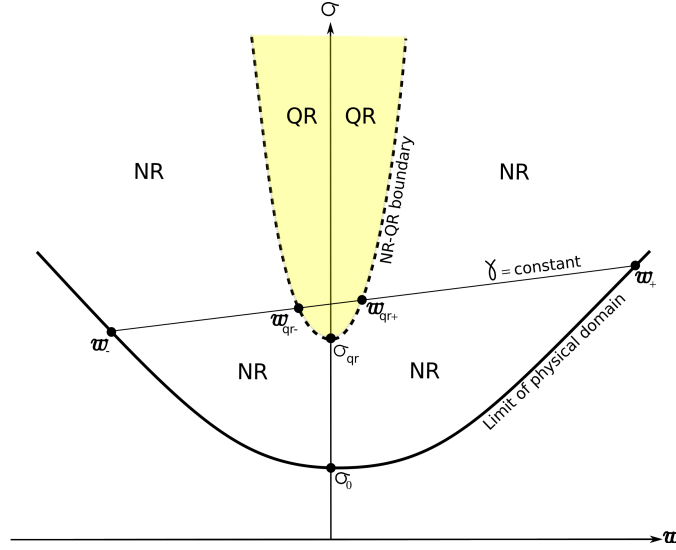


Figure 6. The physical domain of the ϖ - σ plane is above the hyperbolic line \mathcal{B} , of equation $\sigma^2 = \varpi^2 + \sigma_0^2$. The smallest possible value of σ is $\sigma_0 = \omega \sin \alpha / |\Omega|$. The quasi-resonant domain is the shaded area defined by $g \leq 1$ (equation (94)). It is bounded by the dotted line \mathcal{B}_{QR} , represented by equation (97). The smallest value of σ on \mathcal{B}_{QR} , σ_{qr} , is given by equation (97) for $\varpi = 0$. The oblique line is the locus of a constant value of the Lorentz factor γ . It intersects \mathcal{B} at $\varpi = \varpi_-(\gamma)$ and $\varpi_+(\gamma)$ and \mathcal{B}_{QR} at $\varpi = \varpi_{\text{qr}-}(\gamma)$ and $\varpi_{\text{qr}+}(\gamma)$.

$$K_\nu(g) = \frac{\pi}{2} \frac{I_{-\nu}(g) - I_\nu(g)}{\sin \nu \pi}, \quad L_\nu(g) = \frac{\pi}{2} \frac{I_{-\nu}(g) + I_\nu(g)}{\sin \nu \pi}. \quad (93)$$

The definition of the functions K_ν is standard (Abramowitz & Stegun 1964) and applies to integer values of the index in a limit sense. Our definition of the functions L_ν in equation (93) does not make sense for integer ν . However, we only deal here with indices $\nu = 1/3$ or $2/3$. The argument g on which these functions depend is

$$g = \frac{2^{3/2}}{3} \frac{(\sigma - x)^{3/2}}{x^{1/2}}. \quad (94)$$

From equation (92), it can be seen that the variable g is $\mathcal{O}(1)$ or smaller wherever the Nicholson's approximation applies. The latter yields the following approximate representations:

$$J_\sigma(x) \approx \frac{1}{\pi} \sqrt{\frac{2}{3}} \sqrt{\frac{\sigma - x}{x}} K_{\frac{1}{3}}(g), \quad N_\sigma(x) \approx -\frac{\sqrt{2}}{\pi} \sqrt{\frac{\sigma - x}{x}} L_{\frac{1}{3}}(g). \quad (95)$$

$$J'_\sigma(x) \approx \frac{2}{\pi \sqrt{3}} \left(\frac{\sigma - x}{x} \right) K_{\frac{2}{3}}(g), \quad N'_\sigma(x) \approx \frac{2}{\pi} \left(\frac{\sigma - x}{x} \right) L_{\frac{2}{3}}(g). \quad (96)$$

The quasi-resonant contributions to the Faraday coefficients f and h are obtained by substituting equations (95)–(96) into equations (88)–(89), the domain of integration in the ϖ - σ plane then being restricted to the quasi-resonant one. This domain is characterized by the inequality in equation (92), or equivalently, since at quasi-resonance x and σ are nearly equal, by the requirement that the variable g in equation (94) be less than or equal to unity. From equations (94) and (A2), the condition that $g = 1$ translates into

$$\varpi^2 + \sigma_0^2 = 3^{2/3} \sigma^{4/3}. \quad (97)$$

The variable g can then be less than unity only when σ exceeds a threshold σ_{qr} and the Lorentz factor exceeds a related one, γ_{qr} , such that the line $\gamma = \gamma_{\text{qr}}$ in figure 6 be tangent to the boundary \mathcal{B}_{QR} . The Lorentz factor γ_{qr} is of order of the γ variable associated with σ_{qr} and $\varpi = 0$. To sum up,

$$\sigma_{\text{qr}} = \frac{\sigma_0^{3/2}}{\sqrt{3}}, \quad \gamma_{\text{qr}} \approx \sqrt{\frac{u}{3 \sin \alpha}}. \quad (98)$$

Thus, a particle can only quasi-resonantly interact with the radiation when σ exceeds σ_{qr} . Since σ_0 defined in equation (23) is usually large, $\sigma_{\text{qr}} \gg \sigma_0$. The characteristic frequency $\omega_c(\gamma, \alpha)$ of synchrotron emission by particles of Lorentz factor γ_{qr} , defined in equation (101), is almost ω . The figure 6 represents the quasi-resonant domain in the ϖ - σ plane. When $u = \omega / |\Omega|$ becomes very large, σ_{qr} diverges as $u^{3/2}$ while the σ value corresponding to a given Lorentz factor γ diverges as u . This means that at high enough frequency there will be a negligible number of particles in quasi-resonance and the transfer coefficients will then be essentially given by the non-resonant contribution. When on the contrary $\sigma > \sigma_{\text{qr}}$ for relevant values of γ , the

quasi-resonant region partly contributes to f and h . These contributions are:

$$f_{\text{QR}} = 2s_q \frac{\omega_{\text{pr}}^2 \Omega^2}{c \omega^3} \iint_{\text{QR}} \frac{m^3 c^3}{\sin^2 \alpha} d\varpi d\sigma \varpi x \left(\frac{2\sqrt{2}}{\sqrt{3}} \left(\frac{\sigma - x}{x} \right)^{\frac{3}{2}} K_{\frac{2}{3}}(g) L_{\frac{1}{3}}(g) - \frac{\pi}{x} \right) \frac{\partial F_0}{\partial \sigma}, \quad (99)$$

$$h_{\text{QR}} = \frac{\omega_{\text{pr}}^2 \Omega^2}{c \omega^3} \iint_{\text{QR}} \frac{m^3 c^3}{\sin^2 \alpha} d\varpi d\sigma \left(\frac{4x^2}{\sqrt{3}} \left(\frac{\sigma - x}{x} \right)^2 K_{\frac{2}{3}}(g) L_{\frac{2}{3}}(g) + \frac{2\varpi^2}{\sqrt{3}} \left(\frac{\sigma - x}{x} \right) K_{\frac{1}{3}}(g) L_{\frac{1}{3}}(g) \right) \frac{\partial F_0}{\partial \sigma}. \quad (100)$$

where the subscript QR indicates that the integration should be carried over the quasi-resonant domain only.

5.2 Polarization-dependent absorption coefficients

The dissipative coefficients per unit length are given by equations (82)–(84). Since the product of Bessel functions declines exponentially out of the quasi-resonant domain, it is appropriate to use the Nicholson's approximation to represent them (equations (94), (95), (96)). Equations (82)–(84) are then expressed in terms of the Lorentz factor γ and the pitch angle ϑ of the particles, or the difference ψ of the latter to the propagation angle α , which remains small in the quasi-resonant domain. This results in $\partial_\sigma F_0 \approx (\partial_\gamma F_0 - \psi \partial_\vartheta F_0 / \gamma) / u \sin^2 \alpha$. Owing to the smallness of ψ , the angular derivative term may sometimes be neglected. Similarly, the argument g of the K Bessel functions in equations (95) and (96) may sometimes be approximated by $g_0 \approx (\omega / 3\gamma^2 \Omega \sin \alpha) (1 + \gamma^2 \psi^2)^{3/2}$. The critical frequency ω_c of synchrotron emission by a particle of Lorentz factor γ in the direction α is defined by (Westfold 1959):

$$\omega_c = \frac{3}{2} \gamma^2 |\Omega| \sin \alpha. \quad (101)$$

The integration over the particles directions of the right hand sides of equations (82)–(84) can be performed as in Westfold (1959), which gives for the total and linear polarization absorption coefficients:

$$\frac{K_{II}}{c} = - \frac{\omega_{\text{pr}}^2 |\Omega| \sqrt{3} \pi}{c \omega^2} \sin \alpha \int m^3 c^3 \gamma^2 d\gamma \frac{\partial F_0}{\partial \gamma} \frac{\omega}{\omega_c} \int_{\frac{\omega}{\omega_c}}^{\infty} K_{5/3}(u) du, \quad (102)$$

$$\frac{K_{IQ}}{c} = - \frac{\omega_{\text{pr}}^2 |\Omega| \sqrt{3} \pi}{c \omega^2} \sin \alpha \int m^3 c^3 \gamma^2 d\gamma \frac{\partial F_0}{\partial \gamma} \frac{\omega}{\omega_c} K_{2/3} \left(\frac{\omega}{\omega_c} \right). \quad (103)$$

Here, $\partial_\gamma F_0$ is meant to be taken at $\vartheta = \alpha$, the propagation angle. The results (102) and (103) coincide with those of Sazonov (1969a), considering his use of the CGS system of units, the definition of his distribution function, and the presence of an unfortunate typo in the first of his equations (2.2), where $\int_{\nu/\nu_c}^{\infty} K_{5/3}(u) du$ should be replaced by $\frac{\nu}{\nu_c} \int_{\nu/\nu_c}^{\infty} K_{5/3}(u) du$.

The calculation of the absorption coefficient for circular polarization in equation (84) is less straightforward because its dominant order contribution involves the integral of an odd function of ϖ , or ψ , which vanishes. Thus K_{IV}/c generically is much smaller than the other two absorption coefficients. Using the Nicholson's approximation for $J_\sigma(x)$ and $J'_\sigma(x)$, equation (84) becomes:

$$\frac{K_{IV}}{c} = - \frac{4\sqrt{2}}{3} s_q \frac{\omega_{\text{pr}}^2 \Omega^2}{c \omega^3} \iint u^2 m^3 c^3 \sin \vartheta \sqrt{\gamma^2 - 1} d\gamma d\psi \frac{\partial F_0}{\partial \sigma} \varpi \frac{(\sigma - x)^{3/2}}{x^{1/2}} K_{1/3}(g) K_{2/3}(g). \quad (104)$$

The integrand on the right hand side of equation (104) should be expressed in terms of γ and ϑ from equations (A1) and expanded to the first non-vanishing even order in ψ . This implies that the angle derivative term in $\partial_\sigma F_0$ (equation (A6)), which is of order ψ , should be accounted for, that the derivative $\partial_\gamma F_0$ be Taylor expanded about $\vartheta = \alpha$ and that all other factors involved in equation (104) be similarly expanded. This applies in particular to the product of Bessel functions, owing to the fact that the actual value of their argument g , given by equation (94), slightly differs from its lowest order approximation in ψ . With two terms, this argument g may actually be expanded as

$$g = g_0 + g_1 = \frac{\gamma u}{3 \sin \alpha} \left(\psi^2 + \frac{1}{\gamma^2} \right)^{3/2} - \frac{\gamma u \cos \alpha}{6 \sin^2 \alpha} \psi \left(\psi^2 + \frac{1}{\gamma^2} \right)^{3/2}. \quad (105)$$

Integrating the correction to the product of Bessel functions over ψ by parts, these expansions lead to

$$\begin{aligned} \frac{K_{IV}}{c} &= - \frac{2}{3} s_q \frac{\omega_{\text{pr}}^2}{c |\Omega|} \iint \frac{m^3 c^3}{\sin \alpha} \gamma^3 d\gamma d\psi \frac{\partial F_0}{\partial \gamma} \frac{\cos \alpha}{\sin \alpha} \left(2\psi^2 + \frac{2}{\gamma^2} \right) \left(\psi^2 + \frac{1}{\gamma^2} \right)^{3/2} K_{1/3}(g_0) K_{2/3}(g_0), \\ &\quad - \frac{2}{3} s_q \frac{\omega_{\text{pr}}^2}{c |\Omega|} \iint \frac{m^3 c^3}{\sin \alpha} \gamma^3 d\gamma d\psi \left(\frac{\partial^2 F_0}{\partial \gamma \partial \vartheta} - \frac{1}{\gamma} \frac{\partial F_0}{\partial \vartheta} \right) \psi^2 \left(\psi^2 + \frac{1}{\gamma^2} \right)^{3/2} K_{1/3}(g_0) K_{2/3}(g_0), \end{aligned} \quad (106)$$

where, again, all derivatives of F_0 are to be taken at $\vartheta = \alpha$. The integration over ψ is carried out following a procedure similar to that described by Westfold (1959), which gives

$$\frac{K_{IV}}{c} = - \frac{2\pi}{\sqrt{3}} s_q \frac{\omega_{\text{pr}}^2 |\Omega|}{c \omega^2} \cos \alpha \int m^3 c^3 \gamma d\gamma \frac{\partial F_0}{\partial \gamma} \left(\int_{\frac{\omega}{\omega_c}}^{\infty} K_{1/3}(u) du + \frac{\omega}{\omega_c} K_{1/3} \left(\frac{\omega}{\omega_c} \right) \right)$$

$$-\frac{\pi}{\sqrt{3}} s_q \frac{\omega_{\text{pr}}^2 |\Omega|}{c \omega^2} \sin \alpha \int m^3 c^3 \gamma d\gamma \left(\frac{\partial^2 F_0}{\partial \gamma \partial \vartheta} - \frac{1}{\gamma} \frac{\partial F_0}{\partial \vartheta} \right) \int_{\frac{\omega}{c}}^{\infty} K_{1/3}(u) du. \quad (107)$$

The result in equation (107) coincides with that given by Sazonov (1969a) in his equation (2.2).

5.3 Non-resonant contribution to transfer coefficients from Debye's expansion

In the non-resonant regime, the reverse inequality to equation (97) applies, though x and σ both remain large but need not be almost equal. These conditions are suitable for using the Debye expansion of Bessel functions of large indices and argument (Watson 1922; Matviyenko 1992), subject to the condition that $(\sigma - x) \gg \sigma^{1/3}$ and, in our case, that $x < \sigma$. The Debye expansion represents the Bessel functions of large index σ for a given value of the argument-to-index ratio x/σ , represented by a parameter ξ such that

$$\frac{x}{\sigma} = \frac{1}{\cosh \xi}. \quad (108)$$

The Debye expansions of $J_\sigma(x)$ and $N_\sigma(x)$ can be written as (Watson 1922):

$$J_\sigma(x) \equiv J_\sigma \left(\frac{\sigma}{\cosh \xi} \right) = + \frac{e^{\sigma(\tanh \xi - \xi)}}{\sqrt{2\pi\sigma \tanh \xi}} \sum_{m=0}^{\infty} \frac{\Gamma(m+1/2)}{\Gamma(1/2)} \frac{2^m A_m(\xi)}{(\sigma \tanh \xi)^m}, \quad (109)$$

$$N_\sigma(x) \equiv N_\sigma \left(\frac{\sigma}{\cosh \xi} \right) = - \frac{\sqrt{2} e^{\sigma(\xi - \tanh \xi)}}{\sqrt{2\pi\sigma \tanh \xi}} \sum_{m=0}^{\infty} \frac{\Gamma(m+1/2)}{\Gamma(1/2)} \frac{(-1)^m 2^m A_m(\xi)}{(\sigma \tanh \xi)^m}. \quad (110)$$

where the coefficients A_m depend on ξ , but for A_0 that equals unity. $\Gamma(y)$ denotes the gamma function of argument y . The n -th term in the sum is of order σ^{-n} , that is of order $(|\Omega|/\omega)^n$. Here we only need to proceed to second order. It can be checked that at this order the Debye approximation continuously merges into the Nicholson's approximation at their common limit of validity. While σ is regarded as a large parameter in the expansions in equations (109) and (110), the ratio x/σ should be considered of order unity. Approximations to $J'_\sigma(x)$ and $N'_\sigma(x)$ are obtained by derivating equations (109) and (110) with respect to x at fixed σ , taking care of the fact that the auxiliary variable ξ depends on x , and thus also the coefficients A_1 and A_2 . Some terms resulting from this derivation contribute at this order. All calculations done, we obtain

$$J_\sigma(x)N_\sigma(x) = \frac{(-1)}{\pi\sqrt{\sigma^2 - x^2}} \left(1 + \frac{6A_2 - A_1^2}{\sigma^2 - x^2} \right), \quad (111)$$

$$J'_\sigma(x)N_\sigma(x) = \frac{(-1)}{\pi x} \left(1 + \frac{1}{2} \frac{x^2}{(\sigma^2 - x^2)^{3/2}} + \frac{6A_2 + xA'_1 - A_1^2}{\sigma^2 - x^2} + \frac{3}{2} \frac{A_1 x^2}{(\sigma^2 - x^2)^2} \right), \quad (112)$$

$$J'_\sigma(x)N'_\sigma(x) = \frac{\sqrt{\sigma^2 - x^2}}{\pi x^2} \left(1 + \frac{6A_2 + 2xA'_1}{\sigma^2 - x^2} + \frac{2A_1 x^2}{(\sigma^2 - x^2)^2} - \frac{A_1^2}{\sigma^2 - x^2} - \frac{1}{4} \frac{x^4}{(\sigma^2 - x^2)^3} \right). \quad (113)$$

where

$$A_1 = \frac{1}{8} - \frac{5}{24} \frac{\sigma^2}{\sigma^2 - x^2}, \quad A_2 = \frac{3}{128} - \frac{77}{576} \frac{\sigma^2}{\sigma^2 - x^2} + \frac{385}{3456} \frac{\sigma^4}{(\sigma^2 - x^2)^2}, \quad xA'_1 = -\frac{5}{12} \frac{\sigma^2 x^2}{(\sigma^2 - x^2)^2}. \quad (114)$$

The first terms in the parentheses of equations (111)–(113), that are equal to unity, remain in the unmagnetized limit, $\Omega \rightarrow 0$. The non-Bessel terms in equations (86)–(87) are comparable to them. The non-resonant contributions to equations (88) and (89) are obtained by integrating these expansions of the Bessel functions over the non-resonant domain, denoted by the suffix NR:

$$f_{\text{NR}} = \frac{2\pi^2 s_q \omega_{\text{pr}}^2 \Omega^2}{c \omega^3} \iint_{\text{NR}} \frac{m^3 c^3}{\sin^2 \alpha} d\varpi d\sigma \frac{\varpi}{\pi} \frac{\partial F_0}{\partial \sigma} \left(\frac{1}{2} \frac{x^2}{(\sigma^2 - x^2)^{3/2}} + \frac{6A_2 + xA'_1 - A_1^2}{\sigma^2 - x^2} + \frac{3}{2} \frac{A_1 x^2}{(\sigma^2 - x^2)^2} \right). \quad (115)$$

$$h_{\text{NR}} = \frac{\pi^2 \omega_{\text{pr}}^2 \Omega^2}{c \omega^3} \iint_{\text{NR}} \frac{m^3 c^3}{\sin^2 \alpha} d\varpi d\sigma \frac{\partial F_0}{\partial \sigma} \frac{2\sqrt{\sigma^2 - x^2}}{\pi} \left(1 + \frac{6A_2 - A_1^2 + xA'_1}{\sigma^2 - x^2} + \frac{A_1 x^2}{(\sigma^2 - x^2)^2} - \frac{1}{8} \frac{x^4}{(\sigma^2 - x^2)^3} \right) - \frac{\pi^2 \omega_{\text{pr}}^2 \Omega^2}{c \omega^3} \iint_{\text{NR}} \frac{m^3 c^3}{\sin^2 \alpha} d\varpi d\sigma \frac{\partial F_0}{\partial \sigma} \frac{\sigma_0^2}{\pi\sqrt{\sigma^2 - x^2}} \left(1 + \frac{6A_2 - A_1^2}{\sigma^2 - x^2} \right) + \frac{\pi \omega_{\text{pr}}^2 \Omega^2}{c \omega^3} \int_{-\infty}^{+\infty} \frac{m^3 c^3}{\sin^2 \alpha} d\varpi \frac{2\varpi^2 + \sigma_0^2}{\sqrt{\varpi^2 + \sigma_0^2}} F_0(\varpi, \sigma_b(\varpi)). \quad (116)$$

It is remarkable that the terms independent of magnetization have canceled out of equation (115). They also cancel out of equation (116) as we now show. Gathering and arranging them, these terms can be written as

$$h_{\text{NR}}^{(0)} = \frac{\pi \omega_{\text{pr}}^2 \Omega^2}{c \omega^3} \iint_{\text{NR}} \frac{m^3 c^3}{\sin^2 \alpha} d\varpi d\sigma \frac{\partial F_0}{\partial \sigma} \frac{2\varpi^2 + \sigma_0^2}{\sqrt{\varpi^2 + \sigma_0^2}} + \frac{\pi \omega_{\text{pr}}^2 \Omega^2}{c \omega^3} \int_{-\infty}^{+\infty} \frac{m^3 c^3}{\sin^2 \alpha} d\varpi \frac{2\varpi^2 + \sigma_0^2}{\sqrt{\varpi^2 + \sigma_0^2}} F_0(\varpi, \sigma_b(\varpi)). \quad (117)$$

The double integral term may be integrated explicitly over σ at given ϖ since only $\partial_\sigma F_0$ depends on this variable. The integration is on the values of σ between its value $\sigma_b(\varpi)$ on the boundary \mathcal{B} of the physical domain and its value $\sigma_{\text{QR}}(\varpi) = (\varpi^2 + \sigma_0^2)^{3/4} / \sqrt{3}$ on the boundary \mathcal{B}_{QR} between the non-resonant and quasi-resonant domains. The contribution from the

lower boundary, $\sigma_b(\varpi)$, cancels the term that was already in the form of a single integral over ϖ . The contribution from the upper boundary at $\sigma_{\text{QR}}(\varpi)$ remains and could as well be considered to be part of the quasi-resonant contribution since it can be written as an integral over the quasi-resonant domain. Naming this contribution h_{BQR} :

$$h_{\text{BQR}} = \frac{\pi\omega_{\text{pr}}^2\Omega^2}{c\omega^3} \int_{-\infty}^{+\infty} \frac{m^3c^3}{\sin^2\alpha} d\varpi \frac{2\varpi^2 + \sigma_0^2}{\sqrt{\varpi^2 + \sigma_0^2}} F_0(\varpi, \sigma_{\text{bqr}}(\varpi)) = - \frac{\pi\omega_{\text{pr}}^2\Omega^2}{c\omega^3} \iint_{\text{QR}} \frac{m^3c^3}{\sin^2\alpha} d\varpi d\sigma \frac{2\varpi^2 + \sigma_0^2}{\sqrt{\varpi^2 + \sigma_0^2}} \frac{\partial F_0}{\partial \sigma}. \quad (118)$$

We refer to the remainder of the non-resonant contribution to h as the reduced non-resonant contribution \hat{h}_{NR} :

$$\hat{h}_{\text{NR}} = \pi \frac{\omega_{\text{pr}}^2\Omega^2}{c\omega^3} \iint_{\text{NR}} \frac{m^3c^3}{\sin^2\alpha} d\varpi d\sigma \left(2 \left(\frac{6A_2 - A_1^2 + xA_1'}{(\sigma^2 - x^2)^{1/2}} + \frac{A_1x^2}{(\sigma^2 - x^2)^{3/2}} - \frac{1}{8} \frac{x^4}{(\sigma^2 - x^2)^{5/2}} \right) - \sigma_0^2 \left(\frac{6A_2 - A_1^2}{(\sigma^2 - x^2)^{3/2}} \right) \right) \frac{\partial F_0}{\partial \sigma}. \quad (119)$$

The \mathcal{B}_{QR} contribution to h in equation (118) is then associated to the quasi-resonant contribution h_{QR} in equation (100) to form a reduced quasi-resonant contribution \hat{h}_{QR} :

$$\hat{h}_{\text{QR}} = \frac{\omega_{\text{pr}}^2\Omega^2}{c\omega^3} \iint_{\text{QR}} \frac{m^3c^3}{\sin^2\alpha} d\varpi d\sigma \left(\frac{4x^2}{\sqrt{3}} \left(\frac{\sigma - x}{x} \right)^2 K_{\frac{2}{3}}(g) L_{\frac{2}{3}}(g) + \frac{2\varpi^2}{\sqrt{3}} \left(\frac{\sigma - x}{x} \right) K_{\frac{1}{3}}(g) L_{\frac{1}{3}}(g) - \pi \frac{2\varpi^2 + \sigma_0^2}{\sqrt{\varpi^2 + \sigma_0^2}} \right) \frac{\partial F_0}{\partial \sigma}. \quad (120)$$

The combinations of the functions A_1 , A_2 and xA_1' that appear in equations (115) and (119) may be expressed in terms of σ and x by using equation (114). When the integration over the NR domain can be extended to the full domain, this results in equations (28)–(29).

5.4 Non-resonant versus quasi-resonant contribution to the Faraday coefficients

The quasi-resonant contributions to the Faraday coefficients are given by equations (99) and (120) and the non-resonant ones by equations (115) and (119). We now compare them, making a simple Ansatz concerning the distribution function, namely that F_0 is a linear function of ϖ , so that $\partial_\sigma F_0 = F_{0\sigma}(\sigma) + \varpi F_{0\sigma\varpi}(\sigma)$. The $F_{0\sigma}$ term produces a nil contribution to f if, as assumed here, it depends on σ alone. The $\varpi F_{0\sigma\varpi}$ term produces a vanishing contribution to h since its kernel is an even functions of ϖ . This Ansatz is sufficient to give a hint on the dependence of the transfer coefficients on the distribution function. The contributions f_{NR} and f_{QR} to f , or h_{NR} and h_{QR} to h , may then be written in a form involving a kernel depending on σ , such that

$$f_{\text{R}} = 2s_q \frac{\omega_{\text{pr}}^2\Omega^2}{c\omega^3} \int_{\text{R}} \frac{m^3c^3}{\sin^2\alpha} d\sigma K_{\text{R}}^{(f)}(\sigma) F_{0\sigma\varpi}(\sigma), \quad h_{\text{R}} = \frac{\omega_{\text{pr}}^2\Omega^2}{c\omega^3} \int_{\text{R}} \frac{m^3c^3}{\sin^2\alpha} d\sigma K_{\text{R}}^{(h)}(\sigma) F_{0\sigma}(\sigma). \quad (121)$$

where R stands either for the QR or NR domain and $K_{\text{R}}^{(f)}(\sigma)$ and $K_{\text{R}}^{(h)}(\sigma)$ are corresponding one-variable kernels, integrated over ϖ at given σ . For Faraday rotation:

$$K_{\text{NR}}^{(f)}(\sigma) = \int_{\text{NR}} d\varpi \frac{\pi}{2} \frac{\varpi^2 x^2}{(\sigma^2 - x^2)^{3/2}}, \quad K_{\text{QR}}^{(f)}(\sigma) = \int_{\text{QR}} d\varpi \frac{2^{3/2}}{3^{1/2}} \varpi^2 x \left(\frac{\sigma - x}{x} \right)^{3/2} \left(K_{2/3}(g) L_{1/3}(g) - \frac{\pi}{\sqrt{3}g} \right). \quad (122)$$

The quasi-resonant kernel for f , on the right of equation (122), can be expressed in terms of the variable g from equations (H4) and then be integrated over the quasi-resonant domain $g_{\text{m}}(\sigma) < g < 1$. The lower bound g_{m} , defined in equation (H4), approaches zero when σ diverges. The integral on the right of equation (122) converges as g_{m} approaches zero, which it does when σ grows much larger than σ_{qr} . The asymptotic non-resonant part of the kernel of f can be calculated as shown in appendix H. The results, valid for $\sigma \gg \sigma_{\text{qr}}$, are:

$$K_{\text{NR}}^{(f)}(\sigma) \approx \frac{\pi}{3} \sigma^2 \ln \left(\frac{\sigma}{3} \right), \quad K_{\text{QR}}^{(f)}(\sigma) \approx 0.6 \sigma^2. \quad (123)$$

The non-resonant contribution to f slightly dominates when $\sigma \gg \sigma_{\text{qr}}$. These results partly depend on our assumption that the distribution function depends linearly on ϖ . Otherwise, f_{NR} would also have a term proportional to $F_{0\sigma}$ that is absent from equation (121) by parity. We return to this in section 6.3.

The ϖ -integrated kernel for h being defined as in equation (121), its non-resonant part results from equation (119) and is calculated in Appendix H. The quasi-resonant part \hat{h}_{QR} is given by equation (120) and its calculation is also outlined in this Appendix. The kernels $K_{\text{NR}}^{(h)}(\sigma)$ and $K_{\text{QR}}^{(h)}(\sigma)$ turn out to be approximately given, for $\sigma \gg \sigma_{\text{qr}}$ by

$$K_{\text{NR}}^{(h)}(\sigma) \approx -\frac{\pi}{8} \left(\frac{\sigma}{3} \right)^{4/3}, \quad K_{\text{QR}}^{(h)}(\sigma) \approx +\frac{\pi}{2} \sigma^{4/3}. \quad (124)$$

A glance at equation (124) shows that both contributions to the kernel $K^{(h)}$ vary when $\sigma \gg \sigma_{\text{qr}}$ as $\sigma^{4/3}$, the quasi-resonant one being numerically larger.

The scaling in $\sigma^{4/3}$ anticipated for the h kernel from equations (124) does not conflict with the fact that the Faraday conversion coefficient h decreases to zero at high temperature for thermal distributions (Huang & Shcherbakov 2011). We have confirmed this decline of h^{th} with temperature by numerically integrating equation (89) for a thermal distribution function

and checked its compatibility with a kernel in $\gamma^{4/3}$. We return to this in section 6.2. The Faraday conversion coefficient h is largely affected by the quasi-resonant contribution to it, which is of an opposite sign to the non-resonant one. Equations (31) and (32) propose a simple, though crude, way to account for the increasing importance of the quasi-resonant contribution which should be good enough wherever the balance passes from non-resonant to quasi-resonant domination. For a given ω , the QR domain becomes narrower in angle as γ increases and the QR kernel has an effectively compact support in this domain. Therefore our calculation in equation (124) of the quasi-resonant contribution to h should be close to being exact at large γ 's, since $\partial F_0/\partial\sigma$ certainly is almost constant with ϖ over the narrow QR domain, as was assumed in this section.

The condition for the quasi-resonant domain not to contribute to the transfer coefficients is that the distribution function be negligible in it. From equation (92), this happens when for most particles $\sigma - \sqrt{\sigma^2 - \sigma_0^2} > \sigma^{1/3}$, or equivalently when the variable g in equation (94) is larger than unity. Expanding the expression of the latter condition in σ_0/σ and noting that $\sigma = \gamma u \sin^2\alpha$ at $\varpi = 0$, this inequality reduces again to the condition that equation (27) be satisfied. Up to a somewhat arbitrary factor, the parameter on the left of equation (27) is similar to the square of the regime-change parameters X and $\gamma_0 X_A$ respectively defined by Shcherbakov (2008) and Huang & Shcherbakov (2011). When the inequality in equation (27) is not satisfied, the coefficients f and h differ from their high-frequency approximations in equations (145) and (146) below, where the integration is meant to extend over the full ϖ - σ domain. The intrusion of quasi-resonant contributions is at the origin of the change in the trend of the variations of f and h with temperature described by Shcherbakov (2008) for thermal distributions. This author attributes this change to a failure of the high-frequency expansion, which is correct in the sense that the quasi-resonant contribution cannot be expressed in the form of a series expansion, no partial sum of the Debye series being able to represent the Bessel function in the domain of validity of the Nicholson's approximation.

6 LOW-FREQUENCY KERNELS OF FARADAY COEFFICIENTS OF ISOTROPIC DISTRIBUTIONS

6.1 Remarks on the low-frequency limit of isotropic kernels for the Faraday coefficients

In the limit of large γ 's, the quasi-resonant domain contributes little to the Faraday rotation coefficient f , given by equation (88), because it involves the integral of an odd function of the difference $\psi = \vartheta - \alpha$ on the small QR domain. This remark holds also for the integral over this same quasi-resonant domain of the non-resonant contribution. For an isotropic distribution, there is however a non-vanishing NR contribution to f that is proportional to $\partial_\gamma F_0$. Such a contribution is absent for distributions, as considered in section 5.4, that are linear in ϖ .

By contrast, the quasi-resonant domain, if substantially populated with particles, largely contributes the Faraday conversion coefficient h . Particles in the QR domain satisfy the inequality inverse to that in equation (27) in a strong sense. We refer to the case when this strong inequality is satisfied as the low-frequency limit. Since any isotropic distribution function depends on γ only, the Faraday coefficients for such distributions can be reduced to a single quadrature over the Lorentz factor involving a γ -dependent kernel as defined in equations (33). The exact expression of the isotropic kernel for f results from equation (88) in which the variables ϖ - σ should be changed to ϖ - γ , giving on integrating over ϖ at a given γ

$$F^{\text{iso}}(\gamma) = -\frac{2\pi^2 s_q}{\sin^2\alpha} \int_{\varpi_-}^{\varpi_+} d\varpi \varpi x \left(J'_\sigma(x) N_\sigma(x) + \frac{1}{\pi x} \right). \quad (125)$$

The exact isotropic kernel for h is similarly obtained from equation (87), in which the principal value term should be neglected. Using equations (A1)–(A7), the isotropic kernel for h can be written as:

$$H^{\text{iso}}(\gamma) = \frac{\pi^2}{\sin^2\alpha} \int_{\varpi_-}^{\varpi_+} d\varpi \left(x^2 J'_\sigma(x) N'_\sigma(x) - \varpi^2 J_\sigma(x) N_\sigma(x) - \frac{1}{\pi} (\gamma u \sin^2\alpha + 2\varpi \cos\alpha) \right). \quad (126)$$

In equations (125) and (126), the bounds $\varpi_\pm(\gamma)$ are defined by equation (37). The kernel $H^{\text{iso}}(\gamma)$ could have been deduced as well from equation (89), reformulating the line-integral term in it as a surface integral. These different expressions are equivalent because the non-Bessel integrals in them, though apparently different, are actually equal, given the particular values of the bounds.

6.2 Thermal Faraday conversion coefficient in the low-frequency limit

To check the behaviour of the Faraday conversion coefficient h in the low-frequency limit, we have numerically integrated its quasi exact expression in equation (126) with `Mathematica` for a thermal distribution function. At a given frequency, the low-frequency limit would then correspond to the limit of high temperatures. Huang & Shcherbakov (2011) have found that in this limit the Faraday conversion coefficient decreases with temperature. We confirm this and find that this decrease scales as $-T^{-5/3}$ by extending our numerical calculations to high values of the temperature T (see figure 2). This has been possible by using the uniform expansion for high order Bessel functions derived by Olver (1954) which allows a fast and reliable calculation of high order Bessel functions (see Appendix G). Returning the result of the integration over the directions of

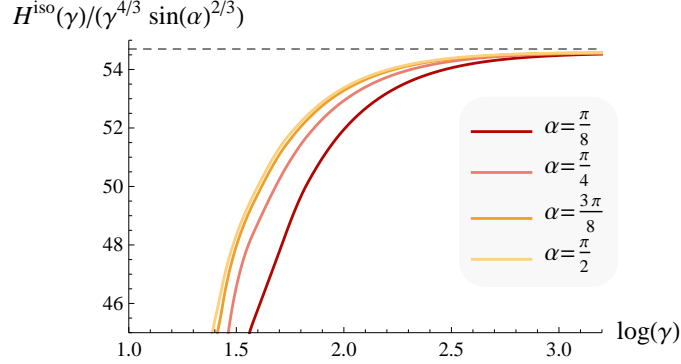


Figure 7. The evolution of $H^{\text{iso}}(\gamma)/(\gamma^{4/3} \sin^2(\alpha)^{2/3})$ (computed via equation (126) using the Olver expansion) as a function of γ for different values of α . The radiation's parameter $u = 15$. For all values of α , this ratio asymptotes to a constant for large γ . The dashed line corresponds to the asymptotic prediction of equation (138).

the particles before performing that over γ reveals the high energy properties of the isotropic kernels derived in sections 6.3 and 6.4. This numerically supports the analytical result, reached in section 6.4 and shown in figure 7, that the kernel of h asymptotically grows with the Lorentz factor as $\gamma^{4/3}$ and shows that this increase with energy of the kernel is consistent with the fast decline with temperature of the thermal Faraday conversion coefficient. Note finally that, considering equations (42) and (33), equation (138) predicts at large γ the result of the numerical integration and the $T^{-5/3}$ asymptote for the thermal distribution.

6.3 Isotropic kernel of the Faraday rotation coefficient in the low-frequency limit

The integral in equation (125) may be separated into non-resonant and quasi-resonant parts as follows. The Faraday rotation kernel $F^{\text{iso}}(\gamma)$ is the sum of the expression in equation (115), integrated over the NR domain and limited to its lowest order term in Ω/ω , and of the QR contribution from equation (99). The integral over the NR domain in equation (115) can be extended to the full domain at the expense of adding, if needed, to the contribution from equation (99) a correction to account for the undue integration over the quasi-resonant domain so introduced. After the necessary change of variables, and considering the result in equation (38), the kernel $F^{\text{iso}}(\gamma)$ assumes the, still exact, form

$$\begin{aligned}
 F^{\text{iso}}(\gamma) &= 4\pi s_q \frac{\omega \cos \alpha}{|\Omega|} \left(\gamma \mathcal{L}(\gamma) - \sqrt{\gamma^2 - 1} \right) - \pi s_q \frac{\Theta_H(\gamma - \gamma_{\text{qr}})}{\sin^2 \alpha} \int_{\text{QR}} d\varpi \frac{\varpi x^2}{(\sigma^2 - x^2)^{3/2}} \\
 &\quad + 2s_q \frac{\Theta_H(\gamma - \gamma_{\text{qr}})}{\sin^2 \alpha} \int_{\text{QR}} d\varpi \varpi \left(\sqrt{3} g K_{2/3}(g) L_{1/3}(g) - \pi \right). \tag{127}
 \end{aligned}$$

The first term on the first line of equation (127) is the non-resonant isotropic kernel, calculated by integration over the full physical domain. The second term on the first line is an integral at given γ over the quasi-resonant domain correcting for the fact that the non-resonant domain really does not extend over the full physical one. The second line is the quasi-resonant contribution proper. The variables σ , x and g are functions of γ and ϖ that may be found from appendix A and equation (94). The QR integration over ϖ is between $\varpi_{\text{qr}-}$ and $\varpi_{\text{qr}+}$ defined in the caption of figure 6.

As γ approaches infinity, the interval $[\varpi_{\text{qr}-}, \varpi_{\text{qr}+}]$ becomes more and more symmetrical about zero while $g(+\varpi, \gamma)$ and $g(-\varpi, \gamma)$ converge to each other. The second and third terms in equation (127) then approach the integral of an odd function over an interval symmetrical with respect to $\varpi = 0$, which then vanishes. As for the circular polarization absorption coefficient K_{IV} calculated in section 5.2, higher order terms determine the QR contribution. Since only isotropic distributions are considered in this section, corrections caused by the anisotropy of the distribution function are absent. However, the interval $[\varpi_{\text{qr}-}, \varpi_{\text{qr}+}]$ is slightly asymmetrical with respect to $\varpi = 0$, which gives rise to a first order "offset" correction. Moreover, $\sigma(+\varpi, \gamma)$ and $\sigma(-\varpi, \gamma)$ slightly differ when $\varpi \ll \gamma u \sin^2 \alpha$, as can be seen from equation (A1), and then $g(+\varpi, \gamma)$ and $g(-\varpi, \gamma)$ differ by the quantity g_1 in equation (105). Thus the integrands in the QR integrals in equation (127) have a small even part that gives rise to a "parity" correction to these integrals. At large γ 's, the offset $\Delta\varpi_{\text{qr}}$ is given by the expansions in equations (J2)–(J3), eventually giving for the offset correction (appendix K):

$$F_{\text{off}}^{\text{iso}}(\gamma) = -\frac{4\pi s_q}{3} \gamma u \cos \alpha + 8s_q \gamma u \cos \alpha \left(\sqrt{3} K_{2/3}(1) L_{1/3}(1) - \pi \right). \tag{128}$$

The parity corrections are evaluated by integrating the even part of the integrands in equation (127) over the symmetric interval $[-3^{1/3}(\gamma u \sin^2 \alpha)^{2/3}, +3^{1/3}(\gamma u \sin^2 \alpha)^{2/3}]$. The even part of the integrand on the second line of equation (127) is obtained by Taylor-expanding in g the function in the parenthesis about g_0 as in equation (105), then performing the integration by using

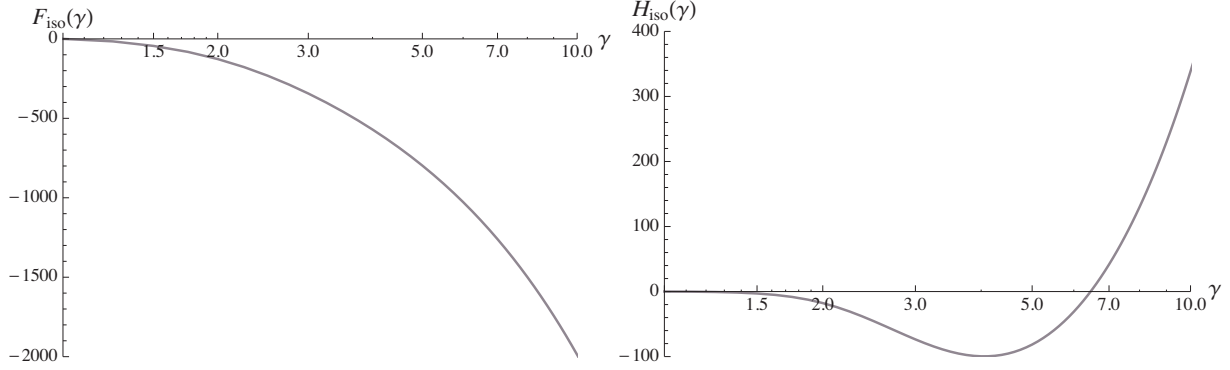


Figure 8. The isotropic kernels $F^{\text{iso}}(\gamma)$ (left panel) and $H^{\text{iso}}(\gamma)$ (right panel) as given by equations (125) and (126). The parameters of the radiation are $\omega = 15 |\Omega|$ and $\alpha = \pi/4$

g as the integration variable. To sufficient accuracy, g is related to ϖ by the lowest-order relation in equation (J6). The minimum value g_m of g , reached at $\varpi = 0$, is given by equation (H4) and approaches zero as γ grows larger. The parity correction from the second line of equation (127) is thus evaluated taking $g_m = 0$. The calculation of the parity correction from the first line is more straightforward. All calculations done (appendix K), it is found that

$$F_{\text{par}}^{\text{iso}}(\gamma) = -\pi s_q \gamma u \cos \alpha \left[\frac{8}{3} \ln(\gamma) + \frac{4}{3} \ln\left(\frac{\sin \alpha}{u}\right) + 2 \ln(4) + \frac{4}{3} \ln(3) - 4 + \frac{8\sqrt{3}}{\pi} \int_0^1 dg g \frac{d}{dg} \left(\sqrt{3} g K_{2/3}(g) L_{1/3}(g) \right) \right]. \quad (129)$$

An asymptotic expansion of F^{iso} for large γ 's is finally obtained by expanding the first term of equation (127) up to order γ , integrating by parts the last term of equation (129), which partly simplifies with the second term of equation (128), and numerically calculating the coefficients of the terms of the expansion. This gives

$$F_{\text{LF}}^{\text{iso}}(\gamma) = \pi s_q \gamma u \cos \alpha \left(\frac{4}{3} \ln\left(\frac{\gamma u}{\sin \alpha}\right) - 1.26072439 \right). \quad (130)$$

6.4 Isotropic kernel of the Faraday conversion coefficient in the low-frequency limit

The integral in equation (126) can be separated into a non-resonant and a quasi-resonant contribution. This is best achieved by writing the kernel $H^{\text{iso}}(\gamma)$ as the sum of the contributions to it from equations (119) and (120), which may be modified by extending the former integral to the full σ - ϖ domain and adding to equation (120) a correction to account for the undue integration over the quasi-resonant domain so introduced. The variables are then changed to γ and ϖ . The extended non-resonant contribution then provides the result in equation (39) while the expression for the correction to the quasi-resonant contribution is similar to that in equation (35), the boundaries of the integral over ϖ being however placed at $\varpi_{qr+}(\gamma)$ and $\varpi_{qr-}(\gamma)$ on the edge of the quasi-resonant domain shown in figure 6. The kernel $H^{\text{iso}}(\gamma)$ then takes the form

$$H^{\text{iso}}(\gamma) = -\frac{\pi}{2} \sin^2 \alpha \left(\gamma(2\gamma^2 - 3) \sqrt{\gamma^2 - 1} + \mathcal{L}(\gamma) \right) + \frac{\Theta_H(\gamma - \gamma_{qr})}{\sin^2 \alpha} \int_{\varpi_{qr-}}^{\varpi_{qr+}} d\varpi \frac{\pi}{8} \left(\frac{2x^4}{(\sigma^2 - x^2)^{5/2}} + \sigma_0^2 \frac{x^2(4\sigma^2 + x^2)}{(\sigma^2 - x^2)^{7/2}} \right) \\ + \frac{\Theta_H(\gamma - \gamma_{qr})}{\sin^2 \alpha} \int_{\varpi_{qr-}}^{\varpi_{qr+}} d\varpi \left(\frac{4x^2}{\sqrt{3}} \left(\frac{\sigma - x}{x} \right)^2 K_{2/3}(g) L_{2/3}(g) + \frac{2\varpi^2}{\sqrt{3}} \left(\frac{\sigma - x}{x} \right) K_{1/3}(g) L_{1/3}(g) - \pi \frac{2\varpi^2 + \sigma_0^2}{\sqrt{\varpi^2 + \sigma_0^2}} \right). \quad (131)$$

The first term on the first line of equation (131) is the non-resonant isotropic kernel, calculated by integration over the full physical domain. The second term on the first line is an integral over the quasi-resonant domain correcting for the fact that the non-resonant domain really does not extend over the full physical one. The second line is the quasi-resonant contribution proper. The low-frequency limit of this kernel is to be obtained from an asymptotic expansion in γ of the right hand side of equation (131). This low-frequency development is valid when $\gamma \gg \gamma_{qr} \approx (u/(3 \sin \alpha))^{1/2}$. The domain of validity of the low-frequency limit is where $\omega \ll 3\gamma^2 \sin \alpha |\Omega|$ (equation (27)), which is equivalent to $\omega \ll \omega_c(\gamma, \alpha)$, where ω_c is the characteristic frequency of synchrotron emission defined in equation (101).

As discussed in section 5.1, the variable g in equation (94) is less than unity in the QR domain. At the order required by the calculations in this subsection, the lowest order approximation to the values of $\varpi_{qr\pm}(\gamma)$ is sufficient, namely

$$\varpi_{qr\pm}(\gamma) \approx \pm (3\gamma^2 u^2 \sin^4 \alpha)^{1/3}. \quad (132)$$

From equations (A1)–(A2), the integrand on the first line of equation (131) can be written in terms of ϖ and γ , or $G =$

$\gamma u \sin^2 \alpha / 3$, as:

$$\begin{aligned} \frac{2x^4}{(\sigma^2 - x^2)^{5/2}} + \sigma_0^2 \frac{x^2(4\sigma^2 + x^2)}{(\sigma^2 - x^2)^{7/2}} &= \frac{162G^4}{(\varpi^2 + \sigma_0^2)^{5/2}} \left(1 + \frac{2\varpi \cos \alpha}{3G} - \frac{\varpi^2 \sin^2 \alpha + \sigma_0^2}{9G^2} \right)^2 \\ &+ \frac{405\sigma_0^2 G^4}{(\varpi^2 + \sigma_0^2)^{7/2}} \left(1 + \frac{2\varpi \cos \alpha}{3G} - \frac{\varpi^2 \sin^2 \alpha + \sigma_0^2}{9G^2} \right) \left(1 + \frac{2\varpi \cos \alpha}{3G} + \frac{5\varpi^2 \cos^2 \alpha - \varpi^2 - \sigma_0^2}{45G^2} \right). \end{aligned} \quad (133)$$

The primitive of this function is shown in Appendix J. The integral over ϖ that appears in the second term of the first line of equation (131) can be obtained from it and expanded to the required order in γ . It is inferred from section 5.4 that this order should be $\mathcal{O}(\gamma^{4/3})$. The expansion procedure, outlined in Appendix J, leads to

$$\frac{\pi}{8 \sin^2 \alpha} \int_{\varpi_{qr-}}^{\varpi_{qr+}} d\varpi \left(\frac{2x^4}{(\sigma^2 - x^2)^{5/2}} + \sigma_0^2 \frac{x^2(4\sigma^2 + x^2)}{(\sigma^2 - x^2)^{7/2}} \right) \approx \pi \sin^2 \alpha \gamma^4 - 2\pi \sin^2 \alpha \gamma^2 - \frac{\pi}{8} \sin^{2/3} \alpha \left(\frac{\gamma u}{3} \right)^{4/3}. \quad (134)$$

The properly quasi-resonant contribution to $H^{\text{iso}}(\gamma)$ originates from the integration over ϖ of the second line in equation (131). This contribution is calculated to order $\gamma^{4/3}$ by changing the variable ϖ for the variable g on which the K and L functions depend, much as was done in section 5.4, but for the fact that the integration over ϖ is now performed at constant γ instead of at constant σ . Some details are presented in Appendix J. From these calculations it is found that the low frequency limit to the quasi-resonant contribution to the kernel $H^{\text{iso}}(\gamma)$ is

$$H_{\text{QR}}^{\text{iso}}(\gamma) = 2(\gamma u)^{4/3} (\sin \alpha)^{2/3} 3^{1/6} \int_0^1 dg g^{2/3} \left(K_{2/3}(g)L_{2/3}(g) + K_{1/3}(g)L_{1/3}(g) - \frac{2\pi}{\sqrt{3}g} \right). \quad (135)$$

The integrand in equation (135) declines rapidly to zero out of the quasi-resonant domain (see section 5.4) and the value of the definite integral over g is, with a relative error of only 10^{-4} , equal to $\pi/(4 \cdot 3^{1/6})$. Adopting this value, we eventually get

$$H_{\text{QR}}^{\text{iso}}(\gamma) \approx \frac{\pi}{2} (\sin \alpha)^{2/3} (\gamma u)^{4/3}. \quad (136)$$

Accounting for the slightly different definitions of $H^{\text{iso}}(\gamma)$ and $K_{\text{QR}}^{(h)}(\sigma)$ in equations (33) and (121), the results in equations (136) and (124) are entirely equivalent since at fixed γ the quasi-resonant domain is concentrated near $\varpi = 0$ at $\sigma = \gamma u \sin^2 \alpha$. This was not unexpected because the quasi-resonant domain is of a very small angular extent, so that the quasi-resonant contribution is insensitive to the fact that the distribution function is isotropic or otherwise. Finally, the asymptotic expansion in γ of the first term in equation (131), limited to the order $\gamma^{4/3}$, is

$$-\frac{\pi}{2} \sin^2 \alpha \left(\gamma(2\gamma^2 - 3) \sqrt{\gamma^2 - 1} + \mathcal{L}(\gamma) \right) \approx -\frac{\pi}{2} \sin^2 \alpha (2\gamma^4 - 4\gamma^2). \quad (137)$$

The complete $H^{\text{iso}}(\gamma)$ kernel in the low-frequency limit is the sum of the three contributions in equations (134), (136) and (137). The large terms proportional to γ^4 and γ^2 cancel out and the net result is, at low frequency:

$$H_{\text{LF}}^{\text{iso}}(\gamma) \approx \frac{\pi}{8} (\gamma u)^{4/3} (\sin \alpha)^{2/3} \left(4 - \frac{1}{3^{4/3}} \right). \quad (138)$$

This result is in complete agreement with those in equation (124) and confirms that in the low frequency limit neither the resonant nor the non-resonant contribution to h predominates.

6.5 Approximate expressions for the isotropic kernels over the full energy range

Equations (38)–(39) provide expressions for the isotropic kernels in the HF regimes that are valid in the interval $[1, \gamma_{\text{qr}}]$, although when γ approaches γ_{qr} from below more terms should be retained in the Debye's expansion. Equations (130) and (138) provide expressions of the kernels in the asymptotic LF regime at $\gamma \gg \gamma_{\text{qr}}$. The transition between the HF regime and the asymptotic LF regime should take place over an interval $\gamma_{\text{qr1}} < \gamma < \gamma_{\text{qr2}}$, where $\gamma_{\text{qr1}} = A_1 \gamma_{\text{qr}}$ and $\gamma_{\text{qr2}} = A_2 \gamma_{\text{qr}}$ and $A_1 < 1$ and $A_2 > 1$ are coefficients of order unity. For the kernel $F^{\text{iso}}(\gamma)$ these coefficients should be close to unity because the change from the HF regime to the LF regime for this coefficient is dim. For $H^{\text{iso}}(\gamma)$, or its derivative $H'^{\text{iso}}(\gamma)$, A_2 is more likely to be of order of several units since figure 7 shows that the asymptotic regime is in this case slowly reached. The figure 8 shows that exact kernels are continuous and at least once differentiable. Our proposed approximation adopts the HF expressions (38) and (39) at $\gamma < \gamma_{\text{qr1}}$ and extends them into the LF domain by a function that connects at γ_{qr1} to the HF expression and to its first order derivative and asymptotically merges into the LF limit in equations (130) or (138). The kernels themselves or their derivatives could be interpolated that way, according to whether one is wishing to use equations (33) as they stand or to calculate them by integrating by parts. We opted for the second method for the coefficient h , which minimizes the inaccuracies due to the existence of singularities in the derivative of the distribution functions of truncated power laws. We interpolate from γ_{qr1} to infinity by connection functions $C_c(\gamma - \gamma_{\text{qr1}})$ that we define for coefficient c ($= f$ or h) and element i in the connection ($i = 1$ for HF and $i = 2$ for LF) by

$$C_{ci}(\gamma - \gamma_{qr1}) = \left(1 - \exp\left(-\frac{(\gamma - \gamma_{qr1})}{\lambda_{ci} \gamma_{qr1}}\right) \right)^2. \quad (139)$$

The fact that this function is a square warrants that the interpolated function and its first derivative are continuous at γ_{qr1} when the functions to be joined are. The extrapolations of the HF expressions to the LF domain that appear on the second lines of equations (140)–(141) must then be continuous and derivable at γ_{qr1} but are otherwise unconstrained. A linear extrapolation proved satisfactory for F^{iso} , taking in this case $\gamma_{qr1} = \gamma_{qr2} = \gamma_{qr}$. Due to the non-negligible gap that the interpolation should bridge between the high-frequency and the low-frequency regime, the interpolation formula for the derivative $H^{\text{iso}}(\gamma)$ of the kernel of the h coefficient is more sophisticated. A value of γ_{qr1} smaller than γ_{qr} has been chosen, and the extrapolation of the HF behaviour in the LF domain at $\gamma > \gamma_{qr1}$ has been endowed with a local bump that is meant to represent the cumulative effect of higher order terms in the Debye expansion when approaching its limit of validity.

The decrement parameter λ_{ci} is a constant, chosen to optimize the fit to the exact kernels in figure 8. For the kernel F^{iso} we have adopted $\lambda_{f1} = \lambda_{f2} = 1/(1.7)$. For the derivative $H^{\text{iso}}(\gamma)$ of the kernel of h we have adopted $\gamma_{qr1} = 0.7\gamma_{qr}$ and different decrement parameters λ_{ci} in equations (139), namely $\lambda_{h1} = 0.4$ and $\lambda_{h2} = 1.8$. Other relevant parameters are described below. The resulting interpolation formulae for $F^{\text{iso}}(\gamma)$ and $H^{\text{iso}}(\gamma)$ at $\gamma > \gamma_{qr1}$ are

$$F_{\text{int}}^{\text{iso}}(\gamma) = \pi s_q u \cos \alpha \left[C_f(\gamma - \gamma_{qr}) \gamma \left(\frac{4}{3} \ln \left(\frac{\gamma u}{\sin \alpha} \right) - 1.26072439 \right) + (1 - C_f(\gamma - \gamma_{qr})) \times \right. \\ \left. \left(4\gamma_{qr} \ln \left(\gamma_{qr} + \sqrt{\gamma_{qr}^2 - 1} \right) - 4\sqrt{\gamma_{qr}^2 - 1} + 4 \ln \left(\gamma_{qr} + \sqrt{\gamma_{qr}^2 - 1} \right) (\gamma - \gamma_{qr}) \right) \right], \quad (140)$$

$$H_{\text{int}}^{\text{iso}}(\gamma) = C_{h2}(\gamma - \gamma_{qr1}) \left(-\frac{\pi}{6} (u^2 \sin \alpha)^{2/3} \left(4 - \frac{1}{3^{4/3}} \right) \gamma^{1/3} \right) + (1 - C_{h1}(\gamma - \gamma_{qr1})) \times \\ \frac{\pi \sin^2 \alpha}{2} \left[4(2\gamma_{qr1}^2 - 1) \sqrt{\gamma_{qr1}^2 - 1} + \frac{4(6\gamma_{qr1}^2 - 5)\gamma_{qr1}}{\sqrt{\gamma_{qr1}^2 - 1}} (\gamma - \gamma_{qr1}) + \eta \frac{\left(\frac{\gamma - \gamma_{qr1}}{\mu \gamma_{qr1}} \right)^2}{1 + \left(\frac{\gamma - \gamma_{qr1}}{\mu \gamma_{qr1}} \right)^3} \right]. \quad (141)$$

The coefficient $\eta = 103$ and $\mu = \lambda_{h1}/1.5$. The transition value γ_{qr} rigorously is the value of γ that causes the line of constant γ in figure 6 to tangent the NR-QR boundary. It slightly differs from the γ value associated to σ_{qr} at $\varpi = 0$ that is approximately representative of it and to which it reduces for $\cos \alpha = 0$. In our numerical evaluations we used the exact value, given by

$$\gamma_{qr} u \sin^2 \alpha = \sqrt{\frac{u \sin \alpha}{3}} (u \sin \alpha - \cos^2 \alpha) \quad (142)$$

In appendix L we give some examples of Faraday coefficients derived from the interpolating formulae (140)–(141) and contrast them with the quasi exact ones obtained by double integration over ϖ and σ of the expressions in equations (25) and (26). The accuracy of the fit provided by the interpolating formulae is of order or better than about 10% in this frequency range.

7 CONCLUSION

7.1 Summary of the results in the different regimes

We have derived an almost exact expression for the Faraday transfer coefficients in the form of equations (25)–(26), which we repeat here, as expressed in terms of the ϖ – σ variables defined in equation (23):

$$f = -\frac{2\pi^2 s_q}{c} \frac{\omega_{\text{pr}}^2 \Omega^2}{\omega^3} \iint \frac{m^3 c^3}{\sin^2 \alpha} d\varpi d\sigma \varpi x \frac{\partial F_0}{\partial \sigma} \left[J'_\sigma(x) N_\sigma(x) + \frac{1}{\pi x} \right]. \quad (143)$$

$$h = \frac{\pi^2 \omega_{\text{pr}}^2 \Omega^2}{c \omega^3} \iint \frac{m^3 c^3}{\sin^2 \alpha} d\varpi d\sigma \left[\frac{\partial F_0}{\partial \sigma} (x^2 J'_\sigma(x) N'_\sigma(x) - \varpi^2 J_\sigma(x) N_\sigma(x)) + \frac{1}{\pi} \left(\varpi \frac{\partial F_0}{\partial \varpi} - \sigma \frac{\partial F_0}{\partial \sigma} \right) \right]. \quad (144)$$

These expressions, which involve a two-real-variables integration, are completely general, applying to isotropic as well as to non-isotropic distributions and encompassing all regimes of particle-wave interaction. The Olver uniform expansions of high order Bessel functions presented in Appendix G can be used to speed up the integration in equations (143) and (144) when very high orders σ must be considered. In the high-frequency limit, when quasi-resonant contributions to these integrals are negligible, the transfer coefficients can be more simply written as

$$f_{\text{HF}} = 2\pi s_q \frac{\omega_{\text{pr}}^2 \Omega^2}{c \omega^3} \iint \frac{m^3 c^3}{\sin^2 \alpha} d\varpi d\sigma \left(\frac{1}{2} \frac{\varpi x^2}{(\sigma^2 - x^2)^{3/2}} \right) \frac{\partial F_0}{\partial \sigma}, \quad (145)$$

$$h_{\text{HF}} = -\pi \frac{\omega_{\text{pr}}^2 \Omega^2}{c \omega^3} \iint \frac{m^3 c^3}{\sin^2 \alpha} d\varpi d\sigma \left(\frac{1}{8} \frac{2x^4(\sigma^2 - x^2) + \sigma_0^2 x^2(4\sigma^2 + x^2)}{(\sigma^2 - x^2)^{7/2}} \right) \frac{\partial F_0}{\partial \sigma}. \quad (146)$$

Within the high-frequency limit, these expressions are also completely general. The integrands in equations (145)–(146) are more regular than those in equations (143)–(146). The integration over ϖ in equations (145) and (146), although it is meant to

cover the non-resonant domain only, extends in the high-frequency limit to the full physical domain by lack of a quasi-resonant contribution, the QR domain then being ill-populated.

We have particularized equations (145)–(146) to a number of different physical situations. For isotropic distribution functions they reduce to equations (38)–(39), which coincide with known results for thermal distribution functions, as shown in section 3.2.4. A quadrupolar anisotropy, represented by a distribution functions as in equation (51), produces the transfer coefficients shown in equations (53)–(54) while anisotropies of higher multipolar orders generate the coefficients compiled in Appendix I. In all these cases, the expression of the transfer coefficients is reduced to a one-variable quadrature over the energy of the particles. For anisotropies that cannot be expanded in a sum of a few multipolar terms, the high-frequency coefficients are obtained by performing the double integrals in equations (145)–(146), either in these variables or in others, as shown in the case of a beam in section 3.3.2.

The high-frequency approximation progressively loses validity as the fraction of particles with a Lorentz factor γ large enough to interact with the wave in the low-frequency mode increases. A regime change occurs when the quasi-resonant contribution ceases to be negligible, which, for a given frequency and a given direction of propagation, happens for Lorentz factors such that their characteristic synchrotron frequency, defined in equation (101), is of order or larger than the frequency of the radiation considered. We offer clear physical and mathematical explanations for this behaviour, that has been previously well observed in the results of Shcherbakov (2008) and Huang & Shcherbakov (2011): the regime change occurs when particles in quasi-resonance make a contribution comparable to the non-resonant one. From a mathematical standpoint, the two-variable kernels in equations (143)–(144) must be represented differently in these two regimes, in terms of the Nicholson’s approximations for quasi-resonance or in terms of the Debye expansion of high order Bessel functions for non-resonance.

In full generality, the QR contributions to the transfer coefficients are given by equations (99)–(100). The QR contribution to h is however better expressed as in equation (120). When quasi-resonant contributions are important, the NR and QR contributions should eventually be added and care should be taken to integrate the QR contributions in equations (99) and (120) over the QR domain only and the NR contributions in equations (145)–(146) over the NR domain only. We have compared the QR and NR contributions to the Faraday coefficients in section 5.4, and shown that in the low-frequency limit none of them predominates. For a given frequency, the quasi-resonant contribution to the Faraday conversion coefficient h grows when $\sigma \gg \sigma_{qr}$ to a value comparable to, and in fact numerically larger than, the non-resonant one. In the limit of large energies, the angular integration over the QR domain covers a very small interval in pitch angle space, as can be seen from equation (91). Across this interval, the partial derivative $\partial_\sigma F_0$ usually varies by only a little amount. Our estimation in section 5.4 of \hat{h}_{QR} is for this reason expected to be a reliable one, that can be written in the low-frequency limit as

$$\hat{h}_{LF}^{QR} = \frac{\omega_{pr}^2 \Omega^2}{c \omega^3} \int_{\sigma \gg \sigma_{qr}}^{\infty} \frac{m^3 c^3}{\sin^2 \alpha} d\sigma \frac{\pi}{2} \sigma^{4/3} \partial_\sigma F_0(\varpi = 0, \sigma). \quad (147)$$

Equation (147) is one among different contributions to h . It is meant to apply only to values of σ that are relevant to the asymptotic low-frequency limit. It is otherwise general and valid for any distribution function whatever the pitch angle distribution, the latter being anyway irrelevant to the quasi-resonant contribution.

The complication of accounting for both NR and QR contributions has been overcome for isotropic distribution functions by actually calculating their sum in the low-frequency limit. This has led to the results in equations (33), (130) and (138). The asymptotic low-frequency contribution to the Faraday coefficients is in this case

$$f_{LF}^{iso} = \pi s_q \frac{\omega_{pr}^2 |\Omega|}{c \omega^2} \cos \alpha \int_{\gamma \gg \gamma_{qr}}^{\infty} m^3 c^3 d\gamma \gamma \left(\frac{4}{3} \ln \left(\frac{\gamma u}{\sin \alpha} \right) - 1.26072439 \right) \frac{dF_0}{d\gamma}, \quad (148)$$

$$h_{LF}^{iso} = \frac{\omega_{pr}^2 |\Omega|^{2/3}}{c \omega^{5/3}} \sin \alpha^{2/3} \frac{\pi}{8} \left(4 - \frac{1}{3^{4/3}} \right) \int_{\gamma \gg \gamma_{qr}}^{\infty} m^3 c^3 d\gamma \gamma^{4/3} \frac{dF_0}{d\gamma}. \quad (149)$$

These simple analytical results, which apply to the asymptotic low-frequency regime $\gamma \gg \gamma_{qr}$, do not seem to have appeared so far in the literature. For example, Shcherbakov (2008) and Huang & Shcherbakov (2011) provide intermediate and low-frequency regime fits to numerical results. For application to specific distributions functions, equations (25)–(26), (31)–(32), (145)–(146) or (147) may of course be expressed in terms of any set of physical variables, such as the Lorentz factor γ and pitch angle ϑ of the particles, as was partly done in sections 3.2 and 3.3.

We proposed in equations (140)–(141) approximate expressions of the kernels of the Faraday coefficients for isotropic distribution functions that interpolate between the high-frequency regime and the asymptotic low-frequency one. These approximations to the kernels generate reasonably accurate expressions of the coefficients f and h that can be written in the form of a simple one-variable quadrature over the entire energy range. In the high-frequency limit, we have similarly reduced to a one-variable quadrature on energy the expression of the Faraday coefficients for a large class of anisotropic distribution functions proportional to Legendre polynomials of low degree depending on the cosine of the pitch angle. These functions may be used as a basis for expanding distribution functions of any simple kind of anisotropy. For distribution functions with sharp anisotropies our results can be made completely explicit by performing a double integration over energy and angle.

7.2 Discussion and prospects

Our analytical results have been deduced from a new, but straightforward, calculation of the anti-hermitian part of the conductivity tensor expressed in a form in which the usual sum over discrete synchrotron resonances is exactly replaced by an integration over a continuous variable. This particular representation of the conductivity tensor has not been hitherto used in this context. The integral over this continuous variable has principal value singularities that can be exactly reduced to the sum of a regular part and of a residual part that has been shown to be safely negligible. As a result, simple, general, quasi exact and non-singular expressions for the transfer coefficients have been obtained in a form that parallels that of the familiar expressions of the synchrotron emission and absorption coefficients, but differs from the form in which Faraday coefficients are usually expressed in the literature. Notwithstanding this difference our results exactly coincide with known exact ones for thermal distributions.

Unlike the hermitian part of the conductivity, which describes synchrotron absorption, the anti-hermitian part is never dominated by the contribution of a small quasi-resonant population traveling close to the direction of propagation of the considered wave. On the contrary, non-resonant particles make most of the contribution to the non-dissipative coefficients in the high-frequency limit and cannot be ignored otherwise.

The transfer properties of relativistic plasmas may sensibly differ from those of cold plasmas, which may be a useful diagnostic. For example the Faraday rotation coefficient f of a symmetric pair plasma, with equal densities of electrons and positrons having identical distribution functions, exactly vanishes but its Faraday conversion coefficient h does not. The study of a field-aligned beam in section 3.3.2 also revealed that the Faraday rotation coefficient is enhanced in this case for radiation travelling in the beam. The knowledge of transport coefficients in all physical regimes, high frequency or low frequency, should allow optimal use of inversion algorithms of multiwavelength polarization data to yield the density and magnetic structure of the source and of the intervening medium.

The reconstruction of the magnetic field distribution in volume, from multiwavelength polarization observations of synchrotron emitting astrophysical media, has been attempted either partially (“Faraday synthesis”, Brentjens & de Bruyn 2005) or fully (Thiébaud et al. 2010), but in the latter case assuming a known distribution of the electronic population(s) responsible for the synchrotron emission and/or the Faraday rotation. In the case of cold plasmas (e.g. the interstellar medium of our Galaxy or nearby galaxies) where the circular polarization is negligible (both from emission and transfer), these assumptions about the underlying electronic spatial distribution(s) are a real limitation to reconstructing the magnetic field structure. However, it was also shown (Thiébaud et al. 2010) that in the case of relativistic sources where a single electronic distribution would be responsible for both synchrotron emission and radiative transfer effects (through their contribution to the dielectric properties of the plasma), the multiwavelength observation of circular polarization (in addition to intensity and linear polarization) should in principle allow the simultaneous reconstruction of the magnetic field *and* electronic spatial distributions. In this context, the Faraday rotation and conversion coefficients derived in this work are of particular interest. The diagnostic of relativistic jets from galactic nuclei and of pulsar winds by these methods would be of particular interest. It should be noted however that our present results only yield the transfer coefficients in the plasma rest frame and should be transformed to the observer’s frame for use in the inversion algorithm.

ACKNOWLEDGMENTS

We thank M. Lemoine and G. Pelletier for early discussions and the “Programme National de Cosmologie et Galaxies” for funding. CP thanks the community of <http://mathematica.stackexchange.com> for technical advice.

REFERENCES

- Agol, E. 2000, *Astrophys. J.* 538, L21
 Abramowitz, M. and Stegun, I., 1964, *Handbook of Mathematical Functions*, 2d edition, National Bureau of Standards
 Beck, R., 2009, *Proc. RMXAC*, 36, 1
 Beckert, T., 2003, *Astrophys. Sp. Sc.*, 288, 123
 Bekefi, G., 1966, *Radiation processes in plasmas*, J. Wiley
 Bicknell, G.V., Jones, D.L., Lister, M., 2004, *New Astr. Rev.*, 48, 1151
 Brentjens, M.A. and de Bruyn, A.G., 2005, *Astron & Astrophys.*, 441, 1217
 Carilli, C.L., Rawlings, S., 2004, *New Astr. Rev.*, 48, 979
 Cioffi, D.F. and Jones, T.W., 1980, *AJ*, 85, 4
 Dovciak, M., Muleri, F., Goosmann, R.W., Karas, V., Matt, G., 2008 *Mon. Not. R. Astron. Soc.*, 391, 32
 Dewdney, P.E., Schilizzi, R.T., Lazio, T.J.L.W., 2009, *Proc. IEEE*, Vol 97, No 8
 Dyks, J., Harding, A.K., Rudak, B., 2004, *Astrophys. J.*, 606, 1125

- Feretti, L., Johnston-Hollitt, M., 2004, *New Astr. Rev.*, 48, 1145
- Gaensler, B.M., Beck, R., Feretti, L., 2004, *New Astr. Rev.*, 48, 1003
- Ginzburg, V.L. & Sirovatskii, S.I., 1969, *Ann. Rev. Astron. Astrophys.* 7, 375
- Gradshteyn, I.S., and Ryzhik, I.M., 1994 *Table of Integrals, Series and Products*, Fifth Edition, Academic Press
- Heyvaerts, J., 1968, *Annales d’Astrophys.* 31, 129
- Heyvaerts, J., 1969, *Astrophysics and Space Science* 5, 36
- Heyvaerts, J., 1970, Thesis (Faculté des Sciences de Paris)
- Homan, D.C., and Wardle, J.F.C., 2004, *Astrophys. J.* 602, L13
- Huang, L., Shcherbakov, R., 2011, *Mon. Not. R. Astron. Soc.*, 416, 2574
- Jones, T.W., O’Dell, S.L., 1977, *Astrophys. J.* 214, 522
- Kanbach, G., Kellner, S., Schrey, F.Z., Steinle, H., Straubmeier, C., Spruit, H.K., 2003, *Proc. SPIE*, 4841, 82
- Matviyenko, G. 1992, Research report of Yale University, Department of Computer science, YALEU/DCS/RR-903
- Mc Donald, J., O’Connor, P., de Burca, D., Golden, A. Shearer, A. 2010, *Mon. Not. R. Astron. Soc.*, 417, 730
- Melrose, D. B., 1997, *J. Plasma Phys.*, 57, 479
- Melrose, D. B., 1997, *J. Plasma Phys.*, 58, 721
- Melrose, D. B., 1997, *J. Plasma Phys.*, 58, 735
- Melrose, D. B., 1997, *Phys. Rev. E*, 56, 3527
- Olver, F.W.J., 1952, *Math. Proc. of the Cambridge Philosophical Soc.*, 48, 414
- Olver, F.W.J., 1954, *Phil. Trans. R. Soc. Lond. A*, 247, 328
- Petiau, G., 1955, *La théorie des fonctions de Bessel*, Editions du CNRS
- Petri, J. and Kirk, J., 2005, *Astrophys. J.* 627, L37
- Qin, H., Phillips, C.K., Davidson, R.C., 2007, *Physics of Plasmas*, 14, 092103
- Ramaty, R., 1968, *JGR*, 11, 3573
- Razin, V.A., 1960, *News of Higher Educational Institutions*, Ministry of Higher Education, Radio Physics Series, 3, 73
- Sazonov, V.N., 1969, *Soviet Astronomy*, 13, 396
- Sazonov, V.N., 1969, *Soviet Phys. JETP*, 29, 578
- Sazonov, V.N., Tsytovitch, V.N., 1968, *Radiofizika*, 11, 1287
- Shcherbakov, R.V., 2008, *Astrophys. J.*, 2008, 688, 695
- Shcherbakov, R.V., 2011, PhD Thesis, Harvard University
- Shcherbakov, R.V., and Huang, L., 2011, *Mon. Not. R. Astron. Soc.*, 410, 1052
- Stirling, A.M., Spencer, R.E., Cawthorne, T.V., Paragi, Z., 2004, *Mon. Not. R. Astron. Soc.*, 354, 1239
- Stepanov, R., Arshakian, T.G., Beck, R., Frick, P., Krause, M., 2008, *Astron. & Astrophys.*, 480, 45
- Thiébaud, J., 2010, Thesis (Université Pierre et Marie Curie, Paris)
- Thiébaud, J., Prunet, S., Pichon, C., Thiébaud, E., 2010, *Mon. Not. R. Astron. Soc.*, 403, 415
- Trubnikov, B.A., 1958, PHD Thesis, Moscow Inst. Engineering and Physics
- Tsyrovitch, V.N., 1951, *Vestnik Moscow Univ.* 6, n° 11, Ser. Fiz.-Mat. Estestven. Nauk, 7, 27
- Watson, G.N., 1922, *The theory of Bessel functions*, Cambridge U. Press
- Westfold, K. C., 1959, *ApJ*, 130, 241
- Wild, J.P., Weiss, A.A and Smerd, S.F. 1963 *Ann. Rev. Astron. Astrophys.*, 1, 291
- Yuen, R., Manchester, R.N., Burgay, M., Camillo, F., Kramer, M., Melrose, D.B., Stairs, J.H., 2012, *Astrophys. J.*, 752, L32
- Zheleznyakov V.V., 1967, *Soviet Phys. JETP*, 24, 381
- Zheleznyakov V.V., Suzorov, E.V. Shaposhnikov, 1974, *Soviet Astronomy*, 18, 142

APPENDIX A: VARIABLES SUITED TO THE RELATIVISTIC PARTICLE-WAVE INTERACTION

The variables σ and ϖ are defined in equation (23). They depend on the propagation angle α of the radiation (figure 5) and may be substituted to other dynamical variables of a particle, such as p_{\perp} and p_{\parallel} , or the modulus p of its momentum (or its Lorentz factor γ) and the pitch angle ϑ of the particle’s velocity. The variables σ , ϖ are convenient since some often-met operators acting on the distribution function take a simple form when expressed in terms of them, as equation (A5) shows. Assuming the vacuum dispersion relation to be valid, equation (23) relates ϖ and σ to γ and p_{\parallel}/mc by

$$\varpi = u \left(\gamma \cos \alpha - \frac{p_{\parallel}}{mc} \right), \quad \sigma = u \left(\gamma - \frac{p_{\parallel}}{mc} \cos \alpha \right), \quad \gamma = \frac{\sigma - \varpi \cos \alpha}{u \sin^2 \alpha}, \quad \frac{p_{\parallel}}{mc} = \frac{\sigma \cos \alpha - \varpi}{u \sin^2 \alpha}. \quad (\text{A1})$$

From this, p_{\perp} and the variable x defined in equation (23) may be deduced. Using the notation $\sigma_0 = u \sin \alpha$, defined in equation (23), we have

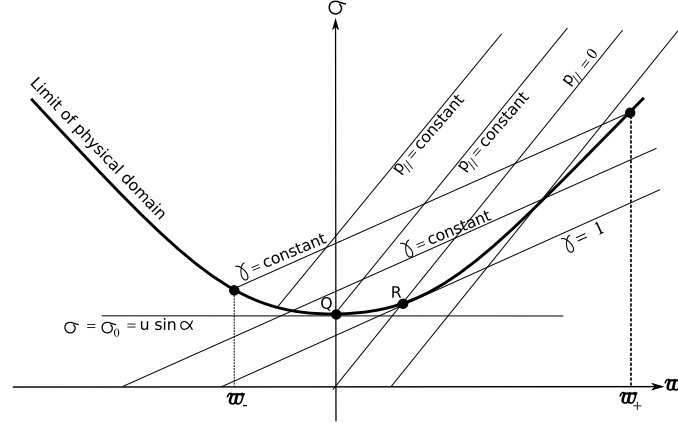


Figure A1. In the w - σ plane, the physical domain is above the thick hyperbolic line that represents states with zero perpendicular momentum. Lines of constant Lorentz factor γ and constant parallel momentum p_{\parallel} are shown. The state of rest is R. The state of lowest value of σ , $\sigma_0 = u \sin \alpha$, at Q, differs from it.

$$\frac{p_{\perp}^2}{m^2 c^2} = \frac{\sigma^2 - w^2 - \sigma_0^2}{\sigma_0^2}, \quad x = \sqrt{\sigma^2 - w^2 - \sigma_0^2}, \quad \text{where} \quad \sigma_0 = u \sin \alpha. \quad (\text{A2})$$

The physical region of the w - σ plane is where σ is positive and p_{\perp}^2 positive, that is, $\sigma^2 \geq w^2 + \sigma_0^2$. Thus σ assumes a minimum value, σ_0 that is usually large and can only be reached when $w = 0$. The dynamical state of particles that are represented by points on the border of the physical domain are those for which $p_{\perp} = 0$. For particles traveling at a velocity close to the speed of light, the sign of w on the boundary of the domain is opposite to that of the field-aligned component of the particle's velocity, as can be seen from equations (A1). Particles with vanishing w are those for which $\gamma \cos \alpha = \sqrt{\gamma^2 - 1} \cos \vartheta$, which means that the field-aligned particle velocity equals the field-aligned wave velocity. For large γ 's this relation approximately reduces to $\vartheta = \alpha$. When w does not vanish, its sign and value are indicative of the direction of the velocity of the particle. This makes the variable w akin to an angular one. By calculating the jacobian of the transformation from p_{\perp}, p_{\parallel} to w, σ , it is found that

$$p_{\perp} dp_{\perp} dp_{\parallel} = \frac{m^3 c^3}{u^2 \sin^2 \alpha} \gamma dw d\sigma, \quad (\text{A3})$$

where γ is the function of w and σ given in equation (A1). The operators acting on the distribution function f_0 that are most often met in these calculations translate in w - σ variables as

$$\frac{\partial f_0}{\partial p_{\perp}} = \frac{u}{m^2 c^2} \frac{p_{\perp}}{\gamma} \left(\frac{\partial f_0}{\partial \sigma} + \cos \alpha \frac{\partial f_0}{\partial w} \right), \quad \frac{\partial f_0}{\partial p_{\parallel}} = -\frac{1}{\gamma m c} \left(w \frac{\partial f_0}{\partial \sigma} + \sigma \frac{\partial f_0}{\partial w} \right). \quad (\text{A4})$$

$$D(f_0) = -\frac{u v_{\perp}}{m c} \left(\frac{\partial f_0}{\partial w} + \cos \alpha \frac{\partial f_0}{\partial \sigma} \right), \quad \left(w \frac{\partial f_0}{\partial p_{\perp}} + k_{\parallel} D(f_0) \right) = \frac{\omega u v_{\perp} \sin^2 \alpha}{m c^2} \frac{\partial f_0}{\partial \sigma}. \quad (\text{A5})$$

Conversely, in terms of the Lorentz factor γ and pitch angle ϑ :

$$\frac{\partial f_0}{\partial \sigma} = \frac{1}{u \sin^2 \alpha} \left(\frac{\partial f_0}{\partial \gamma} - \frac{1}{\sin \vartheta} \left(\frac{\cos \alpha}{\sqrt{\gamma^2 - 1}} - \frac{\gamma \cos \vartheta}{\gamma^2 - 1} \right) \frac{\partial f_0}{\partial \vartheta} \right). \quad (\text{A6})$$

$$\frac{\partial f_0}{\partial w} = \frac{1}{u \sin^2 \alpha} \left(-\cos \alpha \frac{\partial f_0}{\partial \gamma} + \frac{1}{\sin \vartheta} \left(\frac{1}{\sqrt{\gamma^2 - 1}} - \frac{\gamma \cos \vartheta \cos \alpha}{\gamma^2 - 1} \right) \frac{\partial f_0}{\partial \vartheta} \right). \quad (\text{A7})$$

APPENDIX B: THE CONTINUOUS-SPECTRUM REPRESENTATION OF THE CONDUCTIVITY

This appendix gives a few hints to calculate the matrix elements G_{ab} in equation (63), the functions T_a being defined in equation (60). Similar calculations being described in some detail in the paper by Qin et al. (2007), we only sketch here the main methods that should be used. The definitions of some quantities in Qin et al. (2007) may however differ from ours by a sign and the gyrofrequencies are defined in their paper with a sign different from ours. Consider first the case in which $a = b = 1$, the matrix element then being

$$G_{11}(\sigma, x) = \int_0^{2\pi} \frac{d\phi}{2\pi} \int_0^{2\pi} \frac{dw}{2\pi} \exp \left(i \left(\sigma w + x (\sin(\phi - w) - \sin \phi) \right) \right). \quad (\text{B1})$$

The identity $\sin(\phi - w) - \sin \phi = -2 \sin(w/2) \cos(\phi - w/2)$ allows to integrate over ϕ by using the identity

$$\int_0^{2\pi} \frac{d\theta}{2\pi} e^{iy \sin \theta} = J_0(y). \quad (\text{B2})$$

J_0 is the Bessel function of index 0. For some other coefficients, the integration over ϕ yields a result proportional to the first or second derivative of J_0 . Changing the angle w into 2β , G_{11} is reduced to the quadrature (Watson (1922) chap. 5)

$$G_{11}(\sigma, x) = \int_0^\pi \frac{d\beta}{\pi} e^{2i\sigma\beta} J_0(2x \sin \beta) = e^{i\sigma\pi} J_\sigma(x) J_{-\sigma}(x). \quad (\text{B3})$$

Some other elements, like G_{31} , involve after integrating over ϕ the derivative of the Bessel functions J_0 . The integration over w is then completed by integrating by parts. The calculation of elements G_{23} , G_{33} and G_{22} is less straightforward because the integrals over w cannot be directly obtained from the identity in equation (B3). This difficulty is overcome by reducing the matrix element to a form that can be integrated by parts, by using Bessel's equation for $J_0(t)$:

$$\frac{d^2 J_0(t)}{dt^2} + \frac{1}{t} \frac{dJ_0(t)}{dt} + J_0(t) = 0. \quad (\text{B4})$$

Consider for example the matrix element

$$G_{33}(\sigma, x) = \int_0^{2\pi} \frac{d\phi}{2\pi} \cos \phi \int_0^{2\pi} \frac{dw}{2\pi} e^{i\sigma w} \cos(\phi - w) e^{ix(\sin(\phi-w) - \sin \phi)}. \quad (\text{B5})$$

Changing ϕ to θ by $\phi = \theta + w/2 + \pi/2$ and then $w/2$ to β , G_{33} in equation (B5) is changed to

$$G_{33}(\sigma, x) = \int_0^{2\pi} \frac{dw}{2\pi} e^{i\sigma w} \int_0^{2\pi} \frac{d\theta}{2\pi} \left(\sin^2 \theta - \sin^2 \frac{w}{2} \right) e^{2ix \sin \frac{w}{2} \sin \theta} = - \int_0^\pi \frac{d\beta}{\pi} e^{2i\sigma\beta} \left(J_0''(2x \sin \beta) + \sin^2 \beta J_0(2x \sin \beta) \right). \quad (\text{B6})$$

On integrating over θ , use has been made of equation (B2) and of its second derivative with respect to y . The Bessel equation (B4) being written for an argument $t = t_\beta \equiv 2x \sin \beta$, the second derivative term with respect to t in equation (B4) is expressed in terms of derivatives with respect to β . The first order derivative term proportional to $dJ_0(t_\beta)/d\beta$ happens to be $\tan^2 \beta (J_0'(t_\beta)/t_\beta)$. All terms proportional to $J_0'(t_\beta)$ are then eliminated by using equation (B4) again, which yields

$$4x^2 \left(J_0''(t_\beta) + \sin^2 \beta J_0(t_\beta) \right) = \frac{d^2 J_0(t_\beta)}{d\beta^2}, \quad \text{with} \quad t_\beta \equiv 2x \sin \beta. \quad (\text{B7})$$

Using this, the expression of G_{33} in equation (B6) becomes

$$G_{33} = - \int_0^\pi \frac{d\beta}{4\pi x^2} \frac{e^{2i\sigma\beta} d^2 J_0(t_\beta)}{d\beta^2} = - \left[\frac{e^{2i\sigma\beta} dJ_0(2x \sin \beta)}{4\pi x^2 d\beta} \right]_0^\pi + \frac{2i\sigma}{4x^2} \int_0^\pi \frac{d\beta}{\pi} e^{2i\sigma\beta} \frac{dJ_0(2x \sin \beta)}{d\beta}. \quad (\text{B8})$$

which can be integrated by parts again, noting that the square bracket term in equation (B8) vanishes because $J_0'(t)$ vanishes at $t = 0$, to eventually give, using equation (B3)

$$G_{33}(\sigma, x) = + \frac{2i\sigma}{4\pi x^2} \left[e^{2i\sigma\beta} J_0(2x \sin \beta) \right]_0^\pi + \frac{\sigma^2}{x^2} \int_0^\pi \frac{d\beta}{\pi} e^{2i\sigma\beta} J_0(2x \sin \beta) = \frac{i\sigma}{2\pi x^2} \left(e^{2i\sigma\pi} - 1 \right) + \frac{\sigma^2}{x^2} e^{i\sigma\pi} J_\sigma(x) J_{-\sigma}(x). \quad (\text{B9})$$

APPENDIX C: THE DISTRIBUTION ASSOCIATED WITH MULTIPLE RESONANCES

Let us consider the limit for $N \rightarrow \infty$ of the following function of σ :

$$\left(1 - e^{2i\pi N\sigma} \right) \frac{\cos \sigma\pi}{\sin \sigma\pi}. \quad (\text{C1})$$

This function enters expressions involving the integration of its product with a regular function of σ . When N diverges, $\exp(2i\pi N\sigma)$ oscillates infinitely rapidly, leaving in the limit a vanishing integral when multiplied by any regular function, which is the case in any interval containing no integer value. At integer values of σ , the denominator $\sin \sigma\pi$ vanishes, as does also the factor $(1 - \exp(2i\pi N\sigma))$. To find the limit value, we expand by setting $\sigma = n + \eta$, where η is $\mathcal{O}(1/N)$. This gives

$$g(\sigma) \left(1 - e^{2i\pi N\sigma} \right) \frac{\cos \sigma\pi}{\sin \sigma\pi} \approx g(n + \eta) \left(2\pi N^2 \eta - i 2N \frac{\sin 2\pi N \eta}{2\pi N \eta} \right). \quad (\text{C2})$$

Near the singularity, the real term, which is proportional to $2\pi N^2 \eta$, appears as a symmetrical cut replacing the diverging part of the function $\cos \sigma\pi / \sin \sigma\pi$ by an odd function of η that vanishes at $\eta = 0$ in an interval that decreases with N as $1/N$. This means that as $N \rightarrow \infty$, the real part of the diverging integral of $g(\sigma)(\cos \sigma\pi / \sin \sigma\pi)$ should be understood as a principal value. The imaginary part is proportional near the resonance to $2N(\sin 2\pi N \eta / 2\pi N \eta)$ which is large at $\eta = 0$, and then quickly decreases in the vicinity of $\sigma = n$, oscillating rapidly on a scale $\mathcal{O}(1/N)$. The integral of the product with a regular function $g(\sigma)$ in the vicinity of $\sigma = n$ can be evaluated by changing from η to $y = 2\pi N \eta$, which yields, in this vicinity

$$\int d\sigma g(\sigma) \left(-i2N \frac{\sin 2\pi N \eta}{2\pi N \eta} \right) \approx -ig(n) \frac{1}{\pi} \int_{-\infty}^{+\infty} \frac{\sin y dy}{y} = -ig(n). \quad (\text{C3})$$

In the limit $N \rightarrow \infty$, the function in equation (C1) then converges to the distribution

$$\lim_{N \rightarrow \infty} \left(1 - e^{2i\pi N \sigma} \right) \frac{\cos \sigma \pi}{\sin \sigma \pi} \equiv \mathcal{D} \left(\frac{\cos \sigma \pi}{\sin \sigma \pi} \right) = \mathcal{P} \left(\frac{\cos \sigma \pi}{\sin \sigma \pi} \right) - i\pi \sum_n \delta_{\text{D}}(\sigma - n). \quad (\text{C4})$$

where δ_{D} is a Dirac distribution. This leads to the result in equation (69). The distribution $\mathcal{D}(\cos \sigma \pi / \sin \sigma \pi)$ is causal, which was obvious from the beginning since the integration has been carried over positive delay times only. This explicitly shows up in the fact that when σ is close to a singularity, at $\sigma = n$ say, the distribution \mathcal{D} reduces, according to Plemelj's formula, to

$$\frac{1}{\pi} \left(\mathcal{P} \frac{1}{\sigma - n} - i\pi \delta_{\text{D}}(\sigma - n) \right) = \frac{1}{\pi} \frac{1}{(\sigma - n) + i0}. \quad (\text{C5})$$

The presence of the infinitesimal positive imaginary part at the denominator of the right hand side member reveals the causal character of the distribution (see the last paragraph of section 2.2).

APPENDIX D: THE TRANSVERSE COMPONENTS OF THE CONDUCTIVITY

The components XYZ of the tensor \mathbf{M} being given by equations (68), its transverse components in the $x' y' z'$ frame are obtained from them by equations (70)–(71). This first gives

$$\begin{aligned} M_{x'x'} &= \frac{i\pi v_{\perp}}{|\Omega_*|} \left(\omega \frac{\partial f_0}{\partial p_{\perp}} + k_{\parallel} D(f_0) \right) \left(\mathcal{D} \left(\frac{\cos \sigma \pi}{\sin \sigma \pi} \right) J_{\sigma}^2(x) - J_{\sigma}'(x) N_{\sigma}'(x) + \frac{\sigma}{\pi x^2} \right), \\ M_{x'y'} &= \frac{s_q \pi v_{\perp}}{|\Omega_*|} \left(\sin \alpha \left(\omega \frac{\partial f_0}{\partial p_{\parallel}} - k_{\perp} D(f_0) \frac{\sigma}{x} \right) - \cos \alpha \frac{\sigma}{x} \left(\omega \frac{\partial f_0}{\partial p_{\perp}} + k_{\parallel} D(f_0) \right) \right) \left(\mathcal{D} \left(\frac{\cos \sigma \pi}{\sin \sigma \pi} \right) J_{\sigma}(x) J_{\sigma}'(x) - J_{\sigma}'(x) N_{\sigma}(x) - \frac{1}{\pi x} \right), \\ M_{y'x'} &= (-s_q \pi) \left(\sin \alpha \frac{v_{\parallel}}{|\Omega_*|} - \cos \alpha \frac{v_{\perp}}{|\Omega_*|} \frac{\sigma}{x} \right) \left(\omega \frac{\partial f_0}{\partial p_{\perp}} + k_{\parallel} D(f_0) \right) \left(\mathcal{D} \left(\frac{\cos \sigma \pi}{\sin \sigma \pi} \right) J_{\sigma}(x) J_{\sigma}'(x) - J_{\sigma}'(x) N_{\sigma}(x) - \frac{1}{\pi x} \right), \\ M_{y'y'} &= \cos^2 \alpha \frac{i\pi v_{\perp}}{|\Omega_*|} \left(\omega \frac{\partial f_0}{\partial p_{\perp}} + k_{\parallel} D(f_0) \right) \frac{\sigma^2}{x^2} \left(\mathcal{D} \left(\frac{\cos \sigma \pi}{\sin \sigma \pi} \right) J_{\sigma}^2(x) - J_{\sigma}(x) N_{\sigma}(x) - \frac{1}{\sigma \pi} \right) \\ &+ \sin^2 \alpha \frac{i\pi v_{\parallel}}{|\Omega_*|} \left(\left(\omega \frac{\partial f_0}{\partial p_{\parallel}} - k_{\perp} D(f_0) \frac{\sigma}{x} \right) \left(\mathcal{D} \left(\frac{\cos \sigma \pi}{\sin \sigma \pi} \right) J_{\sigma}^2(x) - J_{\sigma}(x) N_{\sigma}(x) \right) + \frac{k_{\perp} D(f_0)}{\pi x} \right) \\ &- \sin \alpha \cos \alpha \frac{i\pi v_{\perp}}{|\Omega_*|} \frac{\sigma}{x} \left(\omega \frac{\partial f_0}{\partial p_{\parallel}} - k_{\perp} D(f_0) \frac{\sigma}{x} \right) \left(\mathcal{D} \left(\frac{\cos \sigma \pi}{\sin \sigma \pi} \right) J_{\sigma}^2(x) - J_{\sigma}(x) N_{\sigma}(x) - \frac{1}{\sigma \pi} \right) \\ &- \sin \alpha \cos \alpha \frac{i\pi v_{\parallel}}{|\Omega_*|} \frac{\sigma}{x} \left(\omega \frac{\partial f_0}{\partial p_{\perp}} + k_{\parallel} D(f_0) \right) \left(\mathcal{D} \left(\frac{\cos \sigma \pi}{\sin \sigma \pi} \right) J_{\sigma}^2(x) - J_{\sigma}(x) N_{\sigma}(x) - \frac{1}{\sigma \pi} \right). \end{aligned}$$

Although this is not obvious, the elements $M_{x'y'}$ and $M_{y'x'}$ differ by only a sign, since their factors of $\sin \alpha$ are equal. This can be seen by calculating the difference of these factors of $\sin \alpha$, accounting for the definition of $D(f_0)$ in equation (20). The expression of $M_{y'y'}$ is improved by arranging the first parenthesis using the definitions in equation (23). The writing of $M_{y'y'}$ can be similarly improved by gathering the terms proportional to Bessel functions on the one hand, and those which are not on the other hand, then changing some factors accompanying $\sin^2 \alpha$ and $\sin \alpha \cos \alpha$ by using equations (20) and (23). Denoting $D(f_0)$ by D for brevity, this eventually gives, for example

$$v_{\parallel} \left(\omega \frac{\partial f_0}{\partial p_{\parallel}} - k_{\perp} D \frac{\sigma}{x} \right) = \frac{v_{\parallel}^2}{v_{\perp}} \left(\omega \frac{\partial f_0}{\partial p_{\perp}} + k_{\parallel} D \right), \quad (\text{D1})$$

$$v_{\perp} \left(\omega \frac{\partial f_0}{\partial p_{\parallel}} - k_{\perp} D \frac{\sigma}{x} \right) + v_{\parallel} \left(\omega \frac{\partial f_0}{\partial p_{\perp}} + k_{\parallel} D \right) = 2v_{\parallel} \left(\omega \frac{\partial f_0}{\partial p_{\perp}} + k_{\parallel} D \right), \quad (\text{D2})$$

$$\begin{aligned} &-v_{\perp} \cos^2 \alpha \frac{\sigma}{x^2} \left(\omega \frac{\partial f_0}{\partial p_{\perp}} + k_{\parallel} D \right) + v_{\parallel} \sin^2 \alpha \frac{k_{\perp} D}{x} + \frac{\sin \alpha \cos \alpha}{x} \left(v_{\perp} \left(\omega \frac{\partial f_0}{\partial p_{\parallel}} - k_{\perp} D \frac{\sigma}{x} \right) + v_{\parallel} \left(\omega \frac{\partial f_0}{\partial p_{\perp}} + k_{\parallel} D \right) \right) \\ &= |\Omega_*| \left(\frac{\omega \sin \alpha \cos \alpha}{k_{\perp}} \frac{\partial f_0}{\partial p_{\parallel}} - (\omega \cos \alpha - k v_{\parallel}) \left(\frac{D \sin \alpha}{k_{\perp} v_{\perp}} + \frac{\cos \alpha}{k_{\perp}^2 v_{\perp}} \left(\omega \frac{\partial f_0}{\partial p_{\perp}} + k_{\parallel} D \right) \right) \right). \end{aligned} \quad (\text{D3})$$

The last equation has been obtained by using the vacuum dispersion relation. The matrix elements can be given a simpler expression by using, instead of p_{\perp} and p_{\parallel} , the variables σ and ϖ defined in equation (23) and presented in Appendix A. This results in the equations (72)–(74).

APPENDIX E: RESIDUAL PRINCIPLE VALUE TERMS ARE NEGLIGIBLE

The integrations which appear in equations (86) and (87) are over the physical domain in the ϖ - σ plane. This domain is bounded from below by the curve \mathcal{B} of equation $\sigma^2 = \varpi^2 + u^2 \sin^2 \alpha$. This constrains σ to be larger than a minimum value, $\sigma_0 = u \sin \alpha$, that is usually large (unless $\sin \alpha$ is very small) because $u = \omega/|\Omega|$ is large. For a given value of σ , ϖ spans the interval $[-\varpi_b(\sigma), +\varpi_b(\sigma)]$, where $\varpi_b(\sigma) = \sqrt{\sigma^2 - \sigma_0^2}$. Each principal value term in equations (86) and (87) can be written as a sum of a few contributions of the form

$$T = \iint d\varpi d\sigma \mathcal{P}\left(\frac{\cos \sigma \pi}{\sin \sigma \pi}\right) A(\varpi, \sigma) B_\sigma(x) \frac{\partial F_0}{\partial \sigma} = \int_{\sigma_0}^{\infty} \mathcal{P}\left(\frac{\cos \sigma \pi}{\sin \sigma \pi}\right) C(\sigma). \quad (\text{E1})$$

where $A(\varpi, \sigma)$ is a function of σ , ϖ or x and $B_\sigma(x)$ is the product of two functions that may be either $J_\sigma(x)$ or its derivative $J'_\sigma(x)$. The function $C(\sigma)$ is the integral over ϖ of $A(\varpi, \sigma) B_\sigma(x) \partial_\sigma F_0$ on the interval $[-\varpi_b(\sigma), +\varpi_b(\sigma)]$. It varies on a scale of order σ . On $[n - 1/2, n + 1/2]$, $C(\sigma)$ may be series-expanded by setting $a = (\sigma - n)$ and can be written, on this interval, as

$$C(\sigma) = C(n) + a C^{(1)}(n) + \frac{a^2}{2} C^{(2)}(n) + \dots + \frac{a^k}{k!} C^{(k)}(n) + \dots \quad (\text{E2})$$

where $C^{(k)}(n)$ is the k -th derivative of $C(\sigma)$ at $\sigma = n$. From this we get

$$\int_{n-1/2}^{n+1/2} d\sigma \mathcal{P}\left(\frac{\cos \sigma \pi}{\sin \sigma \pi}\right) C(\sigma) = \sum_{k=0}^{\infty} \Lambda_k \frac{C^{(k)}(n)}{k!}, \quad \text{where} \quad \Lambda_k = \int_{-1/2}^{+1/2} da \mathcal{P}\left(\frac{a^k \cos a \pi}{\sin a \pi}\right). \quad (\text{E3})$$

The integral defining Λ_k is regular when $k > 0$. The coefficient Λ_k vanishes when k is even because the integrand then is odd in a . Therefore the summation on k on the left of equation (E3) is on odd values $k = 2m + 1$ only. This series is absolutely convergent since each derivative $C^{(2m+1)}(n)$ is expected to be of order $C^{(2m-1)}(n)/n^2$, thus decreasing rapidly with m , so that the factorial $(2m + 1)!$ at the denominator warrants a fast convergence. Moreover, Λ_{2m+1} also decreases with m . Let n_1 be the smallest integer for which $n_1 - 1/2 \geq \sigma_0$, that is, the smallest integer for which the interval $[n_1 - 1/2, n_1 + 1/2]$ is entirely contained in $[\sigma_0, \infty]$. The expression T in equation (E1) can be written as the sum of a contribution from the interval $[\sigma_0, n_1 - 1/2]$ and a sum over $n \geq n_1$ of terms similar to that in equation (E3):

$$T = \int_{\sigma_0}^{n_1 - \frac{1}{2}} d\sigma \mathcal{P}\left(\frac{\cos \sigma \pi}{\sin \sigma \pi}\right) C(\sigma) + \sum_{n=n_1}^{\infty} \left(\sum_{m=0}^{\infty} \Lambda_{2m+1} \frac{C^{(2m+1)}(n)}{(2m+1)!} \right). \quad (\text{E4})$$

It is possible to replace the summation over n by an integral because the terms of the series in n do not change by much when n changes by unity. Noting that $C^{(2m+1)}(\sigma)$ is the derivative of $C^{(2m)}(\sigma)$, the second term can be exactly calculated by integrating over σ , which performs the summation over n as an integral, giving

$$T = \int_{\sigma_0}^{n_1 - \frac{1}{2}} d\sigma \mathcal{P}\left(\frac{\cos \sigma \pi}{\sin \sigma \pi}\right) C(\sigma) + \sum_{m=0}^{\infty} \Lambda_{2m+1} \frac{C^{(2m)}(n_1)}{(2m+1)!} \equiv T_{\text{first}} + T_{\text{sum}}. \quad (\text{E5})$$

We have separated T in equation (E5) into a first term, T_{first} , the second one, T_{sum} , being the sum over all complete unit intervals. T_{sum} is similar to the integral calculated in equation (E3), for the particular value $n = n_1$, the derivatives $C^{(2m)}$ replacing the derivatives $C^{(2m+1)}$. The ratio $C^{(2m)}(n_1)/C^{(2m+1)}(n_1)$ is expected to be of order of n_1 , which itself is close to σ_0 . We may assume that there is an upper bound over all values of m , $K\sigma_0$ say, to the ratio $C^{(2m)}(n_1)/C^{(2m+1)}(n_1)$, so that we may evaluate an upper bound on T_{sum} :

$$T_{\text{sum}} \leq K\sigma_0 \sum_{m=0}^{\infty} \Lambda_{2m+1} \frac{C^{(2m+1)}(n_1)}{(2m+1)!} = K\sigma_0 \int_{n_1 - 1/2}^{n_1 + 1/2} d\sigma \mathcal{P}\left(\frac{\cos \sigma \pi}{\sin \sigma \pi}\right) C(\sigma). \quad (\text{E6})$$

The contribution T_{first} of the first interval, defined in equation (E5), is itself of the same order of magnitude as the factor of $K\sigma_0$ in the last term of equation (E6). It then suffices to show that T_{sum} , as estimated in equation (E6), is negligibly small.

Since n_1 is distant from σ_0 by less than unity, the argument x of the Bessel functions that corresponds to $\sigma = n_1 \leq \sigma_0 + 1$ is very small compared to its index $n_1 \approx \sigma_0$, the ratio x/σ being of order $\sqrt{2/\sigma_0}$. Now, for arguments $x \ll \sqrt{\sigma}$, as is the case here, the Bessel functions of the first kind $J_\sigma(x)$ may be represented by their Carlini approximation (Abramowitz & Stegun 1964) that can be further simplified by using Stirling's formula for $\Gamma(\sigma)$ at large σ (Abramowitz & Stegun 1964). This gives

$$J_\sigma(x) \approx \frac{1}{\sqrt{2\pi\sigma}} \left(\frac{ex}{\sigma}\right)^\sigma, \quad J'_\sigma(x) \approx \frac{e}{\sqrt{2\pi\sigma}} \left(\frac{ex}{\sigma}\right)^{\sigma-1}. \quad (\text{E7})$$

The function A in equation (E1) may be either ϖ^2 , ϖx or x^2 depending on the corresponding Bessel factor B_σ and the variable x is $\sqrt{\sigma^2 - \sigma_0^2 - \varpi^2}$. Setting $\varpi = \lambda \sqrt{\sigma^2 - \sigma_0^2}$, where λ is in the interval $[-1, +1]$, we get

$$C(\sigma) \approx \frac{\sqrt{\sigma^2 - \sigma_0^2}}{2\pi\sigma} \left(\frac{e^2(\sigma^2 - \sigma_0^2)}{\sigma^2}\right)^\sigma \int_{-1}^{+1} d\lambda \left(\frac{\lambda^2(\sigma^2 - \sigma_0^2)}{\lambda \sigma \sqrt{\sigma^2 - \sigma_0^2}}\right) (1 - \lambda^2)^\sigma \frac{\partial F_0}{\partial \sigma} \left(\lambda \sqrt{\sigma^2 - \sigma_0^2}, \sigma\right), \quad (\text{E8})$$

where the upper element in the column vector corresponds to J_σ^2 , the middle one to $J_\sigma J'_\sigma$ and the lower one to $J_\sigma'^2$. The integral over λ is itself a small number owing to the presence of the factor $(1 - \lambda^2)^\sigma$ that is a large power of a number smaller than unity. But it is the factor in front of the integral that makes the whole expression extremely small, since σ does not differ from σ_0 by more than two units, implying that

$$\left(\frac{e^2(\sigma^2 - \sigma_0^2)}{\sigma^2} \right)^\sigma < \left(\frac{4e^2\sigma_0}{\sigma_0^2} \right)^{\sigma_0} = \mathcal{O} \left(\left(\frac{1}{\sigma_0} \right)^{\sigma_0} \right). \quad (\text{E9})$$

For frequencies at the peak of synchrotron emission, σ_0 is of order of the square of the Lorentz factor γ of the emitting particles, which means that the term on the right of equation (E9) is of order $(\gamma^2)^{-\gamma^2}$, entirely negligible even at relatively small values of γ , such as $\gamma = 10$, where its value is about 10^{-200} . Then, setting $\sigma = \sigma_0 + h$ where h is $\mathcal{O}(1)$, substituting σ_0 to σ wherever possible and otherwise approximating $(\sigma^2 - \sigma_0^2)$ by $2\sigma_0 h$, the upper bound on T_{sum} on the right of equation (E6) can be written as

$$T_{\text{sum}} \leq K \frac{\sigma_0^{\frac{5}{2}}}{\pi\sqrt{2}} \left(\frac{2e^2}{\sigma_0} \right)^{\sigma_0} \int_{(n_1 - \sigma_0) - \frac{1}{2}}^{(n_1 - \sigma_0) + \frac{1}{2}} dh \mathcal{P} \left(\frac{\cos \sigma \pi}{\sin \sigma \pi} \right) h^{\sigma_0 + \frac{1}{2}} \begin{pmatrix} (2h/\sigma_0) \\ (2h/\sigma_0)^{\frac{1}{2}} \\ 1 \end{pmatrix} \int_{-1}^{+1} d\lambda \begin{pmatrix} \lambda^2 \\ \lambda \\ 1 \end{pmatrix} (1 - \lambda^2)^\sigma \frac{\partial F_0}{\partial \sigma} (\lambda\sqrt{2h\sigma_0}, \sigma). \quad (\text{E10})$$

Again, the prefactor proportional to $(\sigma_0)^{-\sigma_0}$ causes the whole expression to be negligibly small. This results from the extreme smallness of the Bessel functions of the first kind and large indices when their argument is small.

APPENDIX F: NICHOLSON'S APPROXIMATION

The Nicholson's approximation provides expressions for the Bessel functions of large indices when their argument is close to the index, in our case slightly smaller. Watson (1922), chap. 6, gives the following integral representations of these functions:

$$J_\sigma(x) = \frac{1}{\pi} \int_0^\pi \cos(\sigma\theta - x \sin \theta) d\theta - \frac{\sin \sigma \pi}{\pi} \int_0^\infty \exp(-(\sigma t + x \sinh t)) dt. \quad (\text{F1})$$

$$-N_\sigma(x) = \frac{1}{\pi} \int_0^\pi \sin(\sigma\theta - x \sin \theta) d\theta + \frac{1}{\pi} \int_0^\infty \exp(\sigma t - x \sinh t) dt + \frac{\cos \sigma \pi}{\pi} \int_0^\infty \exp(-(\sigma t + x \sinh t)) dt. \quad (\text{F2})$$

For x and σ large and almost equal, the integrand is rapidly oscillating, or decaying, and any of these integrals may be approximated by the method of stationary phase which consists in expanding the arguments of the trigonometric or exponential functions in the vicinity of the value of θ or t where they are stationary. This gives, for example

$$\frac{1}{\pi} \int_0^\pi \cos(\sigma\theta - x \sin \theta) d\theta \approx \frac{1}{\pi} \int_0^\pi \cos((\sigma - x)\theta + x\theta^3/6) d\theta = \frac{6^{1/3}}{\pi x^{1/3}} \int_0^\infty \cos\left(3 \frac{2^{1/3}(\sigma - x)}{3^{2/3} x^{1/3}} v + v^3\right) dv. \quad (\text{F3})$$

These integrals involve Airy-Hardy integrals of order 3 (Petiau 1955) defined by

$$\text{Ci}_3(g) = \int_0^\infty \cos(3gv + v^3) dv, \quad \text{Si}_3(g) = \int_0^\infty \sin(3gv + v^3) dv, \quad \text{Ei}_3(g) = \int_0^\infty \exp(-3gv + v^3) dv. \quad (\text{F4})$$

The last, negative exponential, term in equations (F1) and (F2) being negligible compared to the others for large and positive x and σ , we are left with

$$J_\sigma(x) \approx \frac{6^{1/3}}{\pi x^{1/3}} \text{Ci}_3\left(\frac{2^{1/3}(\sigma - x)}{3^{2/3} x^{1/3}}\right), \quad -N_\sigma(x) \approx \frac{6^{1/3}}{\pi x^{1/3}} \left[\text{Si}_3\left(\frac{2^{1/3}(\sigma - x)}{3^{2/3} x^{1/3}}\right) + \text{Ei}_3\left(-\frac{2^{1/3}(\sigma - x)}{3^{2/3} x^{1/3}}\right) \right]. \quad (\text{F5})$$

The function Ci_3 reduces to a combination of modified Bessel functions of index $\pm 1/3$, but the functions Si_3 and Ei_3 , separately, do not. However, the combination which appears in equation (F5) does. Correcting a little typo in Watson's book, p.324 equation (8) (Watson 1922), we have

$$\text{Ci}_3(g) = \frac{\pi\sqrt{g} \cos \frac{\pi}{6}}{3 \sin \frac{\pi}{3}} \left(I_{-\frac{1}{3}}\left(2g^{\frac{2}{3}}\right) - I_{+\frac{1}{3}}\left(2g^{\frac{2}{3}}\right) \right), \quad \text{Si}_3(g) + \text{Ei}_3(-g) = \frac{\pi\sqrt{g} (1 + \sin \frac{\pi}{6})}{3 \sin \frac{\pi}{3}} \left(I_{-\frac{1}{3}}\left(2g^{\frac{2}{3}}\right) + I_{+\frac{1}{3}}\left(2g^{\frac{2}{3}}\right) \right). \quad (\text{F6})$$

The results in equation (95) are deduced from equation (F6) and from the definitions in equations (93). Those in equation (96) result from the expressions in equation (95) by derivating with respect to x . Use is made of the recurrence relations for the functions I_ν , which translate into different recurrence relations for the functions K_ν and L_ν , that have different parity under a change of sign of the index

$$\begin{aligned} I_{\nu-1}(y) - I_{\nu+1}(y) &= \frac{2\nu}{y} I_\nu(y), & I_{\nu-1}(y) + I_{\nu+1}(y) &= 2I'_\nu(y), \\ K'_{\frac{1}{3}}(y) &= -K_{\frac{2}{3}}(y) - \frac{1}{3y} K_{\frac{1}{3}}(y), & L'_{\frac{1}{3}}(y) &= +L_{\frac{2}{3}}(y) - \frac{1}{3y} L_{\frac{1}{3}}(y). \end{aligned}$$

The results in equation (96) have been obtained by neglecting subdominant terms that appear as a result of the derivation.

APPENDIX G: OLVER UNIFORM ASYMPTOTIC EXPANSION OF BESSEL FUNCTIONS

The Olver approximation for the Bessel functions and their derivatives at large order and for $z < 1$ is given by Olver (1954)

$$J_\sigma(\sigma z) \sim \left(\frac{4\zeta}{1-z^2}\right)^{1/4} \left(\frac{\text{Ai}(\sigma^{2/3}\zeta)}{\sigma^{1/3}} \sum_{s=0}^{\infty} \frac{A_s(\zeta)}{\sigma^{2s}} + \frac{\text{Ai}'(\sigma^{2/3}\zeta)}{\sigma^{5/3}} \sum_{s=0}^{\infty} \frac{B_s(\zeta)}{\sigma^{2s}} \right), \quad (\text{G1})$$

$$N_\sigma(\sigma z) \sim - \left(\frac{4\zeta}{1-z^2}\right)^{1/4} \left(\frac{\text{Bi}(\sigma^{2/3}\zeta)}{\sigma^{1/3}} \sum_{s=0}^{\infty} \frac{A_s(\zeta)}{\sigma^{2s}} + \frac{\text{Bi}'(\sigma^{2/3}\zeta)}{\sigma^{5/3}} \sum_{s=0}^{\infty} \frac{B_s(\zeta)}{\sigma^{2s}} \right), \quad (\text{G2})$$

$$J'_\sigma(\sigma z) \sim -\frac{2}{z} \left(\frac{4\zeta}{1-z^2}\right)^{-1/4} \left(\frac{\text{Ai}(\sigma^{2/3}\zeta)}{\sigma^{4/3}} \sum_{s=0}^{\infty} \frac{C_s(\zeta)}{\sigma^{2s}} + \frac{\text{Ai}'(\sigma^{2/3}\zeta)}{\sigma^{2/3}} \sum_{s=0}^{\infty} \frac{D_s(\zeta)}{\sigma^{2s}} \right), \quad (\text{G3})$$

$$N'_\sigma(\sigma z) \sim \frac{2}{z} \left(\frac{4\zeta}{1-z^2}\right)^{-1/4} \left(\frac{\text{Bi}(\sigma^{2/3}\zeta)}{\sigma^{4/3}} \sum_{s=0}^{\infty} \frac{C_s(\zeta)}{\sigma^{2s}} + \frac{\text{Bi}'(\sigma^{2/3}\zeta)}{\sigma^{2/3}} \sum_{s=0}^{\infty} \frac{D_s(\zeta)}{\sigma^{2s}} \right), \quad (\text{G4})$$

where Ai and Bi are Airy functions defined as in the appendix of the paper by Olver (1954) and Ai' and Bi' their derivatives. The variable ζ is related to z by

$$\frac{2}{3}\zeta^{3/2} = \cosh^{-1} \frac{1}{z} - \sqrt{1-z^2},$$

and A_s , B_s , C_s and D_s are given by

$$A_s(\zeta) = \sum_{m=0}^{2s} b_m \zeta^{-3m/2} U_{2s-m} \left(\frac{1}{\sqrt{1-z^2}} \right), \quad \zeta^{1/2} B_s(\zeta) = - \sum_{m=0}^{2s+1} a_m \zeta^{-3m/2} U_{2s+1-m} \left(\frac{1}{\sqrt{1-z^2}} \right), \quad (\text{G5})$$

$$\zeta^{1/2} C_s(\zeta) = - \sum_{m=0}^{2s+1} b_m \zeta^{-3m/2} V_{2s+1-m} \left(\frac{1}{\sqrt{1-z^2}} \right), \quad D_s(\zeta) = \sum_{m=0}^{2s} a_m \zeta^{-3m/2} V_{2s-m} \left(\frac{1}{\sqrt{1-z^2}} \right). \quad (\text{G6})$$

The Debye polynomials U_n and V_n are found by solving the following recurrence

$$U_n(x) = \frac{1}{2} (1-x^2) x^2 U'_{n-1}(x) + \frac{1}{8} \int_0^x (1-5t^2) U_{n-1}(t) dt, \quad V_n(x) = x(x^2-1) \left(x U'_{n-1}(x) + \frac{1}{2} U_{n-1}(x) \right) + U_n(x),$$

with $U_0 = 1$ and $V_0 = 1$. The coefficients,

$$a_0 = 1, \quad b_0 = 1, \quad a_s = \frac{(2s+1)(2s+3)\cdots(6s-1)}{s!(144)^s}, \quad b_s = -\frac{6s+1}{6s-1} a_s$$

arise from asymptotic developments of the Airy functions at infinity, such as:

$$\text{Ai}(\sigma^{2/3}\zeta) \sim \frac{1}{2\sigma^{1/6}\zeta^{1/4}\sqrt{\pi}} \exp\left(-\frac{2}{3}\sigma\zeta^{3/2}\right) \sum_{s=0}^{\infty} (-1)^s \frac{a_s}{\sigma^5\zeta^{3s/2}}, \quad \text{Ai}'(\sigma^{2/3}\zeta) \sim -\frac{\sigma^{1/6}\zeta^{1/4}}{2\sqrt{\pi}} \exp\left(-\frac{2}{3}\sigma\zeta^{3/2}\right) \sum_{s=0}^{\infty} (-1)^s \frac{b_s}{\sigma^5\zeta^{3s/2}}.$$

The Debye expansion is recovered by plugging these asymptotic expansions in equation (G1)-(G4), e.g.

$$J_\sigma(\sigma z) \sim \frac{1}{\sqrt{2\pi\sigma}(1-z^2)^{1/4}} \exp\left(-\frac{2}{3}\sigma\zeta^{3/2}\right) \sum_{s=0}^{\infty} \frac{U_s(1/\sqrt{1-z^2})}{\sigma^s}.$$

Making the following change of variables:

$$z = \frac{1}{\cosh \xi}, \quad \frac{2}{3}\zeta^{3/2} = \xi - \tanh \xi.$$

we recover equations (109) and (110). In section 6.2 we make use of equations (G1)-(G4) to first order to compute numerically equation (126). The corresponding implementation in **Mathematica** is available at the following URL: <http://www.iap.fr/users/pichon/olver/>.

APPENDIX H: COMPARISON OF QUASI-RESONANT AND NON-RESONANT CONTRIBUTIONS

We derive in this appendix the estimations presented in section 5.4 for the NR and QR contributions to the ϖ -integrated kernels of the Faraday rotation and conversion coefficients. Let us first consider the non-resonant contributions. Equation (115) gives f_{NR} , which we may reduce to its dominant term, the first one in the parenthesis. Equation (119) gives h_{NR} . The double integrals in these equations are over the non-resonant domain. The latter is represented in figure 6 and the equations

of its lower boundary \mathcal{B} and upper boundary \mathcal{B}_{QR} respectively are $\varpi^2 + \sigma_0^2 = \sigma^2$ and $\varpi^2 + \sigma_0^2 = 3^{2/3}\sigma^{4/3}$. Taking advantage of the symmetry of the integrands, the ϖ -integrated kernels in equation (121) can be written as:

$$K_{\text{NR}}^{(f)} = 2 \int_{\sqrt{3^{2/3}\sigma^{4/3}-\sigma_0^2}}^{\sqrt{\sigma^2-\sigma_0^2}} d\varpi \varpi^2 \left(\frac{\pi}{2}\right) \frac{\sigma^2 - (\varpi^2 + \sigma_0^2)}{(\varpi^2 + \sigma_0^2)^{3/2}}, \quad (\text{H1})$$

$$K_{\text{NR}}^{(h)} = 2 \int_{\sqrt{3^{2/3}\sigma^{4/3}-\sigma_0^2}}^{\sqrt{\sigma^2-\sigma_0^2}} d\varpi \left(\frac{\pi}{8}\right) \left(\frac{2(\sigma^2 - (\varpi^2 + \sigma_0^2))^2}{(\varpi^2 + \sigma_0^2)^{5/2}} + \frac{\sigma_0^2(\sigma^2 - (\varpi^2 + \sigma_0^2))(5\sigma^2 - (\varpi^2 + \sigma_0^2))}{(\varpi^2 + \sigma_0^2)^{7/2}} \right). \quad (\text{H2})$$

To evaluate these integrals in the limit of large σ 's, that is when $\sigma_0/\sigma \rightarrow 0$, we substitute $y = \varpi/\sigma$ to ϖ . The lower bound of the integrations becomes $(3/\sigma)^{1/3}$ and the upper bound unity. The result is

$$K_{\text{NR}}^{(f)} = \pi \sigma^2 \int_{(3/\sigma)^{1/3}}^1 dy \frac{1-y^2}{y} \approx \frac{\pi\sigma^2}{3} \ln((\sigma/3)), \quad K_{\text{NR}}^{(h)} = \left(\frac{-\pi}{2}\right) \int_{(3/\sigma)^{1/3}}^1 dy \frac{(1-y^2)^2}{y^5} \approx -\frac{\pi}{8} \left(\frac{\sigma}{3}\right)^{4/3}. \quad (\text{H3})$$

We now turn to the quasi-resonant contributions which we evaluate in the same limit. Equation (99) gives f_{QR} and equation (120) gives h_{QR} , combined with the boundary term h_{BQR} in equation (118). The variable g is defined in equation (94) and can be expressed in terms of ϖ and σ from equation (A2). At a given σ , g reaches a minimum $g_{\text{m}}(\sigma)$ at $\varpi = 0$. In the quasi-resonant domain, x may be considered equal to σ except where the difference $(\sigma - x)$ is involved, which makes it possible to invert the relation between g and ϖ , yielding, in the quasi-resonant domain:

$$g \approx \frac{(\sigma_0^2 + \varpi^2)^{3/2}}{3\sigma^2}, \quad \varpi^2 + \sigma_0^2 \approx (3g\sigma^2)^{2/3}, \quad x \approx \sigma, \quad \frac{\sigma - x}{x} \approx \frac{3^{2/3}}{2} \left(\frac{g}{\sigma}\right)^{2/3}, \quad g_{\text{m}}(\sigma) = \frac{\sigma_0^3}{3\sigma^2}. \quad (\text{H4})$$

Assuming as in section 5.4 that $\partial_\sigma F_0$ depends linearly on ϖ , equation (120) can be recast in the form of equation (121). When ϖ is changed for g and the limit $\sigma \gg \sigma_{\text{qr}} \sim \sigma_0^{3/2}$ is taken, the ϖ -integrated kernels assume the form

$$K_{\text{QR}}^{(f)} = \sqrt{3}\sigma^2 \int_{g_{\text{m}}}^1 dg g^{2/3} \sqrt{g^{2/3} - g_{\text{m}}^{2/3}} \left(K_{\frac{2}{3}}(g)L_{\frac{1}{3}}(g) - \frac{\pi}{g\sqrt{3}} \right), \quad (\text{H5})$$

$$K_{\text{QR}}^{(h)} = 2 (3^{1/6})\sigma^{4/3} \int_{g_{\text{m}}}^1 dg g^{2/3} \left(K_{\frac{2}{3}}(g)L_{\frac{2}{3}}(g) + K_{\frac{1}{3}}(g)L_{\frac{1}{3}}(g) - \frac{2\pi}{g\sqrt{3}} \right). \quad (\text{H6})$$

The parenthesis in equation (H5) diverges as g approaches zero as $g^{-1/3}$, but the integral still converges as g_{m} approaches zero. Similarly, the parenthesis in equation (H6) diverges as $g^{-4/3}$ at small values of g . Thanks to the factor $g^{2/3}$, the integral over g is however convergent when its lower bound approaches zero, which it does when σ grows very large. The integral in equation (H5) can be calculated numerically for $g_{\text{m}} = 0$, giving the result in equation (123). From numerical calculation, it also appears that the right hand side of equation (H6) converges when σ approaches infinity to a value that is close to $(\pi/2)\sigma^{4/3}$, with a relative accuracy of 10^{-4} . Adopting this convenient approximation, it is found that for $\sigma \gg \sigma_0^{3/2}$

$$K_{\text{QR}}^{(h)}(\sigma) \approx \frac{\pi}{2} \sigma^{4/3}, \quad (\text{H7})$$

which is the result mentioned in equation (124). For large values of g , that is out of the quasi-resonant domain, the parenthesis in equation (H6) decreases quickly to zero, owing to the fact that any product of a K and L function asymptotes to $\pi/(\sqrt{3}g)$ in this limit. The remainder of the parenthesis decreases as g^{-3} whereas each of its terms considered individually decreases only as g^{-1} . The integrand thus declines with g as $g^{-7/3}$, which would cause the integral in equation (H6) to converge if it were to be extended to a bound much larger than unity. Thus, the support of the integrand in equation (H6) does not extend out of the quasi-resonant domain. The decrease of the integrand in equation (H5) is however slower.

APPENDIX I: ANISOTROPIC KERNELS OF HIGHER MULTIPOLAR ORDERS FOR FARADAY COEFFICIENTS AT HIGH-FREQUENCY

Let us parametrize the distribution function as: $F(\gamma, \vartheta) = F_n(\gamma)P_n(\cos \vartheta)$. After a bit of algebra, following the substitutions of Section 3.3, we find that the coefficient f can be written as in equation (52) with the same C_f factor that appears in equation (53), while the function D'_f can be written as $D'_{f0}(\gamma) + D'_{f1}(\gamma)\mathcal{L}(\gamma)$. The factors D'_{f0} (left column) and D'_{f1} (right column) are listed below for $n = 0, \dots, 6$, where P_i denotes the value of a Legendre polynomials P_i at angle α , $P_i \equiv P_i(\cos \alpha)$:

$$\begin{aligned}
& -\frac{4\sqrt{\gamma^2-1}P_1}{\gamma} & 4P_1 \\
& -6P_2 & \frac{2(2\gamma^2+1)P_2}{\gamma\sqrt{\gamma^2-1}} \\
& \frac{4((\gamma^2-1)P_1-(11\gamma^2+4)P_3)}{5\gamma\sqrt{\gamma^2-1}} & \frac{4((6\gamma^2+9)P_3+P_1(1-\gamma^2))}{5(\gamma^2-1)} \\
& \frac{54(\gamma^2-1)P_2-25(10\gamma^2+11)P_4}{21(\gamma^2-1)} & \frac{6(-2\gamma^4+\gamma^2+1)P_2+5(8\gamma^4+24\gamma^2+3)P_4}{7\gamma(\gamma^2-1)^{3/2}} \\
& \frac{8(11\gamma^4-7\gamma^2-4)P_3-(274\gamma^4+607\gamma^2+64)P_5}{18\gamma(\gamma^2-1)^{3/2}} & -\frac{8(2\gamma^4+\gamma^2-3)P_3-5(8(\gamma^2+5)\gamma^2+15)P_5}{6(\gamma^2-1)^2} \\
& \frac{500(10\gamma^4+\gamma^2-11)P_4-441(28\gamma^4+104\gamma^2+33)P_6}{660(\gamma^2-1)^2} & -\frac{20(\gamma-1)^2(8(\gamma^2+3)\gamma^2+3)P_4-21(16\gamma^6+120\gamma^4+90\gamma^2+5)P_6}{44\gamma(\gamma^2-1)^{5/2}} \\
& \frac{5(\gamma^2-1)(274\gamma^4+607\gamma^2+64)P_5-2(1452\gamma^6+8132\gamma^4+5175\gamma^2+256)P_7}{130\gamma(\gamma^2-1)^{5/2}} & -\frac{15(\gamma^2-1)(8(\gamma^2+5)\gamma^2+15)P_5-14(16\gamma^6+168\gamma^4+210\gamma^2+35)P_7}{26(\gamma^2-1)^3}
\end{aligned} \tag{11}$$

The first line corresponds to an isotropic distribution and reflects the result in equation (38). The third line corresponds to the D'_f part of equation (53). Generically, we find that both coefficients scale like $Q_\alpha[\gamma]P_{n-1}(\cos\alpha) + Q_\beta[\gamma]P_{n+1}(\cos\alpha)$ with Q_α and Q_β polynomials in γ . The dependence of the Faraday rotation coefficient on angle α for the considered anisotropy is set by these Legendre polynomials, P_{n-1} and P_{n+1} . The term independent of $\mathcal{L}(\gamma)$ scales like $1/(\gamma^2-1)^{(n-1)/2}$ and the term linear in $\mathcal{L}(\gamma)$ scales like $1/(\gamma^2-1)^{n/2}$. Similarly, the function $D_f(\gamma)$ (equation (52)) can be written as $D_{f0}(\gamma) + D_{f1}(\gamma)\mathcal{L}(\gamma)$. The factors D_{f0} (left column) and D_{f1} (right column) are gathered below for $n = 1, \dots, 6$ (no D_f term is present when $n = 0$). Again, $P_i \equiv P_i(\cos\alpha)$:

$$\begin{aligned}
& \frac{2}{3\gamma} \left(\frac{(5\gamma^2+4)P_2}{\gamma^2-1} - 2 \right) & -\frac{2(-2\gamma^2+(2\gamma^2+7)P_2+2)}{3(\gamma^2-1)^{3/2}} \\
& \frac{(34\gamma^2+86)P_3-24(\gamma^2-1)P_1}{5(\gamma^2-1)^{3/2}} & -\frac{6((2\gamma^4+15\gamma^2+3)P_3-2(\gamma^4-1)P_1)}{5\gamma(\gamma^2-1)^2} \\
& \frac{12(-5\gamma^4+\gamma^2+4)P_2+(74\gamma^4+387\gamma^2+64)P_4}{7\gamma(\gamma^2-1)^2} & -\frac{3((8(\gamma^2+13)\gamma^2+63)P_4-4(2\gamma^4+5\gamma^2-7)P_2)}{7(\gamma^2-1)^{5/2}}
\end{aligned} \tag{12}$$

$$\begin{aligned}
& \frac{(394\gamma^4+3517\gamma^2+1759)P_5-20(17\gamma^4+26\gamma^2-43)P_3}{27(\gamma^2-1)^{5/2}} & -\frac{5((-8\gamma^6-52\gamma^4+48\gamma^2+12)P_3+(8\gamma^6+160\gamma^4+195\gamma^2+15)P_5)}{9\gamma(\gamma^2-1)^3} \\
& \frac{6(276\gamma^6+3764\gamma^4+3789\gamma^2+256)P_6-20(\gamma-1)(\gamma+1)(74\gamma^4+387\gamma^2+64)P_4}{88\gamma(\gamma^2-1)^3} & -\frac{15(2(-8\gamma^6-96\gamma^4+41\gamma^2+63)P_4+(16\gamma^6+456\gamma^4+930\gamma^2+215)P_6)}{44(\gamma^2-1)^{7/2}} \\
& \frac{5(\gamma^2-1)(274\gamma^4+607\gamma^2+64)P_5-2(1452\gamma^6+8132\gamma^4+5175\gamma^2+256)P_7}{130\gamma(\gamma^2-1)^{5/2}} & -\frac{15(\gamma^2-1)(8(\gamma^2+5)\gamma^2+15)P_5-14(16\gamma^6+168\gamma^4+210\gamma^2+35)P_7}{26(\gamma^2-1)^3}
\end{aligned} \tag{13}$$

The second line corresponds to the D_f part of equation (53). The same scalings are found w.r.t. $P_{n-1}(\cos\alpha)$ and $P_{n+1}(\cos\alpha)$. The terms independent of $\mathcal{L}(\gamma)$ scale like $1/(\gamma^2-1)^{(n+1)/2}$ and the terms proportional to $\mathcal{L}(\gamma)$ scale like $1/(\gamma^2-1)^{(n+2)/2}$. The anisotropic coefficient h can also be written as in equation (52), with a prefactor C_h that is identical to that in equation (54) and a function D'_h that can again be written as $D'_{h0}(\gamma) + D'_{h1}(\gamma)\mathcal{L}(\gamma)$. The factors D'_{h0} (left column) and D'_{h1} (right column) are listed below for $n = 0, \dots, 3$:

$$\begin{aligned}
& \frac{\frac{1}{3}\sqrt{\gamma^2-1}(2\gamma^2-3)(P_2-1)}{(6\gamma^4-17\gamma^2-4)(P_1-P_3)} & \frac{P_2-1}{3\gamma} \\
& \frac{7(4\gamma^4-8\gamma^2+19)+5(-20\gamma^4+76\gamma^2+31)P_2+36(2\gamma^4-9\gamma^2-8)P_4}{15\gamma} & \frac{P_3-P_1}{\sqrt{\gamma^2-1}} \\
& \frac{9((36(\gamma^2-3)\gamma^2+493)\gamma^2+104)P_1+7(-132\gamma^6+696\gamma^4+509\gamma^2-248)P_3+100(6\gamma^6-39\gamma^4-80\gamma^2+8)P_5}{210\sqrt{\gamma^2-1}} & \frac{14\gamma^2+94\gamma^2P_2-108\gamma^2P_4-7P_2+7}{42\gamma-42\gamma^3} \\
& \frac{9((36(\gamma^2-3)\gamma^2+493)\gamma^2+104)P_1+7(-132\gamma^6+696\gamma^4+509\gamma^2-248)P_3+100(6\gamma^6-39\gamma^4-80\gamma^2+8)P_5}{1890\gamma(\gamma^2-1)} & \frac{100\gamma^2P_5-9(2\gamma^2+3)P_1+(27-82\gamma^2)P_3}{18(\gamma^2-1)^{3/2}}
\end{aligned} \tag{14}$$

The first line corresponds to the bracket in equation (39) and the third one to that in equation (54). The terms independent of $\mathcal{L}(\gamma)$ scale like $1/(\gamma^2-1)^{(n-1)/2}$ while terms proportional to $\mathcal{L}(\gamma)$ scale like $1/(\gamma^2-1)^{n/2}$. The number of Legendre polynomials now increases with the anisotropy order n . Finally, the similar functions associated to D_h (defined as in equation (52)) are, for $n = 1, \dots, 3$:

$$\begin{aligned}
& -\frac{(2\gamma^2+13)(P_1-P_3)}{15(\gamma^2-1)} & \frac{(4\gamma^2+1)(P_1-P_3)}{5\gamma(\gamma^2-1)^{3/2}} \\
& -\frac{7(-6\gamma^4+17\gamma^2+4)+5(18\gamma^4+65\gamma^2+4)P_2-12(4\gamma^4+37\gamma^2+4)P_4}{105\gamma(\gamma^2-1)^{3/2}} & \frac{(24\gamma^2+5)P_2-12(2\gamma^2+1)P_4+7}{7(\gamma^2-1)^2} \\
& \frac{9(64\gamma^4-258\gamma^2-331)P_1-7(168\gamma^4+854\gamma^2-197)P_3+100(6\gamma^4+83\gamma^2+16)P_5}{630(\gamma^2-1)^2} & -\frac{500(4\gamma^2+3)\gamma^2P_5+9(8\gamma^2(\gamma^2-22)-7)P_1+7(-296\gamma^4+12\gamma^2+9)P_3}{210\gamma(\gamma^2-1)^{5/2}}
\end{aligned} \tag{15}$$

The terms independent of $\mathcal{L}(\gamma)$ scale like $1/(\gamma^2-1)^{(n+1)/2}$ and the terms proportional to $\mathcal{L}(\gamma)$ scale like $1/(\gamma^2-1)^{(n+2)/2}$.

APPENDIX J: FARADAY CONVERSION COEFFICIENT IN THE LOW-FREQUENCY LIMIT

The equation $g = 1$ which defines the values $\varpi_{qr\pm}$ of ϖ at the edge of the QR domain for a given value of γ can be exactly written as:

$$\frac{(\varpi^2 + \sigma_0^2)^{3/2}}{3\gamma^2 u^2 \sin^4 \alpha} = \left(1 + \frac{\varpi \cos \alpha}{\gamma u \sin^2 \alpha}\right)^2 \left(1 - \frac{\varpi^2 + \sigma_0^2}{\gamma^2 u^2 \sin^4 \alpha \left(1 + \frac{\varpi \cos \alpha}{\gamma u \sin^2 \alpha}\right)^2}\right)^{1/4} \left(\frac{1}{2} + \frac{1}{2} \sqrt{1 - \frac{\varpi^2 + \sigma_0^2}{\gamma^2 u^2 \sin^4 \alpha \left(1 + \frac{\varpi \cos \alpha}{\gamma u \sin^2 \alpha}\right)^2}}\right)^{3/2}. \quad (J1)$$

Since $|\varpi_{qr\pm}|$ is much less than $\gamma u \sin^2 \alpha$, the three parentheses on the right are close to unity and the simplest approximation to $\varpi_{qr\pm}$ in the low-frequency limit is given by equation (132). Higher accuracy approximations to $\varpi_{qr\pm}$ can be generated by successively iterating on equation (J1), setting $\gamma u \sin^2 \alpha = 3G$. The result, valid for $|\varpi_{qr\pm}| \gg \sigma_0$, is:

$$\varpi_{qr+} = + (3\gamma^2 u^2 \sin^4 \alpha)^{1/3} \left(1 + \frac{2 \cos \alpha}{3} \frac{1}{G^{1/3}} + \left(\frac{\cos^2 \alpha}{3} - \frac{5}{24}\right) \frac{1}{G^{2/3}} + \left(\frac{10 \cos^3 \alpha}{81} - \frac{5 \cos \alpha}{36}\right) \frac{1}{G} + \dots\right), \quad (J2)$$

$$\varpi_{qr-} = - (3\gamma^2 u^2 \sin^4 \alpha)^{1/3} \left(1 - \frac{2 \cos \alpha}{3} \frac{1}{G^{1/3}} + \left(\frac{\cos^2 \alpha}{3} - \frac{5}{24}\right) \frac{1}{G^{2/3}} - \left(\frac{10 \cos^3 \alpha}{81} - \frac{5 \cos \alpha}{36}\right) \frac{1}{G} + \dots\right). \quad (J3)$$

The primitive of the function in equation (133) is

$$\begin{aligned} \int d\varpi \left(\frac{2x^4}{(\sigma^2 - x^2)^{5/2}} + \sigma_0^2 \frac{x^2(4\sigma^2 + x^2)}{(\sigma^2 - x^2)^{7/2}} \right) &= \frac{81\varpi(7\sigma_0^4 + 10\varpi^2\sigma_0^2 + 4\varpi^4)}{(\varpi^2 + \sigma_0^2)^{5/2}} \left(\frac{G}{\sigma_0}\right)^4 - \frac{36 \cos \alpha \sigma_0^3 (5\sigma_0^2 + 2\varpi^2)}{(\varpi^2 + \sigma_0^2)^{5/2}} \left(\frac{G}{\sigma_0}\right)^3 \\ -18\varpi \frac{4 \sin^2 \alpha \varpi^4 + (9 - 7 \cos^2 \alpha) \sigma_0^2 \varpi^2 + 5\sigma_0^4}{(\varpi^2 + \sigma_0^2)^{5/2}} \left(\frac{G}{\sigma_0}\right)^2 &+ 12 \cos \alpha \frac{2 \sin^2 \alpha \sigma_0 \varpi^4 + 5 \sin^2 \alpha \sigma_0^3 \varpi^2 + (3 - 2 \cos^2 \alpha) \sigma_0^5}{(\varpi^2 + \sigma_0^2)^{5/2}} \left(\frac{G}{\sigma_0}\right) \\ -2 \cos^2 \alpha (1 + \sin^2 \alpha) \ln \left(\sqrt{\varpi^2 + \sigma_0^2} + \varpi \right) &+ \frac{(3 + 6 \cos^2 \alpha - 5 \cos^4 \alpha) \varpi^4 + (6 + 14 \sin^2 \alpha \cos^2 \alpha) \sigma_0^2 \varpi^2 + (3 + 8 \cos^2 \alpha - 6 \cos^4 \alpha) \sigma_0^4}{3(\varpi^2 + \sigma_0^2)^{5/2}}. \quad (J4) \end{aligned}$$

In the low-frequency limit $\sigma_0/|\varpi_{qr\pm}|$ is small, as can be judged from equation (132), this ratio being about $(u/(3\gamma^2 \sin \alpha))^{1/3}$ which is meant to be small in this limit. The right hand side of equation (J4) can then be expanded in σ_0/ϖ , and the definite integral over the interval $[\varpi_{qr-}, \varpi_{qr+}]$ calculated from it at any desired order in γ , using equations (J2)–(J3). It will however be sufficient to extend the expansion to the first non-vanishing order in γ , which from section 5.4 is expected to be $\gamma^{4/3}$. The ratio (G/σ_0) is proportional to γ and, as mentioned above, $\sigma_0/|\varpi_{qr\pm}|$ is of order $1/\gamma^{2/3}$. The factors of all powers of (G/σ_0) in equation (J4) remain finite or approach zero as σ_0/ϖ approaches zero. This implies that terms proportionnal to $(G/\sigma_0)^1$ and $(G/\sigma_0)^0$ are negligible at the order $\gamma^{4/3}$, as are also the logarithmic terms. Similarly, the term proportionnal to $(G/\sigma_0)^3$ does not contribute at this order because its factor is $\mathcal{O}(1/\gamma^2)$. Those parts of equation (J4) that do contribute at order $\gamma^{4/3}$ are the first term, the factor of which should be expanded to order $(\sigma_0/\varpi)^4$ and the term proportionnal to $(G/\sigma_0)^2$, the factor of which would have to be expanded to order (σ_0/ϖ) , had terms of that order been present in its expansion. This leads to equation (J5) below, which only involves the lowest order approximation to $\varpi_{qr\pm}$ from equations (J2)–(J3):

$$\int d\varpi \left(\frac{2x^4}{(\sigma^2 - x^2)^{5/2}} + \sigma_0^2 \frac{x^2(4\sigma^2 + x^2)}{(\sigma^2 - x^2)^{7/2}} \right) \approx \frac{81\varpi}{|\varpi|} \left(4 - \frac{1}{2} \frac{\sigma_0^4}{\varpi^4}\right) \left(\frac{G}{\sigma_0}\right)^4 - \frac{72\varpi}{|\varpi|} \sin^2 \alpha \left(\frac{G}{\sigma_0}\right)^2. \quad (J5)$$

We then obtain, using equation (J5), the definition $G = \gamma u \sin^2 \alpha / 3$ and the lowest order expressions for $\varpi_{qr\pm}$, the integral over ϖ on the first line of equation (131) in the form of equation (134).

Let us now evaluate, along the lines described in section 6, the quasi-resonant contribution to H^{iso} . In the low-frequency limit, the variable g assumes, for a given Lorentz factor γ , a value less than unity in the quasi-resonant domain, which reaches near $\varpi = 0$ a small minimum, g_m , given by equation (H4). The relation between the variables g and ϖ at a given γ results from equations (A1), (A2) and (94). In the low-frequency limit, it becomes

$$g \approx \frac{(\varpi^2 + \sigma_0^2)^{3/2}}{3\gamma^2 u^2 \sin^4 \alpha}, \quad \text{or} \quad \varpi^2 = (3\gamma^2 u^2 \sin^4 \alpha)^{2/3} \left(g^{2/3} - g_m^{2/3}\right). \quad (J6)$$

From equations (J6) and (A2) we also get

$$\left(\frac{\sigma - x}{x}\right) \approx \left(\frac{3g}{2^{3/2}\gamma u \sin^2 \alpha}\right)^{2/3}. \quad (J7)$$

These results are used to convert the second line of equation (131) into functions of g , so that eventually:

$$\begin{aligned} H_{\text{QR}}^{\text{iso}}(\gamma) &= \frac{2}{\sin^2 \alpha} (\gamma u \sin^2 \alpha)^{4/3} 3^{1/6} \int_{g_m}^1 \frac{dg}{g^{1/3} \sqrt{g^{2/3} - g_m^{2/3}}} \left(g^{4/3} \left(K_{2/3}(g) L_{2/3}(g) + K_{1/3}(g) L_{1/3}(g) - \frac{2\pi}{\sqrt{3}g} \right) \right) \\ &\quad - \frac{2}{\sin^2 \alpha} (\gamma u \sin^2 \alpha)^{4/3} 3^{1/6} \int_{g_m}^1 \frac{dg}{g^{1/3} \sqrt{g^{2/3} - g_m^{2/3}}} \left(g_m^{2/3} g^{2/3} \left(K_{1/3}(g) L_{1/3}(g) - \frac{\pi}{\sqrt{3}g} \right) \right). \quad (J8) \end{aligned}$$

The products $K_{2/3}(g)L_{2/3}(g)$ and $K_{1/3}(g)L_{1/3}(g)$ diverge at small g as $g^{-4/3}$. Therefore both integrals in equation (J8) converge in the limit $g_m \rightarrow 0$, since the second integrand is less than $g^{4/3}(K_{1/3}L_{1/3} - \pi/(\sqrt{3}g))$. Evaluating these integrals in the limit of vanishing g_m , we obtain equation (135) of the main text.

APPENDIX K: FARADAY ROTATION COEFFICIENT IN THE LOW-FREQUENCY LIMIT

We derive here the low-frequency limit of equation (127), which corresponds to $\gamma \gg \gamma_{\text{qr}}$ (equation (98)). The offset correction results from the small displacement $\Delta\varpi_{\text{qr}}$ of the center of the interval $[\varpi_{\text{qr}-}(\gamma), \varpi_{\text{qr+}}(\gamma)]$ with respect to zero. Approximations to $\varpi_{\text{qr}\pm}(\gamma)$ are given in equations (J2)–(J3). $\Delta\varpi_{\text{qr}}$ being small, the integral of an odd function $f_{\text{odd}}(\varpi)$ on $[\varpi_{\text{qr-}}, \varpi_{\text{qr+}}]$ is about twice $\Delta\varpi_{\text{qr}} f_{\text{odd}}(+\varpi_{\text{qr0}})$, ϖ_{qr0} being the dominant term in equation (J2). From the definition of the QR domain, $g(\gamma, \varpi_{\text{qr}\pm})$ is unity. This gives the offset correction associated with the second and third terms in equation (127). Since in the low-frequency limit $(\sigma - x) \ll \sigma$ and $\varpi_{\text{qr0}} \ll \sigma_0$ the raw expressions may be simplified to equation (128):

$$F_{\text{off}}^{\text{iso}} = -\frac{4\pi s_q}{3} \gamma u \cos \alpha + 8s_q \gamma u \cos \alpha \left(\sqrt{3}K_{2/3}(1)L_{1/3}(1) - \pi \right). \quad (\text{K1})$$

The parity correction is the integral over the symmetrical interval $[-\varpi_{\text{qr0}}, +\varpi_{\text{qr0}}]$ of the almost odd integrands in equation (127). Any of these two integrands can be factored as $\varpi \Phi(\varpi)$. Only the small odd part of $\Phi(\varpi)$, which is defined by $\Phi_{\text{odd}}(\gamma, \varpi) = (\Phi(\gamma, +\varpi) - \Phi(\gamma, -\varpi))/2$, contributes to the integral over the interval $[-\varpi_{\text{qr0}}, +\varpi_{\text{qr0}}]$. Using the relation $\sigma^2 - x^2 = \varpi^2 + u^2 \sin^2 \alpha$ the function Φ_{odd} associated with the integrand on the first line of equation (127) can be written as

$$\Phi_{\text{odd}}^{(1)}(\gamma, \varpi) = \frac{1}{2} \frac{4\gamma u \varpi \sin^2 \alpha \cos \alpha}{(\varpi^2 + u^2 \sin^2 \alpha)^{3/2}}. \quad (\text{K2})$$

The associated integral in equation (127) can be calculated by integration by parts, giving

$$\int_{-\varpi_{\text{qr0}}}^{+\varpi_{\text{qr0}}} d\varpi \frac{\varpi^2}{(\varpi^2 + \sigma_0^2)^{3/2}} = \ln \left(\frac{\sqrt{\varpi_{\text{qr0}}^2 + \sigma_0^2} + \varpi_{\text{qr0}}}{\sqrt{\varpi_{\text{qr0}}^2 + \sigma_0^2} - \varpi_{\text{qr0}}} \right) - 2 \frac{\varpi_{\text{qr0}}}{\sqrt{\varpi_{\text{qr0}}^2 + \sigma_0^2}}. \quad (\text{K3})$$

This exact relation is expanded for large γ up to terms of order γ^0 included, leading to an associated parity correction

$$F_{\text{par}}^{(1)} = -\pi s_q \gamma u \cos \alpha \left(\frac{8}{3} \ln(\gamma) + \frac{4}{3} \ln \left(\frac{\sin \alpha}{u} \right) + 2 \ln(4 \cdot 3^{2/3}) - 4 \right). \quad (\text{K4})$$

The parity correction associated with the integral on the second line of equation (127) involves the calculation of the odd part of the function $gK_{2/3}(g)L_{1/3}(g)$, where $g(\gamma, \varpi)$ is defined by equation (94). For small $\varpi/\gamma u \sin^2 \alpha$, g may be expanded by using equation (A1) and the second relation in equation (A2) into

$$g = g_0 + g_1 \quad \text{where} \quad g_0(\gamma, \varpi) = \frac{1}{3} \frac{(\varpi^2 + \sigma_0^2)^{3/2}}{(\gamma u \sin^2 \alpha)^2} \quad \text{and} \quad g_1 = -2g_0 \frac{\varpi \cos \alpha}{\gamma u \sin^2 \alpha}, \quad (\text{K5})$$

where $g_1 \ll g_0$ in the low-frequency limit. Denoting $g(\gamma, \pm\varpi)$ by g_{\pm} , the functions $g_{\pm}K_{2/3}(g_{\pm})L_{1/3}(g_{\pm})$ are then Taylor-expanded about g_0 to provide an approximation of the odd part of $gK_{2/3}(g)L_{1/3}(g)$, that is

$$\frac{1}{2} (g_+K_{2/3}(g_+)L_{1/3}(g_+) - g_-K_{2/3}(g_-)L_{1/3}(g_-)) \approx -\frac{2\varpi \cos \alpha}{\gamma u \sin^2 \alpha} g_0 \frac{d}{dg_0} \left(g_0K_{2/3}(g_0)L_{1/3}(g_0) \right). \quad (\text{K6})$$

The parity correction associated with the integral on the second line of equation (127) can then be written as

$$F_{\text{par}}^{(2)} = -\frac{8\sqrt{3}s_q \cos \alpha}{\gamma u \sin^4 \alpha} \int_0^{+\varpi_{\text{qr0}}} d\varpi \varpi^2 g_0 \frac{d}{dg_0} \left(g_0K_{2/3}(g_0)L_{1/3}(g_0) \right). \quad (\text{K7})$$

Using equation (K5), the integral in equation (K7) is expressed in terms of the integration variable g_0 , noted g below, which ranges from $g_m = g_0(\gamma, \varpi = 0)$ to unity. For large γ , $g_m \rightarrow 0$. To the same order as in equation (K1), it suffices to calculate the integral over g in equation (K7) to order $\mathcal{O}(\gamma^0)$, which gives

$$F_{\text{par}}^{(2)} = -8\sqrt{3}s_q \gamma u \cos \alpha \int_0^1 dg g \frac{d}{dg} \left(gK_{2/3}(g)L_{1/3}(g) \right). \quad (\text{K8})$$

The corrections in equations (K1), (K4) and (K8) are then added to the non-integrated term in equation (127). For consistency, the latter is expanded for large γ as $\gamma \ln(\sqrt{\gamma^2 - 1} + \gamma) - \sqrt{\gamma^2 - 1} \approx \gamma \ln(2\gamma) - \gamma$. The integral over g in equation (K8) may be integrated by parts, resulting in the cancellation of the Bessel term in equation (K1) and leaving us with

$$F_{\text{LF}}^{\text{iso}}(\gamma) = \pi s_q \gamma u \cos \alpha \left[\frac{4}{3} \ln \left(\frac{\gamma u}{\sin \alpha} \right) - \frac{4}{3} - \frac{4}{3} \ln(3) - 8 + \frac{8\sqrt{3}}{\pi} \int_0^1 gK_{2/3}(g)L_{1/3}(g) dg \right]. \quad (\text{K9})$$

The integral over g in equation (K9) is numerically evaluated to 2.162372 finally giving the result quoted in equation (130).

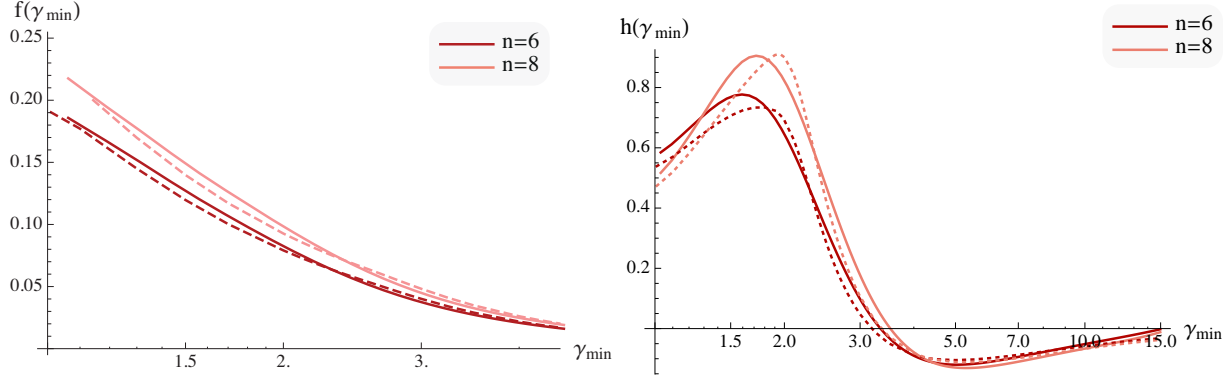


Figure L1. *Left:* quasi exact values of the Faraday rotation coefficient f for power-law distributions obtained by numerically calculating the double integral in equation (25) (full lines) compared to those obtained from the interpolating formula (140) for the kernel $F^{\text{iso}}(\gamma)$ (dashed lines), for a range of values of the low-energy cutoff γ_{min} and for two different exponents n , as labeled. *Right:* Similar plots for the Faraday conversion coefficient h , from equations (26) and (141). The radiation's parameters are $\omega = 15 |\Omega|$ and $\alpha = \pi/4$.

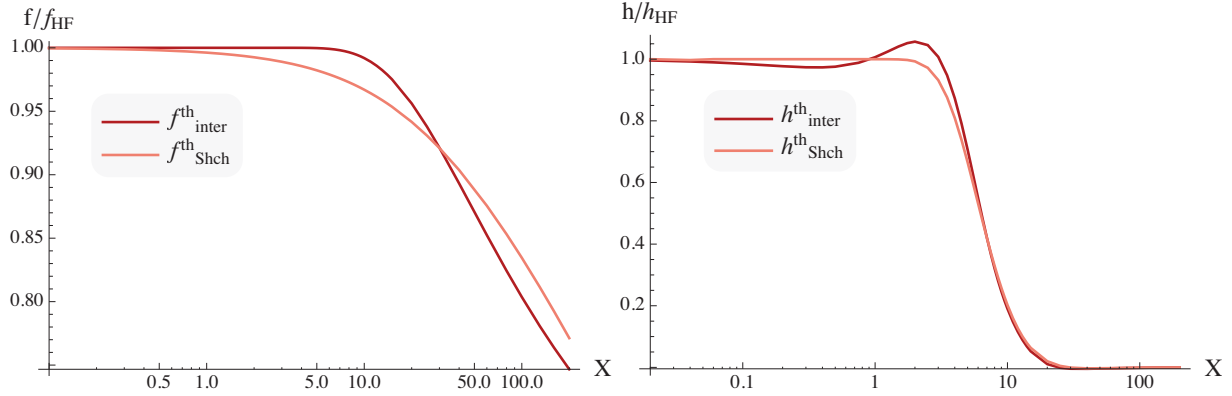


Figure L2. *Left:* The thick line represents the ratio of the Faraday rotation coefficient $f_{\text{inter}}^{\text{th}}$ for a thermal plasma as deduced from the interpolating formula for the kernel $F_{\text{int}}^{\text{iso}}$ in equation (140), to the high-frequency expression $f_{\text{HF}}^{\text{th}}$ deduced from equations (33) and (38). The thin line represents the fit by Shcherbakov (2008) to the ratio of the exact value of f to the high-frequency formula. These quantities are plotted as a function of the regime-change parameter X defined by Shcherbakov (2008) and in equation (47). *Right:* Similar plots for the thermal Faraday conversion coefficient h , from equations (141), (33) and (39). The radiation's parameters here are $\omega = 1000 |\Omega|$ and $\alpha = \pi/4$, allowing a comparison between these figures and figures 4 and 5 of Shcherbakov (2008).

APPENDIX L: TRANSFER COEFFICIENTS FROM INTERPOLATED ISOTROPIC KERNELS

The figures L1 and L2 illustrate how the interpolation formulae in equations (140) and (141) perform in calculating the actual Faraday transfer coefficients in a plasma characterized by an isotropic power-law energy distribution with a low-energy cutoff (figure L1) or in a thermal plasma (figure L2). Figure L1 compares the quasi exact values of the transfer coefficients in figure 3 to those derived from the interpolation formulae (140)–(141) for the kernel or its derivative. The accuracy generally is of order 10% for h and somewhat better than 10% for f . Figure L2 displays the ratio, which Shcherbakov (2008) refers to as the multiplier, of the Faraday transfer coefficients for a thermal plasma, calculated from the interpolated kernels (140) and (141), to their high-frequency expression deduced from equations (38), (39) and (33). In figures 4 and 5 of his paper, Shcherbakov (2008) presents similar ratios of numerically computed exact transfer coefficients and corresponding high-frequency expressions, which he displays as a function of the regime-change parameter X defined by equation (47). He proposes fitting formulae for these ratios (his equations (28) and (29)). The figures 4 and 5 of Shcherbakov (2008) can then be compared to our figures L2, similar parameters having been adopted for the radiation. From this comparison it appears that within the range of parameters represented here our interpolation formula approaches the real value of the Faraday rotation coefficient somewhat closer than his proposed fit, while our interpolation also well represents the Faraday conversion coefficient, though slightly less accurately than his.